Performance of Geosynthetic-Reinforced Unpaved Roads

A THESIS

SUBMITTED IN PARTIAL FULFILMENTS OF THE REQUIREMENTS FOR THE

AWARD OF DEGREE OF

DOCTOR OF PHILOSOPHY

IN

CIVIL ENGINEERING

BY

MEENAKSHI SINGH

Under the Supervision of

Prof. A. Trivedi
Professor, Department of Civil Engineering
Delhi Technological University, Delhi-110042
&
Prof. S. K. Shukla
Adjunct Professor, Department of Civil Engineering
Delhi Technological University, Delhi-110042
&
Founding Research Group Leader
Geotechnical and Geoenvironmental Engineering
School of Engineering, Edith Cowan University
270 Joondalup Drive, Joondalup, Perth, WA 6027, Australia

DEPARTMENT OF CIVIL ENGINEERING
DELHI TECHNOLOGICAL UNIVERSITY
DELHI- 110042, INDIA
FEBRUARY 2021

ACKNOWLEDGMENT

I would like to express deep sense of gratitude to several persons for their support in accomplishing the research work. It is a pleasant aspect that I have now the opportunity to express my gratitude for all of them.

Firstly, I would like to express my profound sense of gratitude to my supervisors and motivators **Prof. Ashutosh Trivedi**, Civil Engineering Department, Delhi Technological University and **Prof. Sanjay Kumar Shukla**, Associate Professor and Program Leader, Discipline of Civil and Environmental Engineering, School of Engineering, Edith Cowan University, Australia, for their invaluable suggestions, co-operation and help in providing necessary facilities and resources during the entire period of my research work. I thank them for encouraging me to stay in the laboratory and field for long hours. Their wide knowledge and logical way of thinking have helped me to complete my research work. They always made themselves available for discussions despite their busy schedules and to acquire a knowledge from their research expertise.

I express my gratitude to **Prof. Narendra Dev** and **Prof. V. K. Minocha** for their continued morale-boosting efforts and support towards the completion of my research work.

I am also thankful to **Dr. B. B. Prasad** from Ajay Kumar Garg Engineering College for allowing me to conduct laboratory tests and his valuable suggestions in research work.

I am grateful to **Delhi Technological University** for providing the land for conducting field tests in the campus and help during the moving wheel load tests.

I express special thanks to my father-in-law **Mr. Sukhpal Singh** for his valuable assistance, support and encouragement throughout the research work. Also, my heartiest thanks go to my family, my son, and my husband whose proximity, love & affection, made it possible to complete this research work.
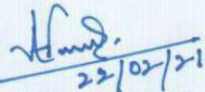
CERTIFICATE

This is to certify that the thesis entitled "**Performance of Geosynthetic-Reinforced Unpaved Roads**" which is being submitted by Mrs. **Meenakshi Singh** with roll no. **2k14/phd/ce/02** as a **full-time** research scholar, for the award of degree of Doctor of Philosophy in Civil Engineering, Delhi Technological University, Delhi, is a record of student's own work carried out by her under our supervision and guidance. The matter embodied in this thesis has not been submitted in part or full to any other university or institute for award for any others degree.

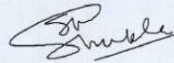Date: 22/02/21

Prof. Ashutosh Trivedi

(Supervisor)

Professor

Department of Civil Engineering

Delhi Technological University

Delhi-110042, India

23/02/2021

Prof. Sanjay Kumar Shukla

(Co-Supervisor)

Adjunct Professor

Department of Civil Engineering

Delhi Technological University

Delhi-110042, India

ABSTRACT

Geosynthetics have been used to improve the performance of pavement. The performance of an unpaved road can be measured by determining the California bearing ratio (*CBR*) and this value represents the strength of subgrade soil. Unpaved roads constructed on weak soil subgrade are frequently subjected to severe damage and hence, they require regular maintenance and repair. One of the main stabilization methods of improvement of the serviceability of these roads is to reinforce them with geosynthetics.

In the present research, firstly an experimental investigation was carried out to evaluate the performance of the subgrade soil by placing a single layer and double layers of geosynthetic reinforcements horizontally at varying depths from the top surface of subgrade soil. Through a series of *CBR* tests in the laboratory, an attempt was made to determine the optimum depth of the reinforcement layer. The single layer of reinforcement has been placed at the middle, one-third and one-fourth of the height of the *CBR* specimen from the top surface of the soil in the *CBR* mould. The double layers of reinforcement were placed at one-fourth of the specimen height from the top surface and the bottom surface. The results show the significant contribution in terms of increased *CBR* value of the soil, resulting in reduced design thickness of the pavement layers above the subgrade soil. The results indicate that for the maximum benefit, the Tenax 3D grid reinforcement should be placed in between 0.3H and 0.36H where H is the height of the soil specimen. For Glasgrid and Tenax multimat reinforcements, the maximum effect of reinforcement is obtained when they are placed between 0.41H and 0.62H.

An attempt has been made to conduct laboratory *CBR* tests on unreinforced and reinforced soil-aggregate composite systems. The improvement in the strength of subgrade-aggregate composite system was determined through the tests conducted in the standard CBR mould in terms of *CBR* value. Unreinforced soil–aggregate composite system is prepared by compacting

the soil layer in the mould, and placing the aggregates layer above the soil, where the soil represents the existing subgrade and aggregate layers, represents the base course material of an unpaved road. In reinforced soil–aggregate composite system, the reinforcing layer was installed at the soil-aggregate interface. The geosynthetics used in the study as reinforcing layers are geotextile, geogrid and geomat. Some more tests were conducted on reinforced soil–aggregate composite system with double layers of reinforcement such that the first reinforcing layer was laid at the soil-aggregate interface and another reinforcing layer was laid at middle half of the compacted aggregate layer. Unreinforced and reinforced soil–aggregate composite systems were subjected to standard penetrating load while performing the tests, and the performance of reinforced soil–aggregate composite system was compared with that of the unreinforced systems. The effect of type of reinforcement on the load–penetration curve and the relative performance of various types of geosynthetics have also been investigated.

In this thesis, an effort has been made to analyses the geosynthetic reinforced unpaved roads using digital static and dynamic cone penetrometer tests. DCP test has been used widely as a pavement evaluation technique. Field experiments were conducted on unpaved test sections reinforced with geotextile and geogrid, with the potential use of dynamic cone penetrometer (DCP) and digital static cone penetrometer (SCP) to assess benefits of geotextile and geogrid reinforcement. Digital SCP was used to measure the load–displacement behavior of geosynthetic-reinforced test section in the field. The field test results of DCP were expressed in terms of dynamic cone penetration index (DCPI, mm/blow). DCPI value represents the penetration depth of the cone per hammer blow and recorded along with the depth profile. Reinforced test section observed reducing DCPI value as compared to the unreinforced test section. DCP results were able to detect transition zone and significant change in the strength of unpaved test section along with penetration depth. The field results indicate the greater resistance to penetration in the geosynthetic-reinforced test section and the penetrometer

resistance increases with the depth. Higher penetration resistance offered by the geotextile has more contribution to the performance improvement of the test section.

In addition, this thesis also presents a fuzzy logic-based modeling approach which is employed for geosynthetic-reinforced subgrade soil of unpaved roads. A review of the literature reveals that fuzzy logic has not been used for predicting the behavior of geogrid-reinforced subgrade. FL-based two models were developed with fuzzy Triangular and Gaussian membership functions for input and output variables. It consists of eight input parameters/factors, namely, reinforced/unreinforced section, depth of reinforcement, plasticity index, plastic limit, liquid limit, optimum moisture content, maximum dry unit weight, and soaked/unsoaked condition and California bearing ratio (*CBR*) as an output parameter. The fuzzy rules are deduced from the experimental data. The laboratory *CBR* tests were performed on the subgrade soil reinforced with geogrid. The precision of models was examined by comparing the predicted *CBR* values with the experimental *CBR* values for Triangular and Gaussian membership functions. The sensitivity analysis reflects a set of dominant parameters. The results indicated a significant improvement in the *CBR* value of geogrid-reinforced subgrade soil due to the inclusion of geogrid. The range for optimal depth of geogrid reinforcement is found to be 36% to 60% of the thickness of the soil layer. The potentialities of FL were found to be satisfactory.

Furthermore, to show the influence of geosynthetic reinforcement on rutting in unpaved roads, field test results of unpaved test section have been presented. The common cause of pavement failure during the unpaved road construction is rutting. Geosynthetic is a solution to this pavement distress and have been widely used for reinforcing unpaved roads. Moving wheel load tests were carried out on unpaved road test sections to investigate the influence of geosynthetic reinforcement in the improvement of pavement surface deformation. One unreinforced and two geosynthetic-reinforced unpaved test sections were constructed in a test

pit of dimension 2700mm $\times$ 9000mm $\times$ 800mm at the Delhi Technological University. Geogrid and geotextile were used for reinforcing the unpaved test sections and this geosynthetic reinforcement layer was embedded at the base-subgrade interface. Unreinforced and geosynthetic-reinforced test sections were examined after moving wheel load tests. Rut depth was measured at three grid locations of each test sections in the transverse direction of the wheel path after certain numbers of vehicle passes. A total number of 350 vehicle passes were applied to the unpaved test section. The contributions of geosynthetic reinforcement were evaluated by calculating traffic benefit ratio (TBR) based on the rut depth measurements in the fields. Test results indicate that inclusion of geosynthetic reinforcement significantly improves the rutting resistance and stability of reinforced test sections comparing to the unreinforced test section.

TABLE OF CONTENTS

LIST OF FIGURES

LIST OF TABLES

CHAPTER 1

INTRODUCTION

This chapter explains the objectives of this research and include the need of sustainable solution to the problem considered in this thesis. This is followed by the scope and an explanation of how this thesis has been structured for easy understanding and convenience of the reader. Some part of this chapter is based on the paper published in Materials Today: Proceedings, Elsevier, as listed in Section 1.6.

1.1 General

The development of road network is essential for rapid growth in economic development of a country. Roads provide connectivity to remote areas and facilitate access to markets, trade, transport, and investment. The road network in India reached to 58.98 lakh kms as on march 2017 and it is second largest road network in the world. Out of the total road length in India, 1.94% is National highways, 2.97% is State highways, 9.94% is District roads, 70.65% is Rural roads, 9.27% is Urban roads and Project roads constituted 5.58% (MORTH, 2017). Rural roads have the highest share in total road length as presented in Fig. 1.1. The percentage of the unsurfaced rural roads to the total rural road length is 66.23% which are also called as unpaved roads (MORTH, 2017). Unpaved roads are basically low volume roads without any permanent surfacing of asphalt or concrete layers and these are generally constructed on locally available subgrade soil. Unpaved roads have aggregate layer which is placed directly above the subgrade soil.

One of the common problems in road construction is dealing with weak subgrade. Unpaved road constructed on weak subgrade, generally causes severe damages to the pavement and requires regular maintenance and repair when they are subjected to the traffic load. This failure may happen because of the inadequate strength of the component layers. In such situations

geosynthetics can be used as a stabilization method of improvement of the serviceability of these roads by reinforcing them with geosynthetics. Inclusion of geosynthetic reinforcement provide better stress distribution, reduces the surface heave and the stresses transferred to the subgrade soil (Koerner 2005). Geosynthetics placed either at the subgrade-base interface or within the granular layer may perform the desired function of separation, confinement or reinforcement as shown in Fig. 1.2.
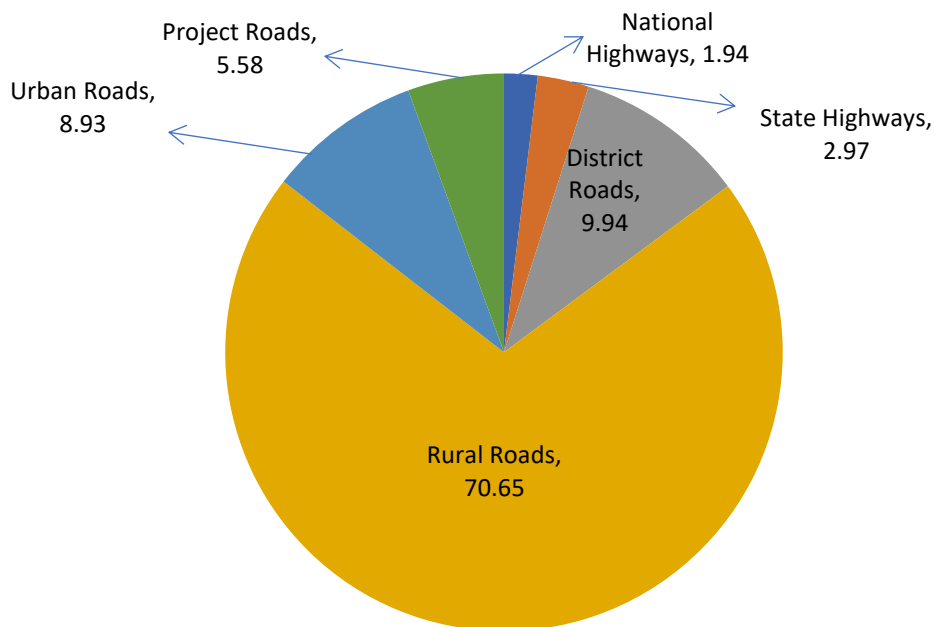
Figure 1.1 Percentage share of road length in total length by various categories.

The use of geosynthetics in unpaved roads provides a reinforcing benefit to the roadway section by reducing the thickness of the granular layer which makes the construction economical and extends their service life. The geosynthetic is typically placed at the base-subgrade interface or within the base course layer to increase the structural or load-carrying capacity of a pavement system (Hufenus et al., 2006). Reinforcement with geosynthetics has become common practice for stabilization of unpaved roads.

2
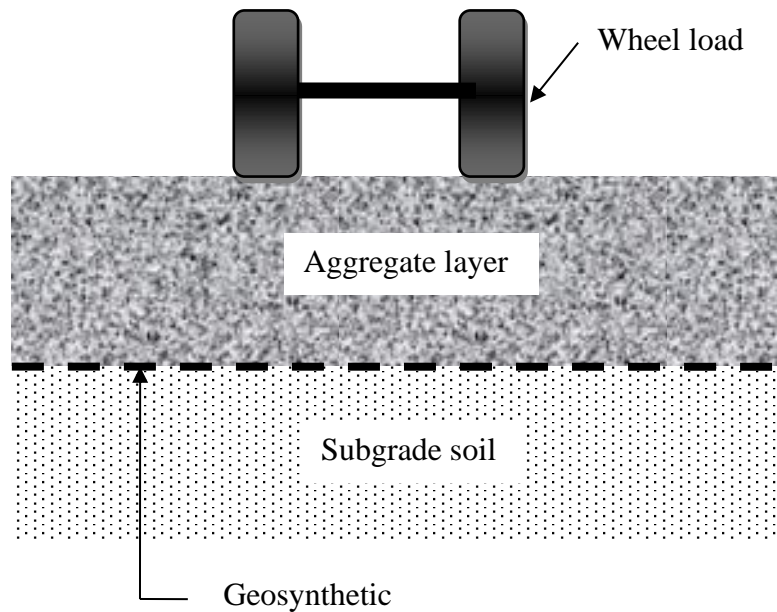
Figure 1.2 A typical cross-section of a geosynthetic-reinforced unpaved road.

1.2 Geosynthetics

Geosynthetics are manufactured from the polymeric materials and used in contact with soil, rock, or any other civil engineering-related material as an integral part of a man-made project, structure, or system. Geosynthetics are available in a variety of planar products, such as geotextiles, geogrids, geocomposits, geonets, geocells, geofoams and geomembrane (Shukla, 2016). The geosynthetic products most commonly used in pavement applications include geotextiles and georids. It can be used to deliver one or more particular functions of geosynthetics in pavement applications. Geotextile is a polymeric, permeable, planar product in the form of a flexible sheet. It is classified as woven and non-woven geotextile based on the manufacturing process. Geogrid is a planar, polymeric product consisting of net like structure with ribs and junction.

Geosynthetic performs various functions in pavements like reinforcement, separation, filtration, drainage, fluid barrier and protection (Shukla, 2012). Geosynthetic application may

perform a single geosynthetic function or a combination of such functions for enhancing the pavement performance. The primary function of geosynthetics in unpaved road construction is considered to be separation and the secondary function would be reinforcement and filteration. Geosynthetics, when used to serve as separation function then it will prevent the intermixing of granular material into the subgrade soil under cyclic loading. The primary function allocated to geotextiles is separation, but the reinforcement function may be acquired from both geogrids and geotextiles (Cuelho and Perkins 2017). Benefits of geosynthetic reinforcement in the roadway applications depends on many factors such as subgrade strength, geosynthetics properties, location of reinforcement in pavement section and base course layer thickness etc. (Hass et al., 1988; Kenny, 1998; Webster, 1992; Cancelli and Montanelli, 1999; Collin et al., 1996; Perkins et. al. 1999).

1.3 Reinforcement Mechanism

Geosynthetics can improve the performance of unpaved roads through the reinforcing mechanisms which include separation between base and subgrade, tensioned membrane effect, vertical restraint of the subgrade soil and lateral restraint of the base course (Perkins et. al, 1999; Hufenus et al. 2006; Giroud and Noiray, 1981; Giroud and Han 2004; Maxwell et al. 2005; Perkins and Ismeik, 1997; Want et al. 2005). Among these mechanisms, lateral restraint of the granular material and vertical restraint of the subgrade soil becomes the dominant mechanisms responsible for enhancing the performance of unpaved roads within tolerable deformation as shown in Fig. 1.3. When the large deformation occurs in the subgrade then the tensioned membrane effect comes to play an important role. The mechanism behind the reinforcement function serve by geotextile is the tensioned membrane effect. If the subgrade undergoes large deformation due to the influence of traffic load, due to which the geosynthetic will exhibits a concave shape under the wheels. This deformed concave shape of geosynthetic is under tension.
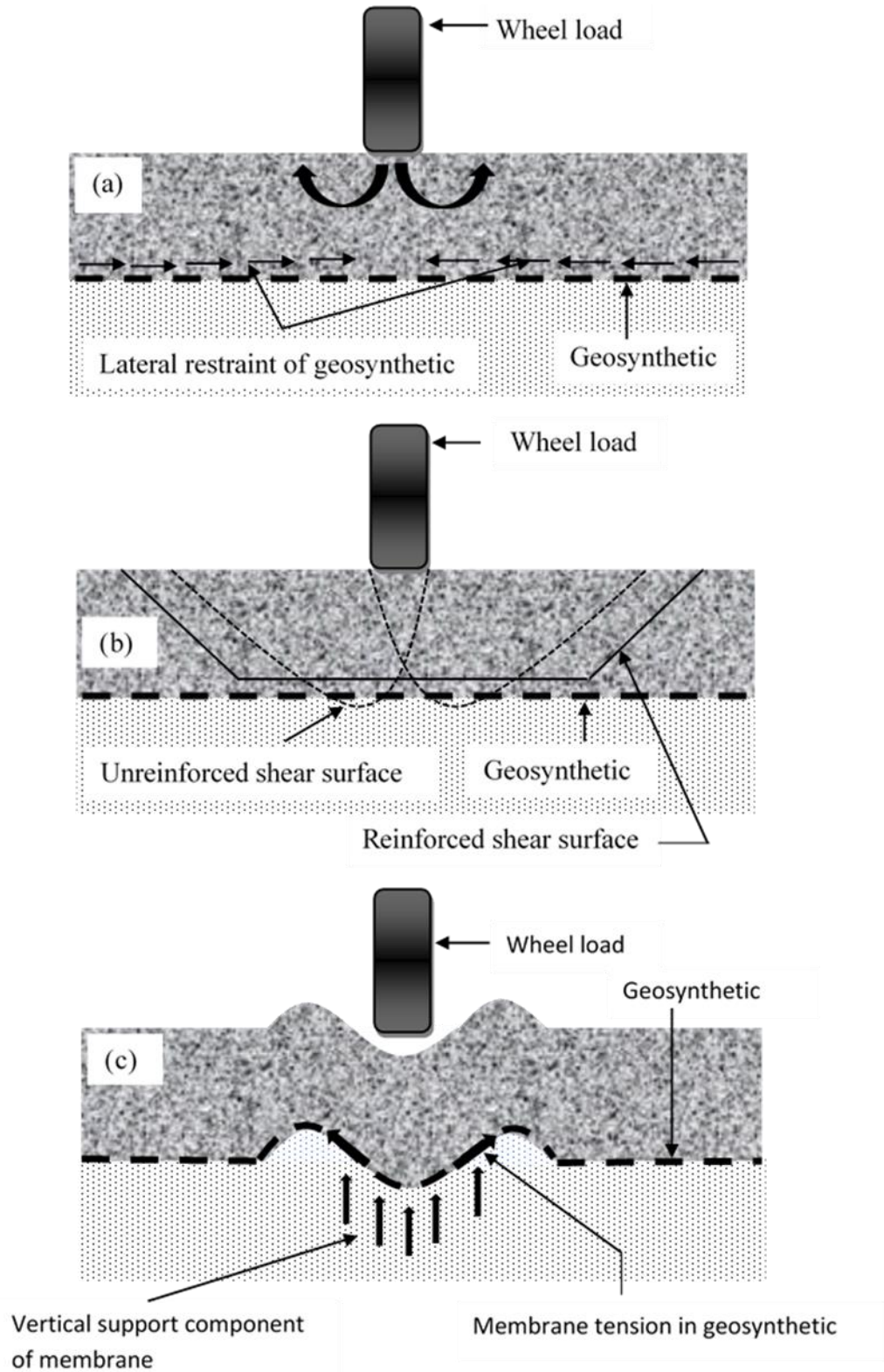
Figure 1.3 Reinforcement mechanisms induced by geosynthetics (Haliburton et al. 1981): (a) Lateral restraint; (b) Increased bearing capacity; (c) Membrane tension support.

Vertical component of this developed tension in geosynthetics will distribute the traffic load to a wider area in the subgrade. Geogrid improve the performance of granular layer through the improvement of wheel load distribution and lateral restraint of granular materials. These reinforcement mechanisms were dependent of the interaction between the geosynthetic and granular material, which prevents lateral spreading of the granular material and imparts tensile stiffness to the base course. The role of granular layer in unpaved roads is to distribute the traffic loads. If the stiffness and thickness of the granular layer is sufficient, the maximum vertical stresses in the subgrade are below the stress level that causes excessive deformation in subgrade. Geosynthetics at the interface of subgrade-base course is the most efficient and convenient location to get the maximum benefits in roadway construction (Das and Shin, 1998; Han and Thakur, 2014). The reinforcement mechanism responsible for the improvement in road performance based on the subgrade-base interaction is intermixing of base and subgrade material. Geotextiles are typically used to perform the separation function which prevents the intrusion of fine particles from the subgrade into the granular base course. Geogrids can be used to perform the separation function at the subgrade-base interface, which provide some degree of separation depending on its aperture size. The interlocking action between the geogrid and granular material will be reduced if the fine particles intrude into the base course from subgrade soil. Hence, the performance of unpaved roads will be affected because interlocking by a geogrid is the main mechanism of improvement in a pavement.

1.4 Significance of the Current Research

Unpaved roads include haul roads, forest roads, access roads and aggregate surfaced roads, which allow the movement of fewer vehicles at slower speed than those on paved roads. An unpaved road has been designed for up to 100000 equivalent single axle loads as per MORTH (1993). The most relevant deformation related to unpaved road performance is rutting.

Excessive rutting should be avoided because this deformation may cause discomfort to drivers, instability of vehicles and damage to vehicles.

Geosynthetics have been used for base course reinforcement and subgrade stabilization for construction of unpaved roads. Geosynthetics can be introduced at base-subgrade interface or within the granular layer for improving the performance of unpaved roads. Contribution of geosynthetic leads to increase the traffic volume carried by a given base course thickness, reduction in the thickness of granular layer, or combinations of both increased traffic and reduced thickness. Another potential benefit of geosynthetics is to use the locally available granular material (Giroud and Han 2004).

Geosynthetics has gain wide acceptance in geotechnical engineering and highway applications. Despite the benefits of geosynthetics in pavement, its use is still limited on rural and low-volume roads (Keller 2016). The main reason for the limited use of the geosynthetics material in low-volume roads is due to lack of understanding in the geosynthetics reinforcement mechanisms. The benefits of geosynthetic reinforcement can be assessed by using experimental laboratory tests or full-scale field tests. Introduction of geosynthetic reinforcement layer at the base-subgrade interface leads to change the overall behavior of geosynthetic-reinforced unpaved roads. Thus, elucidating the need to study the performance of geosynthetic-reinforced unpaved roads for the better understanding of reinforcement mechanism.

1.5 Scope and Objectives of the Research

Major objective of this research is to evaluate the contribution of geosynthetic reinforcement on the behaviour of unpaved roads in enhancing their performance. The research scope includes experimental studies, field studies and model studies for performance evaluation of geosynthetic-reinforced unpaved roads. The following specific objectives have been chosen for further investigation:

- Evaluate the performance of unreinforced and geosynthetic-reinforced unpaved test sections reinforced with different types of geosynthetics: geotextile and geogrid.

- Experimental studies and field studies on unreinforced and geosynthetic-reinforced section for investigating the optimum location of geosynthetic reinforcement in subgrade soil thickness, influence of different types of geosynthetic reinforcement on unpaved roads and reinforcement mechanism responsible for the improvement.

- Study the strength behavior of subgrade-aggregate composite system through California Bearing Ratio tests.

- To assess the benefits of geosynthetics reinforcement placed at base-subgrade interface of unpaved test sections through field studies, with the potential use of dynamic cone penetrometer (DCP) and digital static cone penetrometer.

- To develop a model for predicting the California Bearing Ratio value of subgrade soil reinforced with geogrid layers at various depths using a fuzzy logic approach.

- Evaluate the performance of unreinforced and geosynthetic-reinforced unpaved test sections under moving wheel load tests for the analysis of the rut measurement and Comparison of geosynthetic-reinforced section with unreinforced section.

1.6 Publications Based on the Present Work

Attempts were made during the progress of the research to prepare the thesis as research papers for submission to peer-reviewed international journals and conference proceedings to be considered for publication. The details of the published or prepared papers are as follows:

1. Singh M, Trivedi A, Shukla SK. Strength Enhancement of the Subgrade Soil of Unpaved Road with Geosynthetic Reinforcement Layers. *Transportation Geotechnics* 2019; 19: 54-60. doi: 10.1016/j.trgeo.2019.01.007.

2. Singh M, Trivedi A, Shukla SK. Influence of Geosynthetic Reinforcement on Unpaved Roads Based on CBR, and Static and Dynamic Cone Penetration Tests. *Int. J. of Geosynth. and Ground Eng.* 2020; 6: 1-13. https://doi.org/10.1007/s40891-020-00196-0.

3. Singh M, Trivedi A, Shukla SK. Fuzzy-Based Model for Predicting Strength of Geogrid-Reinforced Subgrade Soil with Optimal Depth of Geogrid Reinforcement. *Transp. Infrastruct. Geotech.* 2020; 7: 664-683. https://doi.org/10.1007/s40515-020-00113-y.

4. Singh M, Trivedi A, Shukla SK. Effect of Geosynthetic Reinforcement on Strength Behaviour of Subgrade-Aggregate Composite System. In: Kanwar V., Shukla S. (eds) Sustainable Civil Engineering Practices. *Lecture Notes in Civil Engineering. 2020*; 72: 61-70. Springer, Singapore. https://doi.org/10.1007/978-981-15-3677-9_7.

5. Singh M, Trivedi A, Shukla SK. Unpaved Test Sections Reinforced with Geotextile and Geogrid. *Materials Today: Proceedings* 2020; 32(4): 706-711. https://doi.org/10.1016/j.matpr.2020.03.260.

6. Singh M, Trivedi A, Shukla SK. Moving Wheel Load Tests for Rutting Evaluation of Geosynthetic-Reinforced Unpaved Roads. *Journal of Transportation Engineering*. (under preparation).

1.7 Structure and Organization of the Thesis

This thesis is organized in eight chapters: general introduction, literature review, six research papers, and summary of conclusions and recommendations for future research.

Chapter 1 presents the brief introduction of geosynthetic-reinforced unpaved roads and also presents the highlights on the contribution of geosynthetic reinforcement in unpaved roads.

Chapter 2 discusses the detailed summary of the literature of past studies pertinent to current research. Experimental, theoretical, and field studies on geosynthetics-reinforced unpaved roads are also presented to recognize the limitations that can be linked to research for achieving the objective of the present study.

Chapter 3 describes the test results of California bearing ratio tests conducted on subgrade soil with single and double layer of geosynthetic reinforcement to evaluate their performance. Except with limited modifications in layout for consistency in the thesis, this chapter has been based on Transportation Geotechnics, of Elsevier/ScienceDirect Publication.

Chapter 4 deals with the experimental investigation on unreinforced and geosynthetic reinforced soil-aggregate composite systems. Except with limited modifications in layout for consistency in the thesis, this chapter has been based on the book chapter published in Lecture Notes in Civil Engineering, Singapore, Springer.

Chapter 5 is devoted to field investigation on unreinforced and geosynthetic-reinforced unpaved test sections with the potential use of dynamic cone penetrometer and digital static cone penetrometer. Except with limited modifications in layout for consistency in the thesis, this chapter has been based on the paper in International Journal of Geosynthetics and Ground Engineering, Springer Publication.

Chapter 6 develops a model for predicting the behavior of geogrid-reinforced subgrade soil based on fuzzy logic approach and sensitivity analysis reflects a set of dominant parameters. Except with limited modifications in layout for consistency in the thesis, this chapter has been based on the paper in Transportation Infrastructure Geotechnology, Springer Publication.

Chapter 7 describes a comprehensive summary of the field tests on unpaved road test section to investigate the influence of geosynthetic reinforcement in the improvement of pavement

surface deformation under moving wheel load tests. Test results indicate significant improvement in rutting resistance and stability of reinforced test section.

Chapter 8 outlines the conclusions of the present study and highlights the major contributions to knowledge through this research and suggests potential future research paths.

References

Cancelli A, Montanelli F, Rimoldi P, Zhao A. Full scale laboratory testing on geosynthetics reinforced paved roads. *International Symposium on Earth Reinforcement* 1996, Fukuoka, pp. 573–578.

Collin JG, Kinney TC, Fu X. Full scale highway load test of flexible pavement systems with geogrid reinforced base courses. *Geosynthetics International* 1996; 3 (4), 537–549.

Cuelho EV, Perkins SW. Geosynthetic subgrade stabilization – Field testing and design method calibration. *Transportation Geotechnics* 2017; 10: 22–34. http://dx.doi.org/10.1016/j.trgeo.2016.10.002.

Das BM, Shin EC. Strip foundation on geogrid-reinforced clay: Behavior under cyclic loading. *Geotextiles and Geomembranes* 1998; 13(10), 657–666.

Giroud, JP, Han J. Design method for geogrid-reinforced unpaved roads. I. Development of design method. J. *Geotech. Geoenviron* 2004; 130(8), 775–786. https://doi.org/10.1061/(ASCE)1090-0241(2004)130.

Giroud JP, Noiray L. Geotextile-reinforced unpaved road design. *J Geotech Eng* 1981; 107 (9):1233–54.

Han J, Thakur JK. Sustainable roadway construction using recycled aggregates with geosynthetics. *Sustainable Cities and Society* 2014. http://dx.doi.org/10.1016/j.scs.2013.11.011.

Haas R, Walls J, Carroll RG. Geogrid reinforcement of granular bases in flexible pavements. *Transportation Research Report* 1988; 19–27.

Haliburton TA, Lawmaster JD, McGuffey VC. Use of engineering fabrics in transportation related applications. *Federal Highway Administration*; 1981. FHWA DTFH61-80-C-00094.

Hufenus R, Rueegger R, Banjac R, Mayor P, Springman SM, Brönnimann R. Full-scale field tests on geosynthetic reinforced unpaved roads on soft subgrade. *Geotextile and Geomembrane* 2006; 24: 21–37. https://doi.org/10.1016/j.geotexmem.2005.06.002.

Keller GR. Application of geosynthetics on low-volume roads. *Transportation Geotechnics* 2016; 8:119-131. https://dx.doi.org/10.1016/j.trgeo.2016.04.002.

Kenny MJ. The bearing capacity of a reinforced sand layer overlying a soft clay subgrade. *Sixth International Conference on Geosynthetics* 1998, vol. 2. Atlanta, pp. 901–904.

Koerner RM. Designing with geosynthetics. 5th edition, upper saddle River, 2005, New Jersey.

Maxwell S, Kim W-H, Edil TB, Benson CH. Geosynthetics in stabilizing soft subgrades with breaker run. *Wisconsin Highway Research Program*. Final Report No. 0092-45-15; 2005. p. 88.

MORTH, Addendum to ministry's technical circulars and directives on national highways and centrally sponsored road and bridge projects, New Delhi, India.

MORTH, Basic Road Statistics of India (2016-2017), New Delhi, India.

Perkins SW, Ismeik M. A Synthesis and Evaluation of Geosynthetic-Reinforced Base Layers in Flexible Pavements: Part I. *Geosynth Int* 1997;4(6):549–604.

Perkins, SW, Ismeik M, Fogelsong ML. Influence of geosynthetic placement position on the performance of reinforced flexible pavement systems. *Geosynthetics Conference* 1999, vol. 1. Boston, pp. 253–264.

Shukla SK. An introduction to geosynthetic engineering. 2016, CRC Press, London.

Shukla SK. Handbook of geosynthetic engineering. 2012, ICE Publishing, London.

Watn A, Eiksund G, Jenner C, Rathmayer H. Geosynthetic reinforcement for pavement systems: *European perspectives. In: Proceedings: Geo- Frontiers* 2005, ASCE geotechnical special publications 130- 142. Reston, VA: American Society of Civil Engineers; 2005. p. 3019–37.

Webster SL, Grau RH, Williams RP. Description and application of dual mass dynamic cone penetrometer. Vicksburg, MS, U.S. Army Engineer Waterways Experiment Station 1992. Report Number GL-92-3.

CHAPTER 2

LITERATURE REVIEW

This chapter details the excerpts from relevant literature. Published research works have been collated to reflect the existing and current practices in the relevant research area. A summary of previous work undertaken in national and international scenario in this regard is presented in this chapter.

2.1 Introduction

Geosynthetics have been successfully used to reinforce unpaved roads built on soft subgrade. Different types of geosynthetics are available in the market such as, geotextiles, geogrids, geomembranes, geonets, geocells, geocomposites, prefabricated vertical drains, and geosynthetic clay liner. Geosynthetic materials provide an economical solution for various functions such as, separation, reinforcement, filtration, drainage, barriers, containment, erosion control, and protection. Inclusion of geosynthetics in pavements reduces construction cost as well as construction time due to their ability to utilize locally available material and their ease of handling. One of the common distress in unpaved road is surface rutting, which take place when the pavement was constructed on weak subgrade and it do not have enough strength to support the traffic loads. In such situations geosynthetics can be used as a stabilization method for improvement of the serviceability of these roads by reinforcing them with geosynthetics. Subgrade stabilization is typically applicable for unpaved roads, temporary roads such as haul roads, and construction platforms to support permanent roads. These roads are generally characterised as low-volume roads that can tolerate deeper ruts under heavy vehicle trafficking. Geosynthetics placed either at the subgrade-base interface or within the granular layer may perform the desired function of separation, confinement or reinforcement. Geosynthetics, when used to serve as separation function then it will prevent the intermixing of granular material

into the subgrade soil under cyclic loading. The primary function allocated to geotextiles is separation, but the reinforcement function may be acquired from both geogrids and geotextiles (Cuelho and Perkins 2017). Sometimes, geosynthetics serve more than one function providing unique advantages. Several studies have shown the benefits of geotextile and geogrid reinforcement to improve the performance of unpaved roads (Abu-Farsakh et al., 2016; Gongora and Palmeira, 2012). Geosynthetics can offer an environmental-friendly and economical solution for geosynthetic-reinforced pavements.

2.2 Application of Geosynthetic Reinforcement in Pavements

Advantage of incorporating geosynthetic in pavements has been widely studied by researchers for subgrade stabilization and base reinforcement but the reinforcement mechanism of geosynthetics is still not fully understood. Geotextile and geogrid reinforcement are the most commonly used reinforcement materials for pavement reinforcement applications. These can be used at the base-subgrade interface or within the granular layer of pavement to increase its service life and reduce the required thickness of pavement (Giroud and Han, 2004; Saghebfar et al., 2016). Table 2.1 shows the application of geosynthetic reinforcement in pavements.

Geosynthetic reinforcement layer is installed at the interface of subgrade and base layer to serve the separation function. Intrusion of granular particles into the subgrade soil occurs under the traffic loads. The intermixing of materials at subgrade-base interface can reduce the pavement thickness which leads to the failure of pavements constructed on soft subgrade. Functional and structural integrity of granular fill and soft soil is maintained by preventing the intermixing of dissimilar materials through the geosynthetic reinforcement. Another application of geosynthetic reinforcement in pavements is stabilization of base materials. Geosynthetic are used to maintain the stiffness of the granular layer materials by placing it at the bottom of granular layer or within the aggregate base layer thickness. If geotextile is used for stabilization of base materials then interface frictional effectiveness should be properly

selected and in case of geogrid reinforcement, particle size of aggregate material and aperture size of geogrid should be properly selected (Palmeira and Gongora, 2016).

Table 2.1 Application of geosynthetics in pavements

	Application Areas		
	Separation	Stabilization of base materials	Stabilization of soft subgrade materials
Objective	Prevent the mixing of base course material with the subgrade soil	Decrease the modulus of base course material	Increase the bearing capacity of subgrade soil
Mechanism	Minimized the intrusion of aggregate particles into the subgrade	Lateral restraint mechanism	Improvement of tension membrane effect
Geosynthetic functions	Separation, Filtration	Reinforcement	Reinforcement, Filtration, Separation
Significance in road performance	Minimized the decrease in thickness of base course and maintain the quality of aggregate material	Decreases the lateral movement of aggregate material which helps in achieving better aggregate modulus and wide distribution of vertical loads	Decreased the vertical stresses in the subgrade under the wheel path

Lateral displacement of granular materials occurring under the traffic loads is a mechanism responsible for the degradation of mechanical properties of base aggregate. Higher modulus of granular layer is attained with the inclusion of geosynthetic reinforcement which helps in wider distribution of vertical loads and ultimately decreases the maximum vertical stresses assessing at the subgrade-base interface (Zornberg, 2017).

Table 2.1 presents the application of geosynthetic reinforcement is subgrade stabilization. Bearing capacity of the subgrade soil is improved with the use of geosynthetic at subgrade-base interface to achieve subgrade stabilization. Bearing capacity increases with the contribution of geosynthetic reinforcement function whereas, the stiffening function leads to decrease the lateral displacement within the base. Higher deformation are acceptable in unpaved roads and the geosynthetic acts as a tension membrane under the wheel loads. Geosynthetic develops a concave shape, so the tension develops a vertical component that directly resists against the applied vertical load (Koerner, 2005).

2.3 Literature Review

The benefits of geosynthetic reinforcement in pavement were assessed by various researchers through laboratory studies, field studies, numerical model and analytical studies. Experimental studies confirm the importance of geosynthetics in pavement by improving the performance in terms of reducing permanent surface deformation and extending their service life. Field tests performed for research purposes, generally offers better control over study variables such as proper preparation of subgrade. It is difficult to achieve uniform conditions throughout a field test utilizing the natural subgrade (Fannin and Sigurdsson, 1996; Hufenus et al., 2006). Whereas, laboratory tests can be performed more quickly with more variables and alternatives can be included. This chapter discusses and summaries the technical literature related to the experimental and field studies on geosynthetic reinforced pavements.

2.3.1 Laboratory studies

2.3.1.1 Cyclic plate load tests

Al-Qadi et al. (1994) performed laboratory experimental investigation to evaluate the performance of geosynthetics reinforced and unreinforced pavements. Four pavement test sections were constructed in a concrete box of 3.1m × 1.8m × 2.1m size to model secondary roads built over weak silty sand subgrades. The loading was accomplished using the computer controlled pneumatic actuator. The cyclic load of 40 kN was applied to the pavement sections through the steel plate of 300 mm diameter. The corresponding frequency of loading was 0.5 Hz, which resulted in a contact pressure of 550 kPa over the pavement surface. The subgrade soil of silty sand was compacted at a CBR of 2 to 4%. The thickness of base course varied from 250 mm to 200mm whereas the hot-mix asphalt thickness of 70mm was maintained constant for all the pavement sections. Two woven geotextiles of different stiffness and one geogrid were used and placed at the base-subgrade interface. It was found that geotextile and geogrid can substantially improve the performance of test section constructed on weak subgrade. In this study, reinforcing mechanism of both the geosynthetics was different. Separator function of geotextile was found to be a key parameter which proved to be more important than the reinforcement function of geogrid. The investigator also found that the geotextile stiffness does not have any influence on the pavement performance.

Som and Sahu (1999) carried out an experimental investigation on improvement in bearing capacity of geotextile reinforced unpaved road. A number of model pavements were constructed in 700mm diameter steel tank having a height of 700mm. The pavement sections were subjected to loading through the rigid circular footing of 150 mm diameter. The base course of unpaved road sections was constructed for variable thickness from 75 to 100mm while the subgrade soil of 450mm thick was maintained constant. Two types of geotextile named as woven and nonwoven were used and placed at the subgrade-base course interface.

The investigators observed the improvement in load carrying capacity for geotextile reinforced section. The observed mobilized bearing capacity factor was found to be in good agreement with the studies reported by Giroud and Noiray (1981).

Tingle and Jersey (2005) investigated the influence of geotextile and geogrid reinforcement in unbound aggregate road sections constructed over soft subgrade soil. The pavement sections were constructed in a large steel box of 1.83m × 1.83m × 1.37m deep. Before the pavement construction, the test box was lined with plastic membranes, to impede the moisture loss. Six model pavement sections of varying base course and subgrade thickness were constructed. Cyclic plate load tests were conducted on road sections to evaluate their performance under simulated truck traffic. The investigators observed improvement in resistance to deformation for all the reinforced pavement sections. The thicker reinforced pavement does not show the greater influence of reinforcement as seen in thin reinforced pavement. The investigators further concluded that the geotextiles improvement was attributed to the separation than to reinforcement via tensioned membrane effect.

Palmeira and Antunes (2010) studied the use of nonwoven geotextile and geogrid to reinforce unpaved roads on poor subgrade. The reinforcing layers were installed at the fill-subgrade interface and large equipment was used to perform the tests under cyclic loading. The tests were performed under three loading stages and it was carried out to a maximum rut depth of 25mm. The fill surface was repaired at the end of a loading stage. Presence of both the geosynthetic reinforcement increases the number of load cycles required for the established rut depth to be achieved. It was found that the TBR value lies in between 2.3-9.2, depending on the loading stage and type of reinforcement. The geogrid reinforcement was more efficient than the geotextile reinforcement in restraining lateral movement of the fill material along with the gain in fill passive resistance. The presence of reinforcement layer increased the load spreading

angle from 25° for the unreinforced road to 43° for geotextile reinforced road and 48° for the geogrid reinforced roads.

Abu-Farsakh and Chen (2011) evaluated the performance of geogrid base reinforcement in flexible pavements using cyclic plate load testing. Test sections were constructed inside a steel test box with dimensions of 2m × 2m ×1.7m. A 40kN cyclic load was applied through a 305mm diameter steel plate. Aperture size of geogrid, location of geogrid, and tensile modulus of geogrid were selected as parameters for model tests. Stress distribution, permanent vertical strain and developed pore water pressure in the subgrade, and the strain distribution along the geogrid were also investigated. Test results showed that the inclusion of geogrid base reinforcement can significantly improve the performance of flexible pavement and traffic benefit ratio can be increased up to 15.3 at a rut depth of 19.1 mm. The optimal location of geogrid reinforcement was found to be at the upper one-third of the granular layer. Presence of geosynthetic reinforcement within the granular layer helps in reducing permanent deformation in the subgrade through the wider distributing of load on top of the subgrade layer.

Gongora and Palmeria (2012) carried out tests on unreinforced and geogrid reinforced unpaved roads using a large-scale apparatus aiming to simulate field condition under cyclic loading. Recycled rubble and gravel were used as fill materials and obtained from the construction and demolition works. Geogrid was placed at the fill-subgrade interface with its extremity folded and embedded up to 250 mm length in the fill material to increase reinforcement anchorage strength. The presence of reinforcement significantly increased the number of load repetitions sustained by the road. The performance of a geogrid reinforced road was a function of geogrid tensile stiffness and aperture stability modulus.

Qian et al. (2013) investigated the performance of geogrid reinforced bases at different base thicknesses over weak subgrade under cyclic loading tests. Laboratory cyclic plate load tests

were conducted in a large geotechnical testing box of 2m × 2.2m × 2m on unreinforced and reinforced bases at the University of Kansas. The test investigates the influence of geogrid on permanent deformation and vertical stresses at the base-subgrade interface. Geogrids significantly reduced the maximum vertical stress on the subgrade and resulted in a more uniform stress distribution as compared with the unreinforced bases. The key mechanism responsible for the improvement of the reinforced base course was confinement provided by the geogrid-aggregate interlocking.

Ravi et al. (2014) carried out a series of model-scaled cyclic load tests to understand the performance of reinforced unpaved roads. Geosynthetic reinforcement layer was placed on the prepared subgrade surface and the sub-base was placed over it and all the tests were performed with varied thickness of aggregate layer and strength of subgrade soil. The test results indicate that with the provision of reinforcement the settlement of the road bed has reduced substantially. The improved performance was dependent on the strength and stiffness of the subgrade and it was found to be more when the subgrade was relatively weak. The thickness of the aggregate layer can be reduced by 50% with the provision of reinforcement.

Sun et al. (2015) evaluated the influence of the geogrid on the resilient deformation and radial stresses of the aggregate bases and subgrade. Nine test sections were prepared in a geotechnical test box of 2.2m × 2m × 2m. A cyclic plate load was applied through a 0.3m diameter plate on aggregate bases of varied thicknesses of 0.15m, 0.23m, and 0.3m. The intensity of load increased from 5kN-50kN with an increment of 5kN and surface permanent deformation greater than 75mm was considered as failure. The permanent and resilient deformations on the subgrade and surface was monitor by a displacement transducer. Whereas, pressure cells were installed to monitor radial and vertical stresses within the granular and subgrade layers. Test results showed that geogrid stabilized sections had greater resilience than

the unstabilized sections. The lateral confinement of the geogrid changed the stress distribution of the radial stress and confined it into a smaller area close to the center of the load plate.

Abu-Farsakh et al. (2016) performed cyclic plate load test to quantify the benefits of geosynthetics for enhancing the performance of pavement constructed over soft subgrade. Six test sections were constructed inside a 2m × 2m × 1.7m test box with varying types and layers of geosynthetics and base thickness. A variety of sensors were installed for each section to measure the load-associated pavement response and performance. Inclusion of geosynthetic significantly reduced the pavement rutting. The test sections reinforced with double layer of reinforcement performs much better than all other test sections. The instrumentation measurements indicate the geosynthetics placed at the base-subgrade interface function more as stabilization of weak subgrade soil than as base aggregate reinforcement.

Nair and Latha (2016) studied the laboratory repeated plate load tests on unreinforced and reinforced model sections of unpaved road. Test results discussed the effect of type and form of reinforcement on the stress-strain hysteresis of unpaved road sections. Reinforced sections shows higher load resistance and developed less plastic settlements as compared to the unreinforced sections. The load-deformation behavior shows that unreinforced section could bear a pressure of 253 kPa beyond which the settlements were very high even for a slight increase in load. The load-deformation response shows that the benefit of geogrid reinforcement was evident only after a settlement of 3mm. The stronger geogrid performs better than a weaker geogrid because the stronger geogrid sustained the applied bearing pressure with less settlement due to its higher stiffness.

Suku et al. (2017) examined the performance of geogrid reinforced unpaved sections at higher stresses in order to achieve the objective of reducing the thickness of base layer required in the field. Optimum depth of geogrid reinforcement in granular base layer was determined

through experimental studies using repeated plate load tests. The plate load tests were carried out in a tank size of 1.5m × 1.5m × 1m. For this study, the optimum depth of placing the geogrid in order to minimize the permanent deformation was found to be 50mm. Placing of the geogrid at optimum depth reduced the permanent deformation by 40%. Inclusion of reinforcement reduced the permanent deformation by at least 50% in all the reinforced and unreinforced sections of different thicknesses. Geogrid effectively reduced the pressure on top of the subgrade by 66% when compared to unreinforced section of similar thickness.

2.3.1.2 California Bearing Ratio (CBR) tests

Kamel et al. (2004) investigated the beneficial effects of reinforcing subgrade soils with geogrid and their behavior under static and cyclic loading. California Bearing Ratio, static triaxial and unconfined compression tests were conducted on soil samples reinforced with geogrid at different depths within the sample height. The geogrid was placed in a single layer at different positions, namely 20%, 40%, 60%, and 80% of the specimen height from the top surface. The results indicate that the maximum effect of geogrid reinforcement was obtained when reinforcement layer was placed at 72 to 76% height of the specimen from the top surface. At the optimum position of reinforcement, CBR value of subgrade soil increases by 50 to 100% depending on the stiffness of geogrid and type of the subgrade soil. Stiffness of geogrid played an important role in control of rutting in pavement system.

Williams and Okine (2008) investigated the change in strength characteristics of different granular base materials reinforced with geogrid. Standard proctor compaction tests and CBR tests were performed on the subgrade soil with and without geosynthetic materials. Geogrid reinforcement was placed at the middle half of the subgrade soil specimen. Inclusion of geosynthetic material in subgrade soils improved the strength of soil and increased the load carrying capacity of soils. Soil with low *CBR* had higher benefits in terms of improved strength than those with higher in-situ *CBR* values.

Nagrale et al. (2010) studied the experimental program to investigate the effect of geosynthetic reinforcement on poor subgrade soil. CBR tests were conducted on unreinforced and reinforced subgrade soil with single layer of geogrid placed at 20%, 40%, 60%, and 80% of the specimen height from the top surface. CBR value was increased considerably to 50-100% with the inclusion of geogrid reinforcement. The improvement in the performance depends on the type of soil and geogrid stiffness. The highest increase in CBR value was achieved when the geogrid was embedded at 80% of the specimen height from top. Geogrid reinforcement was more useful when used with the weaker subgrade soil than the strongest one.

Nair and Latha (2010) carried out CBR tests on unreinforced and reinforced soil-aggregate system for determining the equivalent California bearing ratio of the composite system. The objective was to understand the effect of anchorage and type of reinforcement on the bearing resistance of soil-aggregate system. Geotextile, biaxial geogrid, and geonet were used in this study as geosynthetic reinforcement. Five experiments were carried in conventional CBR mould of 150mm diameter with 175 mm height and eight experiments were carried in the modified CBR mould of 300 mm diameter. For preparing the soil-aggregate system, lower half of the mould was filled with subgrade soil and aggregates were filled in the collar of 50mm height. Geosynthetic reinforcement layer was placed at the aggregate –subgrade interface. Test results showed that reinforced soil-aggregate systems performed better than the unreinforced soil-aggregate system. Among the three geosynthetics used in this study, geonet was not effective as reinforcement because of its low tensile strength. Anchorage of geosynthetic reinforcement did not provide any benefit to the reinforced soil-aggregate system.

Rajesh et al. (2016) carried out CBR tests for determining the index and engineering properties of different types of soil subgrade reinforced with geogrid. CBR tests were carried out on all unreinforced and reinforced soil sample in the laboratory and field with the inclusion

of geogrid at mid-height of soil specimen. Field CBR test was conducted in the test pit of size 0.5m × 0.5m × 0.5m. The loading was applied using reaction loading technique supported by the truck. Same variation in the moisture content has been observed for both unreinforced and reinforced specimens after soaking condition irrespective of the presence of geogrid. CBR value of the subgrade soil was increased substantially with the inclusion of geogrid. Plasticity of soil and percent fines influences the index properties and compaction characteristics. The tensile stiffness and soil-geosynthetic interaction was responsible for soil's resistance to penetration. Higher CBR values were observed for higher geogrid capacities and lower fines content.

2.3.1.3 Accelerated pavement testing

Collin et al. (1996) performed a full-scale laboratory loading test program that used a 20 kN moving wheel load to determine the benefits of using geogrid at the subgrade-base interface of a flexible pavement. Four model road sections were constructed in the long box of dimension 14.6m × 2.4m × 1.2m. Out of these four model sections, one was unreinforced section which served as control section, two sections were reinforced with geogrid at the subgrade-base interface, and fourth section was reinforced with two layers of geogrid, one at the subgrade-base interface and second layer placed within the aggregate base. The speed of the wheel was maintained to 1.2 m/s. Test results demonstrated that the presence of geogrid at the subgrade-base interface substantially enhances the pavement performance and decreased the initial pavement deformations. The maximum values of traffic benefit ratio were developed at surface deflections of 25mm or less for base thickness greater than 250mm. But for thinner base thickness, the maximum values were reached after greater deflections.

Tang et al. (2008) identified the mechanical and physical properties of geogrid that are critical to their effectiveness in the stabilization of pavement subgrade. This study focused on correlating these properties of geogrid with the results of bench-scale testing and accelerated

pavement testing. Accelerated testing was conducted on the geogrid reinforced pavement sections using the one-third scale model mobile load simulator (MMLS3). The load exerted by each wheel of MMLS3 was 2.7kN, with a corresponding tyre pressure of 621kPa. Two sets of accelerated pavement testing were performed for a different subgrade CBR value of 3 and 1.5. Aperture size, tensile strength at small strain, junction strength and flexural rigidity were recognized as the most important attributes of geogrid in pavement subgrade stabilization.

Al-Qadi et al. (2012) performed a full scale accelerated pavement test on a full-scale instrumented pavement section. The study was conducted to quantify the effectiveness of geogrid in low-volume flexible pavements and to specify the optimal location of geogrid installation in a low volume pavement system. Nine test sections were constructed divided in to three categories based on the total thickness of pavement system, hot-mix asphalt layer thickness, geogrid stiffness and its location. The Accelerated Transportation Loading Assembly (ATLAS) was used to apply the loading to the pavement sections through the moving wheel load. The experimental program consisted of response testing with different loading criteria. Response testing parameters included three wheel loads of 26, 35, and 44 kN, three tire pressures of 550, 689, and 758 kPa, and two tire speeds of 8 and 16km/h. The study found that loading wander is significant near the surface and becomes negligible as the pavement depth decreases. Inclusion of geogrid reduced the granular base shear flow in the traffic direction and in thin pavements. The optimal location for installing geogrids in pavements was in the upper one-third of the layer and additional geosynthetic layer was needed at the subgrade-base interface for the stability.

Wu et al. (2015) investigated the effect of geogrid reinforcement on unbound granular pavement base material through Loaded Wheel tester (LWT). Three unbound granular materials were utilized to evaluate the reinforcement effects of four types of geogrids with different apertures and stiffness. In the LWT test, the compacted base course specimens were

tested under the repeated wheel loading and the rut depths of the base specimen were measured along the loading path. The LWT results were also compared to those from a traditional cyclic axial load plate test on the same materials. The result shows that the LWT test was an effective method to characterize the reinforcement effects of different combination of geogrids and base courses. Traffic Benefit Ratio (TBR), Rutting Reduction Ratio (RRR), and Rate of Deflection (ROD) were determined for the evaluation of the potential contribution of geogrid reinforcement. All the reinforced river sand and gravel base courses exhibited significant improvement in rutting resistance comparing to the unreinforced base courses.

Saghebfar et al. (2016) assessed the effectiveness of geotextile reinforcement on pavement design through full-scale accelerated pavement testing. Six test lane sections were constructed and each test section had a length of 3.05m in the direction of moving axle and width of 4.9m in perpendicular direction to the traffic. One control test section and five geotextile reinforced test sections were subjected to full-scale accelerated pavement testing. A variety of sensors were used in the instrumented test sections to measure load-associated pavement response. Test sections were loaded to 250000 to 400000 repetitions of an 80-kN single axle load. Results showed that reinforced test sections outperformed the control test section in terms of rutting with similar cross-sections. Permanent deformation accumulated with an increased number of load cycles. During the early stage of loading, rutting increased quickly but later rutting decreased with an increased number of load cycles.

Ingle and Bhosale (2017) developed a full-scale laboratory accelerated pavement testing set up for examining the behavior of unreinforced and geotextile reinforced unpaved road. Full-scale unreinforced and geotextile reinforced unpaved road were subjected to 35000 loading cycles of standard axle load. Test result shows that the inclusion of geotextile reinforcement significantly reduced the magnitude of vertical stress in the reinforced road due to the lateral restraint reinforcement mechanism for limited number of load cycles. This study confirmed

about 22% reduction in base course thickness for the tested 35000 cycles due to geotextile reinforcement. Also, observed the improvement in effective CBR of subgrade soil due to the inclusion of geotextile that may be used to design the pavement. Table 2.2 presents the details of accelerated pavement testing facility.

Table 2.2 Details of accelerated pavement testing (APT) facility

References	APT Facility dimensions (m)	Applied load	Geosynthetic	Loading cycles	Location
Collin et al., 1996	14.6×2.4×1.2	20 kN	Stiff biaxial geogrids	1014 to 40,000 loading cycles	University of Alaska
Qian and Han, 2013	2.0×2.2×2.0	40 kN	Triangular aperture geogrid	1700 loading cycles	University of Kansas
Al-Qadi et al., 1994	3.1×1.8×2.1	40 kN	Woven geotextile and geogrid	800 to 1600 loading cycles	University of Illinois, Urbana-Champaign
Wu et al., 2015	0.6×0.4×0.1	0.35 kN	Four types of geogrids with different apertures and stiffness	16,000 loading cycles	University of Tennessee, Knoxville
Saghebfar et al., 2016	3.05×4.9×0.3	80 kN	Geotextile	250,000 to 400,000 loading cycles	Kansas State University, Kansas
Ingle and Bhosale, 2017	2×3.75×0.97	80 kN	Woven geotextile	35,000 loading cycles	-

2.3.2 Field studies

Fannin and Sigurdsson (1996) described the construction, instrumentation, and response to vehicle trafficking of an unpaved road on soft ground by a vehicle of standard axle loading. Five test sections of an unpaved road were constructed which comprised of one unreinforced section, three sections reinforced with different geotextiles, and a section with geogrid reinforcement. Inclusion of geosynthetic at the base-subgrade soil interface led to a significant improvement in trafficability. The improvement in reinforced sections was greatest for the thinner base course layers of 0.25 m and diminished with increasing base layer thickness. Rut depth of 20 cm was recorded in a program of controlled trafficking to a total of 500 cumulative passes. Geotextiles outperformed the geogrid on the thinner base course layer, for which separation appears to be the dominating function. Whereas, geogrid outperformed the geotextiles on the thicker base course layers for which reinforcement was the dominating function rather than separation. Reinforcement function comes to play on the thicker base course layer, where an efficient mobilization of tensile strength depends on both stiffness and interlocking effect.

Hufenus et al. (2006) investigated the full-scale field performance of geosynthetics reinforced unpaved roads on soft subgrade soil. The test track was constructed adjacent to an existing road, with a length of about 130 m. The test track was divided in to 12 fields of length 8.0m. Out of the total fields, two were the preliminary test fields where only a separator was laid and other fields were reinforced with geogrids, woven and nonwoven geotextiles. The pavement sections were loaded through the truck comprised of front and rear axle of 30 cm wide truck tires with 850 kPa tire pressure. The subgrade CBR was maintained in between 3 to 4%. The investigators found the significant improvement in bearing capacity for geosynthetics pavement with thin base course and weak subgrade soil of CBR less than 2%, whereas the influence of it was marginal for stronger subgrade and thicker base course layer. The combined

effect of geogrid and geotextile was found to reduce the optimal interlocking with coarse grained soil; this resulted in sliding of geogrid on the geotextile.

Latha et al. (2010) carried out the field studies on geosynthetics reinforced unpaved roads constructed on weak subgrade. Total seven unpaved road section were constructed of 2m × 1m. One section was kept as a control section and others were reinforced with geotextile, uniaxial and biaxial geogrid and geocell. The geosynthetic reinforcement was placed at the base subgrade interface of the unpaved road. The single cylinder scooter of 1235mm wheel base and load of 106 kg was used to apply the traffic loading over the pavement sections. The investigators observed performance of pavement sections in terms of sustaining the numbers of vehicle passes for same rut depth. The geotextile and geogrid reinforced sections sustained 100 and 250 vehicle passes respectively whereas control section was able to stand only for 17 vehicle passes. In case of geotextile reinforced unpaved section, the improvement was obtained through the separation followed by tension membrane effect, whereas the biaxial geogrid performed better than the geotextile sections because of the interlocking mechanism. The biaxial geogrid provided greater stiffness to the road section.

Tang et al. (2015) performed full-scale moving wheel load tests to six heavily instrumented test sections built over native soft Louisiana soil. The objective of this study was to quantify the benefits and assess the effectiveness of geosynthetic for reinforcing/stabilizing pavements. Each test section was 24m long and 4m wide and instrumented by a variety of sensors to measure the load- and environment-associated pavement responses and performance. Accelerated load facility applied unidirectional trafficking to the test sections with a nominal speed of 16.8Km/h. Test results demonstrated the contribution of geosynthetic reinforcement-stabilization in reducing the permanent deformation in the pavement system. An important finding was that the majority of the permanent deformation of the surface was attributed to the

aggregate base layer instead of the soft subgrade soil. The permanent strain developed in the geosynthetic was around 0.2% at the end of the accelerated load facility.

Chen et al. (2018) evaluated the benefits of using geosynthetics for enhancing the performance of pavement constructed on soft subgrade. Six full-scale test sections were constructed by using geogrid and high strength geotextile to reinforce the base layer and stabilize the weak subgrade soil. These test sections were instrumented by a variety of sensors to measure the load- and environment-associated pavement response and performance. Results of the full scale accelerated load testing demonstrated the benefits of geosynthetics in significantly reducing the total permanent deformation in the pavement structure. The geosynthetic benefit to reducing the maximum stress on top of the subgrade is more distinguishable at a higher load level. When geosynthetic was placed at the base-subgrade interface was able to improve the performance of both subgrade and base layers. The performance of base layer was further enhanced by placing an additional layer of geosynthetic at the upper one-third of the base layer.

Imjai et al. (2019) studied the performance of geosynthetic as reinforcement in flexible pavements through a series of full-scale trials carried out at Thailand. Geosynthetics were embedded at different pavement depths in four test sections and the structural response was monitored by using pressure sensors, strain gauges, deflection plates and deflection points. The result shows the reduction in the vertical static stress developed at the base of the pavement by 66% and 72% for dynamic stresses. The presence of reinforcement layer near to the base helps in reducing the lateral spreading and experiences the highest lateral strain of 0.13%. All reinforcement configurations helped in improving the rut resistance with maximum traffic benefit ratio of 13.7, minimum rutting reduction ratio of 0.74 and effectiveness ratio of 12.7. The performance of geosynthetic as pavement reinforcement depends on the material characterization such as reinforced position, tensile stiffness and elongation.

2.3.2.1 Dynamic cone penetrometer (DCP) equipment

Dynamic cone penetrometer is one of the lowest cost alternatives for characterization of pavement layer qualities. This instrument has been extensively used in the past literature for evaluating the penetration resistance in granular base course and subgrade layers of pavement because of its ease to operate and analyze the DCP data.

Chen et al. (1999) analyzed the falling weight deflectometer (FWD) data and DCP data from six Kansas Department of Transportation pavement projects to develop a relationship between the DCP values and FWD-backcalculated subgrade moduli. Developed model provides a new approach towards interpreting DCP test results that were consistent and reliable for pavement evaluation and design applications.

Gabr et al. (2000) investigated the potential use of DCP data for evaluating the pavement distress state. A model was developed to predict the distress level and validated using the field data from four test sites located in Davidson Country. DCP tests were performed at the testing stations of dimension 600mm × 600mm. proposed model predict the pavement condition rating index based on the coupled contribution of the subgrade and the ABC materials. Condition rating index value was found to be 4 and 3 for unconfined PR-ABC values less than 4mm/blow, PR-subgrade values less than 25mm/blow, as well as an ABC thickness exceeded 152mm.

Kwon and Tutumluer (2009) discuss the benefits of using geogrid for improving the performance of pavement by using Dynamic Cone Penetrometer (DCP) equipment for in-situ evaluation of unreinforced and geogrid-reinforced pavements. Full-scale pavement test results showed the performance benefits of using geogrids, especially in the reduced horizontal base course movements. Inclusion of geogrid reinforcement increased the base course strength and stiffness as a result of compaction during construction and subsequently caused by trafficking. It was demonstrated by the DCP evaluation test that geogrid-reinforced test sections were much

stiffer than the unreinforced test section because of the geogrid aggregate interlocking mechanism providing better pavement strength with less material.

Boutet et al. (2011) developed a model that described the relation between the strength properties of soil, the resilient properties, and the penetration index values obtained from the dynamic cone penetrometer test. Laboratory tests were performed on five coarse-grained reconstituted soils and field tests were performed on ten fine grained soils along with four subgrade soils. Laboratory test results were compared to the field test results and analyzed in order to develop the relation between the strength and the resilience for different types of soils. The models were not recommended for coarse-grained soils with a penetration index less than 10mm/blow because these values were beyond the confidence interval of the proposed relations.

Rolt and Pinard (2014) suggested the environmentally optimized design approach for low-volume roads in which the in-situ strength of the subgrade and pavement layers were preferred to use for design rather than soaked values. It described how the assumptions and simplifications inherent the traditional CBR design approach tends to produce less than optimum solutions as compared with the DCP method. DCP method was advantageous in the designing of low-volume roads because material strength and pavement layer thickness can be obtained very quickly. It allows the engineer to design a statically reliable pavement because of the amount of data that becomes available.

Schnaid et al. (2017) developed a analytical method for the interpretation of dynamic penetration resistance from penetration tests without the need to resort to empirical factors. The principles of wave propagation and energy conservation provide the necessary background for calculating dynamic penetration resistance which was same as the static cone penetration resistance. Results concluded that the combination of static penetration tests and cone

penetration tests profiles has the greatest potential for characterizing sites correctly. Both the tests were influenced by the same soil parameters and environmental variables.

Amadi et al. (2018) studied the quality and strength of unstabilized lateritic pavement layers of a 14 km long single carriageway road under construction and monitored by the DCP tests. The dynamic cone penetrometer index values were found to be in a ranged from 3 mm/blow to 10 mm/blow for subgrade layer. The dynamic cone penetrometer index values were found to be in a ranged from 5 mm/blow to 16 mm/blow for sub-base layer. The result showed good correlation exists between the dynamic cone penetrometer index and unsoaked CBR values. Laboratory evaluation reveled that subgrade CBR values ranged from 27 % to 74 % which quantify as good to excellent subgrade materials whereas the sub-base CBR values from 15 % to 50 % and rated as poor to good sub-base. Poor quality sub-base layer attributable to poor material selection and somewhat poor compaction followed by a good quality subgrade was delineated.

2.3.3 Analytical studies

Giroud and Noiray (1981) observed the benefit of geotextile as increasing the bearing capacity of subgrade soil from elastic to the ultimate bearing capacity. Empirical formula deduced from this study was able to calculate the thickness of aggregate layer as a function of traffic and soil properties. Theoretical analysis developed the equations for geotextile reinforced and unreinforced unpaved roads and compared them. Incorporation of geotextile reinforcement, results in the reduction of aggregate layer thickness. The investigators considered the deformed shape of the geotextile as parabolic in nature and assume the pyramidal load distribution through base course layer at an arbitrary distribution angle. The theoretical analysis did not consider traffic into account. The test results were presented in the form of charts which were established by combining the empirical formula and the theoretical analysis. The thickness of

the aggregate layer can be determined from these charts for geotextile reinforced unpaved roads.

Sellmeijer (1990) developed a model to analyze the behavior of soil-geotextile-aggregate system. The model was studied, based on the combined effect of membrane action and lateral restraint function of geosynthetics. Elasto-plastic behavior of the aggregate allows the interaction between geotextile and soil to control the degree of strain. The strength and stiffness of the soil-geotextile-aggregate system were increased considerably due to the effect of lateral restraint which allows the aggregate to work as a slab. The limitation of this model was that it was suitable for the design of paved roads only because the analysis was carried out on the basis of smaller deflections. Hence, the applicability of this model was restricted to low-volume roads and parking pools.

Perkins and Edens (2003) developed a mechanistic-empirical model for geosynthetic reinforced pavements and used in a parametric study involving the analysis of 465 cases to describe the reinforcement benefits to the geometry and properties of the reinforced pavement cross-section. The model was expressed with design parameters influencing the reinforcement benefits and includes thickness of the structural section, strength of subgrade, tensile modulus of geosynthetic and few more properties of geosynthetics based on its type and structure. The model was calibrated against the test results of large-scale reinforced pavement test sections. Developed model was capable of indicating that reinforcement benefit increases with increasing tensile modulus of geosynthetic, decreasing subgrade strength and was sensitive to the pavement structural thickness. The reinforcement benefits were modeled by placing the geosynthetic at the bottom of the base aggregate layer. The limitation of the designed model was that it may not be suitable for lightly loaded traffic or for excessive heavily loaded traffic. Another limitation of this model was that it cannot account for situations where it was desired to place the geosynthetic in upper region of base aggregate layer.

Giroud and Han (2004) developed a theoretically based and empirically calibrated design method for geogrid-reinforced unpaved road that include the effect of parameters, such as interlock between geogrid and base course material, strength of base course material, in-plane aperture stability modulus of geogrid, and distribution of stresses. In addition to these parameters, this study also considered the influence of subgrade strength, traffic volume, wheel loads, rut depth, and tire pressure on the design pavement thickness. The design method was developed for geogrid-reinforced unpaved roads but it can also be used for unreinforced and geotextile reinforced unpaved roads with appropriate values of relevant parameters. The bearing capacity factors established for unreinforced roads, geotextile-reinforced roads, and geogrid-reinforced roads were 3.14, 5.15, and 5.71 respectively.

Perkins et al. (2012) developed a mechanistic-empirical model for reinforced unpaved roads and compared the model to several sets of large laboratory-scale test sections. During the development of this model, it includes a new component that accounts for the significant influence of pore water pressure generation in the subgrade. Mechanistic-empirical modeling methods previously developed for geosynthetics base reinforced flexible pavements has been applied to reinforced unpaved roads. Results from instrumented unpaved road test sections were used to calibrate and compared with the model predictions. Thicker aggregate base unreinforced test section shows the stable behavior and sustained a higher level of traffic. Reinforcement influences the induced stresses in the subgrade the most and lowers the excess pore water pressure resulting from these stress increments.

2.4 Conclusions

Based on the literature review, the following research gaps have been identified, which require further investigation:

- The performance of geosynthetics in unpaved roads through the full-scale field tests has not been extensively studied.

- Very conflicting results have appeared in literature for the position of geosynthetic as a reinforcement layer to get maximum benefits.

- Limited studies are available on the use of dynamic cone penetrometer and digital static cone penetrometer devices for performance evaluation of geosynthetic-reinforced pavements.

- No major attempt has been made to apply the fuzzy logic to model the effect of geogrid reinforcement on the strength behavior of subgrade soil.

- The complexity of geosynthetic mechanism is still not fully understood. Hence, more full-scale experimental investigations are needed to understand the governing reinforcement mechanism.

References

Abu-Farsakh MY, Akond I, Chen Q. Evaluating the performance of geosynthetic-reinforced unpaved roads using plate load tests. *International Journal of Pavement Engineering* 2016; 17:901–12. http://dx.doi.org/10.1080/10298436.2015.1031131.

Abu-Farsakh MY, Chen Q. Evaluation of geogrid base reinforcement in flexible pavement using cyclic plate load testing. *International Journal of Pavement Engineering* 2011; 12(03):275-88. DOI: 10.1080/10298436.2010.549565.

Abu-Farsakh M, Hanandeh S, Mohammad L, Chen Q. Performance of geosynthetic reinforced/stabilized paved roads built over soft soil under cyclic plate loads. *Geotext Geomembranes* 2016; 44:845–53. doi: 10.1016/j.geotexmem.2016.06.009.

Al-Qadi IL, Brandon TL, Valentine RJ, Lacina BA, Smith TE. Laboratory evaluation of geosynthetic-reinforced pavement sections. *Transp Res Rec* 1994; 25–31.

Al-Qadi IL, Dessouky SH, Kwon J, Tutumluer E. Geogrid-reinforced low-volume flexible pavements: Pavement response and geogrid optimal location. *Journal of transportation engineering* 2012; 138(9):1083-90. DOI: 10.1061/(ASCE)TE.1943-5436.0000409.

Amadi AA, Sadiku S, Abdullahi M, Danyaya HA. Case study of construction quality control monitoring and strength evaluation of a lateritic pavement using the dynamic cone penetrometer. *International Journal of Pavement Research and Technology* 2018; 11(5):530-539. https://doi.org/10.1016/j.ijprt.2018.07.001.

Boutet M, Dore G, Bilodeau J, Pierre P. Development of models for the interpretation of the dynamic cone penetrometer data. *International Journal of Pavement Engineering* 2011; 12(3):201–214. http://dx.doi.org/10.1080/10298436.2010.488727

Chen J, Hossain M, Latorella TM. Use of Falling Weight Deflectometer and Dynamic Cone Penetrometer in Pavement Evaluation. *Transportation Research Record* 1999; 1655(1):145–51.

Chen Q, Hanandeh S, Abu-Farsakh M, Mohammad L. Performance evaluation of full-scale geosynthetic reinforced flexible pavement. *Geosynthetics International* 2018; 25(1):26-36. https://doi.org/10.1680/jgein.17.00031

Collin JG, Kinney TC, Fu X. Full scale highway load test of flexible pavement systems with geogrid reinforced base courses. *Geosynthetics International* 1996; 3(4):537-49.

Cuelho EV, Perkins SW. Geosynthetic subgrade stabilization – Field testing and design method calibration. *Transportation Geotechnics* 2017; 10:22–34. http://dx.doi.org/10.1016/j.trgeo.2016.10.002.

Duncan-Williams E, Attoh-Okine NO. Effect of geogrid in granular base strength - An experimental investigation. *Construction and Building Materials* 2008; 22:2180–4. doi: 10.1016/j.conbuildmat.2007.08.008.

Fannin RJ, Sigurdsson O. Field Observations on Stabilization of Unpaved Roads with Geosynthetics. *J Geotech Eng* 1996; 122:544–53. doi:10.1061/(ASCE)0733-9410(1996)122:7(544).

Gabr BMA, Hopkins K, Coonse J, Hearne T. DCP Criteria for Performance Evaluation of Pavement Layers. *Journal of Performance of Constructed Facilities* 2000; 14:141–148.

Giroud JP, Han J. Design Method for Geogrid-Reinforced Unpaved Roads. I. Development of Design Method. *Journal of Geotechnical and Geoenvironmental Engineering* 2004; 130 (8): 775–786. DOI: 10.1061/(ASCE)1090-0241(2004)130:8(775).

Giroud J P, Noiray L. Geotextile-reinforced unpaved road design. *J Geotech Eng* 1981;107(9):1233-54.

Góngora IAG, Palmeira EM. Influence of fill and geogrid characteristics on the performance of unpaved roads on weak subgrades. *Geosynth Int* 2012; 19:191–9. doi:10.1680/gein.2012.19.2.191.

Hufenus R, Rueegger R, Banjac R, Mayor P, Springman SM, Brönnimann R. Full-scale field tests on geosynthetic reinforced unpaved roads on soft subgrade. *Geotext Geomembranes* 2006; 24:21–37. doi: 10.1016/j.geotexmem.2005.06.002.

Imjai T, Pilakoutas K, Guadagnini M. Performance of geosynthetic-reinforced flexible pavements in full-scale field trials. *Geotextiles and Geomembranes* 2019; 47:217-229. https://doi.org/10.1016/j.geotexmem.2018.12.012.

Ingle GS, Bhosale SS. Full-Scale Laboratory Accelerated Test on Geotextile Reinforced Unpaved Road. *Int. J. of Geosynth. and Ground Eng* 2017; 3:33. DOI: 10.1007/s40891-017-0110-x.

Kamel MA, Chandra S, Kumar P. Behaviour of subgrade soil reinforced with geogrid. *Int J Pavement Eng* 2004; 5:201–9. doi:10.1080/1029843042000327122.

Koerner RM. Designing with geosynthetics. 5th edition, upper saddle River, 2005, New Jersey.

Kwon J, Tutumluer E. Geogrid Base Reinforcement with Aggregate Interlock and Modeling of Associated Stiffness Enhancement in Mechanistic Pavement Analysis. *Transportation Research Record* 2009; 2116:85–95.

Latha G, Nair A, Hemalatha M. Performance of geosynthetics in unpaved roads. *International journal of geotechnical engineering* 2010; 4(3):337-49. DOI: 10.3328/IJGE.2010.04.02.337-349.

Nagrale, P.P., Sawant, P.H., Pusadkar, S.S.: Laboratory investigation of reinforced sub grade soils. Indian Geotechnical Conference, GEOtrendz. 637–640 (2010).

Nair AM, Latha GM. Repeated load tests on geosynthetic reinforced unpaved road sections. *Geomechanics and Geoengineering* 2016; 11(2):95-103. DOI: 10.1080/17486025.2015.1029012.

Nair AM, Latha GM. Modified CBR Tests on Geosynthetic Reinforced Soil-aggregate Syatems. Indian Geotechnical Conference-2010, GEOtrendz, 16-18 December 2010, IGS Mumbai Chapter & IIT Bombay, pp. 297-300.

Palmeira EM, Antunes LGS. Large scale tests on geosynthetic reinforced unpaved roads subjected to surface maintenance. *Geotext Geomembranes* 2010; 28:547–58. doi: 10.1016/j.geotexmem.2010.03.002.

Palmeria EM, Gongora IAG. Assessing the Influence of Some Soil-Reinforcement Interaction Parameters on the Performance of a Low Fill on Compressible Subgrade. Part I: Fill Performance and Relevance of Interaction Parameters. *International Journal of Geosynthetics and Ground Engineering* 2016; 2(1): 1–17.

Perkins SW, Christopher BR, Lacina BA, Klompmaker J. Mechanistic-Empirical Modeling of Geosynthetic-Reinforced Unpaved Roads. *International Journal of Geomechanics* 2012; 12 (4): 370–380. DOI: 10.1061/(ASCE)GM.1943-5622.0000184.

Perkins SW, Edens MQ. A Design Model for Geosynthetic-reinforced Pavements. *International Journal of Pavement Engineering* 2003; 4(1): 37-50. DOI: 10.1080/1029843031000097562.

Qian Y, Han J, Pokharel SK, Parsons RL. Performance of triangular aperture geogrid-reinforced base courses over weak subgrade under cyclic loading. *Journal of Materials in Civil Engineering* 2013; 25(8):1013-21. DOI: 10.1061/(ASCE)MT.1943-5533.0000577.

Rajesh, U., Sajja, S., Chakravarthi, V.K.: Studies on engineering performance of geogrid reinforced soft subgrade. *Transp. Res. Procedia* 2016; 17: 164–173. https://doi.org/10.1016/j.trpro.2016.11.072.

Ravi K, Dash SK, Vogt S, Braeu G. Behaviour of geosynthetic reinforced unpaved roads under cyclic loading. *Indian Geotechnical Journal* 2014; 44(1):77-85. DOI: 10.1007/s40098-013-0051-9.

Rolt J, Pinard MI. Designing low-volume roads using the dynamic cone penetrometer. Transportation 2016; 169:163-172.

Saghebfar M, Hossain M, Lacina BA. Performance of geotextile-reinforced bases for paved roads. *Transportation Research Record* 2016;2580(1):27-33.

Schnaid F, Lourenço D, Odebrecht E. Interpretation of static and dynamic penetration tests in coarse-grained soils. *Geotechnique Letters* 2017; 7:1–6. http://dx.doi.org/10.1680/jgele.16.00170

Sellmeijer JB. Design of geotextile reinforced paved roads and parking areas. Proceedings of the Conference Geotextiles, Geomembranes and Related Products 1990; (pp. 177-182).

Som N, Sahu RB. Bearing capacity of a geotextile-reinforced unpaved road as a function of deformation: a model study. *Geosynthetics International* 1999;6(1):1-7.

Suku L, Prabhu SS, Babu GLS. Effect of geogrid-reinforcement in granular bases under repeated loading. *Geotextiles and Geomembranes* 2017; 45 (4): 377–389. doi.org/10.1016/j.geotexmem.2017.04.008.

Sun X, Han J, Kwon J, Parsons RL, Wayne MH. Radial stresses and resilient deformations of geogrid-stabilized unpaved roads under cyclic plate loading tests. *Geotextiles and Geomembranes* 2015; 43(5): 440-449. http://dx.doi.org/10.1016/j.geotexmem.2015.04.018.

Tang X, Abu-Farsakh M, Hanandeh S, Chen Q. Performance of reinforced–stabilized unpaved test sections built over native soft soil under full-scale moving wheel loads. *Transportation Research Record* 2015; 11(1):81-9.

Tang X, Chehab GR, Palomino A. Evaluation of geogrids for stabilising weak pavement subgrade. *International Journal of Pavement Engineering* 2008; 9(6):413-29. DOI: 10.1080/10298430802279827.

Tingle JS, Jersey SR. Cyclic Plate Load Testing of Geosynthetic-Reinforced Unbound Aggregate Roads. *Transportation Research Record* 2005; 1936:60–69.

Wu H, Huang B, Shu X, Zhao S. Evaluation of geogrid reinforcement effects on unbound granular pavement base courses using loaded wheel tester. *Geotextiles and Geomembranes* 2015; 43 (5): 462–469. doi.org/10.1016/j.geotexmem.2015.04.014.

Zornberg JG. Functions and applications of geosynthetics in roadways. *Procedia engineering* 2017; 189: 298-306. https://doi.org/10.1016/j.proeng.2017.05.048

CHAPTER 3

STRENGTH ENHANCEMENT OF THE SUBGRADE SOIL WITH GEOSYNTHETIC REINFORCEMENT LAYERS

This chapter is based on the paper published in Transportation Geotechnics, Elsevier, as listed in Section 1.6. The details are presented here with some changes in the layout in order to maintain a consistency in the presentation throughout the thesis.

3.1 Introduction

In the current construction practice, the geosynthetic layers are often utilized for improving the weak/unsuitable soil subgrade for paved and unpaved roads. The geosynthetic layer as a reinforcement can be used effectively to reinforce the unpaved road built on soft soil subgrades, resulting in increased life of the road. The benefits obtained from the use of geosynthetic layers in unpaved roads can be observed not only with respect to performance and durability but also with respect to construction and economy (Shukla, 2002). The concept of using geosynthetic as reinforcement in paved/unpaved road construction started in the 1970s. Since then, many experimental and numerical studies have been reported in the literature to evaluate the benefits of using the geosynthetics in road construction (Al-Qadi et al., 1994; Vinod and Minu, 2010). Due to the successful application of geosynthetics in roads, different types of geosynthetics have been developed worldwide and their market is steadily growing.

Several researchers have shown the benefits of geosynthetic reinforcement in unpaved roads over weak subgrades to improve their performance (Giroud and Noiray, 1981; Fannin and Sigurdsson, 1996; Som and Sahu 1999; Hufenus et al., 2006). The position of the reinforcement layer in the subgrade also influences the performance of the road (Perkins and Ismeik, 1997; Raymond and Ismail, 2003; Subaida et al., 2009). Several field trials and full-scale laboratory investigations have illustrated that the geosynthetics used to reinforce the

unpaved roads on soft ground facilitate confinement, reduce the depth of ruts, improve load-bearing capacity, extend the service life and reduce the necessary fill thickness (Farsakh and Akond, 2016; Farsakh et al., 2016; Hufenus and Rueegger, 2006; Gongora and Palmeira, 2012). Relatively thicker pavement sections and base-course layers indicate that more material is required for construction, and therefore it increases the cost. Geosynthetics have been used as an alternative to reduce the cost of these materials and improve the performance of reinforced road sections. Some studies have been carried out to quantify the benefit of using the geogrid base reinforcement (Farsakh et al., 2012). Initial cost and maintenance cost of reinforced road section has been an important factor which should be considered for evaluating the benefits of geosynthetic reinforcement. Palmeira and Antunes, (2010) have shown that the presence of geosynthetic reinforcement in unpaved road reduces the maintenance cost which yields to the important savings in the overall cost of the road construction.

The behaviour of the road surface depends on the strength of the fill material and the subgrade of the pavement. The strength of the subgrade is most often expressed in terms of the California Bearing Ratio (*CBR*), which is the ratio of test load to standard load at a specific penetration, by a standard plunger (IS: 2720 (part 16) – 1987). Many functions of geosynthetics have been reported such as separation, reinforcement, filtration, drainage, fluid barrier and protection (Shukla, 2016). One of the important applications of geosynthetics is reinforcement which is used to improve the strength of weak soil, that is to increase in *CBR* of soils (Adams et al., 2015; Choudhary et al., 2012; Kuity and Roy, 2013; Rajesh et al., 2016). The soils with low *CBR* value have higher benefits of geosynthetic reinforcement in terms of improved strength than those soils with higher *CBR* values (Williams and Okine, 2008). The improvement in subgrade performance can facilitate compaction, reduces the aggregate layer thickness, delay rut formation and extend the service life of unpaved roads, particularly in cases of very soft subgrades with *CBR* value less than three (Hufenus et. al., 2006). In the literature

very conflicting results have appeared for the position of geosynthetic as a reinforcement layer. Some researchers believe that the maximum effect of reinforcement layer is obtained when geosynthetic is placed near the load or at bottom half of the height of specimen in the CBR mould, while others have found that placing the geosynthetic reinforcement at the centre of the CBR mould is most beneficial (Kamel et al., 2004).

This work presents a study on the use of three different types of geosynthetics as the reinforcement at different depths within the subgrade soil for improvement of its *CBR* value. The main objective of research is to investigate the optimum position of geosynthetic reinforcement layer within the subgrade soil thickness, which has not been given due attention in the past.

3.2 Materials Used

3.2.1 Subgrade soil

The soil used in the present research was locally available soil obtained from the campus of Delhi Technological University, Delhi. The soil is classified as silty sand (SM) using the particle-size analysis and Atterberg limit tests as per Indian Soil Classification System (IS: 2720). The particle-size distribution curve of the soil is shown in Fig. 3.1. The basic properties of the soil are also determined in the laboratory and they are given in Table 3.1.
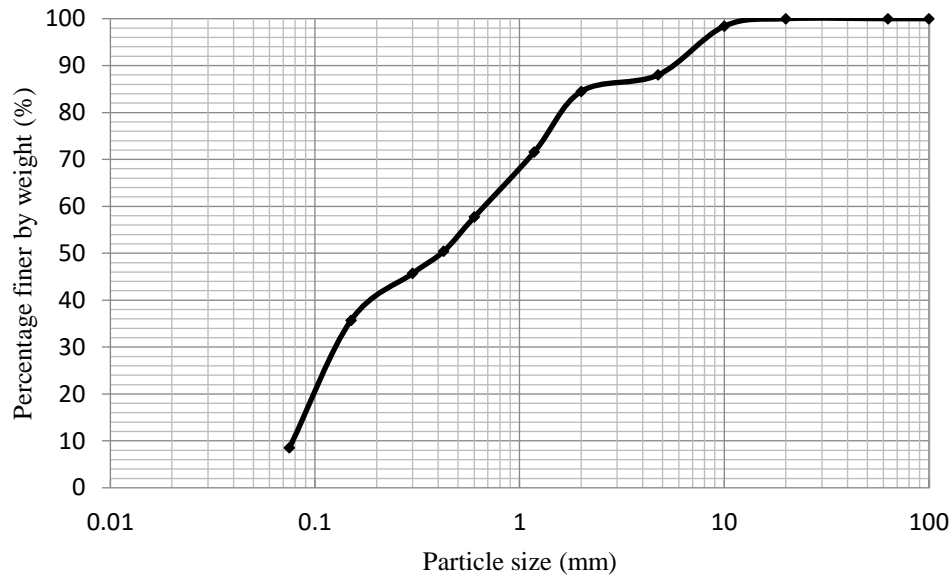
Figure 3.1 Particle-size distribution of subgrade soil

Table 3.1 Engineering properties of subgrade soil

S. No.	Particulars	Subgrade soil
1	Specific gravity	2.55
2	Liquid limit (%)	29
3	Plastic limit (%)	20
4	Plasticity index (%)	9
5	IS Classification	SM
6	Optimum moisture content (%)	13.91
7	Maximum dry unit weight (kN/ m^3)	18.74
8	California bearing ratio (*CBR*) (%)	1.66

3.2.2 Reinforcement

Two types of geogrids (Glasgrid, Tenax 3D grid) and one geomat (Tenax multimat) were used as the geosynthetic reinforcement. The geosynthetic samples are shown in Fig. 3.2. The properties of geogrids and geomat as provided by the manufacturer are given in Table. 3.2.

Glasgrid is a high strength, open fiberglass grid custom knitted in a stable construction and coated with a patent-pending elastomeric polymer and self-adhesive glue. Every component of the matrix shall be stabilized against ultraviolet degradation and inert to chemicals normally found in a natural soil environment. Tenax 3D grid is manufactured from a unique extrusion technique resulting in a perforated sheet that is specifically shaped in three directions (3D). This unique extrusion technique produces a structure with vertical longitudinal ribs capable to guarantee the best possible interaction mechanism between geogrids and granular soils by restricting the horizontal movement of soil particles and preventing further displacements. This increase in interaction from the 3D Grids enables consistent reductions in aggregate layer thickness. Tenax multimat is a three-dimensional mat composed by extruded and bi-oriented polypropylene grids, laid one upon each another and tied up by means of a black polypropylene yarn.

(a)   (b)   (c)
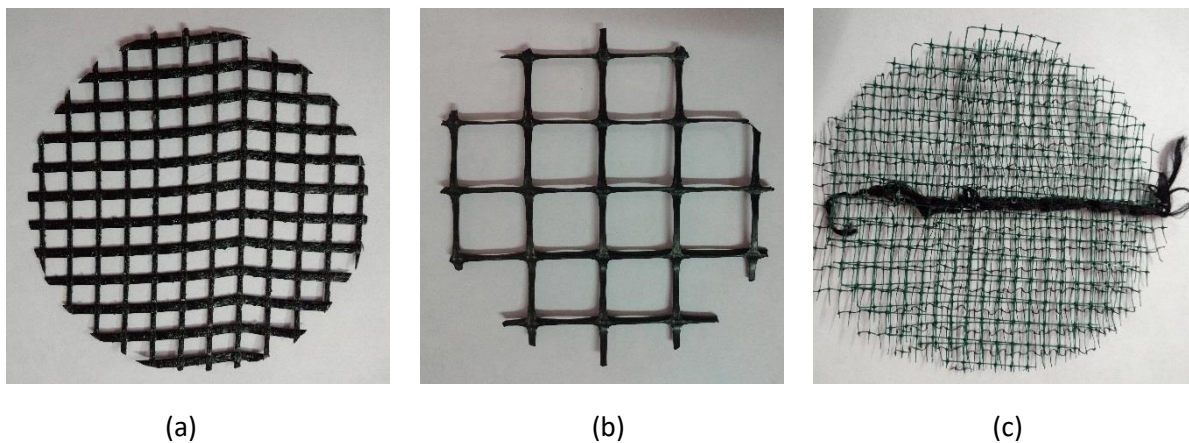
Figure 3.2 Geogrids and geomat used in the study: (a) Glasgrid, (b) Tenax 3D grid, (c) Tenax multimat

Table 3.2 Properties of geogrids and geomat (Courtesy of H. M. B. S Textile Private Limited, New Delhi)

Geosynthetics	Description	Value	Unit	Test method
Glasgrid	Mass per unit area	405	g/m^2	ASTM D5261
	Grid size	12.5 × 12.5	mm	
	Material	Fiberglass reinforcement with modified polymer coating and pressure sensitive adhesive backing	-	-
	Tensile strength (Ultimate)	115 × 115 +/-15 (MD × TD)	kN/m	ASTM D6637 EN-ISO 10319:2008
	Tensile elongation (Ultimate)	2.5 +/-0.5%	-	ASTM D6637 EN-ISO 10319:2008
	Tensile resistance @ 2% strain	95 × 95 +/-20	kN/m	ASTM D6637 EN-ISO 10319:2008
	Secant stiffness EA @ 1% strain	4600 × 4600 +/-600 (MD × TD)	N/mm	ASTM D6637 EN-ISO 10319:2008
	Damage during installation	< 5%	-	Internal test method
Tenax 3D grid	Structure	Bi-oriented geogrids	-	-
	Mesh type	Quadrangular apertures	-	-
	Polymer type	Polypropylene	-	-
	Aperture size [c, d]	30 × 30 (MD × TD)	mm	-
	Transversal rib width [e]	2.6	mm	-
	Longitudinal rib thickness [e]	3.8	mm	-
	Junction thickness [e]	6	mm	-
	Stiffness at 0.5 % strain [a, b, c]	550 × 350 (MD × TD)	kN/m	ISO 10319
	Installation damage factor	1	-	ASTM D5818

Tenax multimat	Structure	Three dimensional geomat composed by 3 layers	-	-
	Mesh type	Rectangular apertures	-	-
	Polymer type	Polypropylene	-	-
	Peak tensile strength [c, f]	3.8×13 (MD $\times$ TD)	kN/m	ISO 10319
	Yield point elongation [a, c]	23×23 (MD $\times$ TD)	%	ISO 10319
	Mass per unit area [a]	180	g/m^2	ISO 9864
	Thickness [a]	8	mm	ASTM D6525
	Aperture size [a, c]	7×9 (MD $\times$ TD)	mm	-

Notes;

a) Typical values

b) Tests performed using extensometers

c) MD: machine direction (longitudinal to the roll) – TD: transverse direction (across roll width)

d) Aperture tolerance: ± 5mm

e) Thickness/width tolerance: -5%

f) 95% lower confidence limit values, ISO 2602

Geosynthetics are available with a variety of geometric and polymer compositions to meet a wide range of functions and applications. Selection of geosynthetic may have specific requirement depending on the type of application. Geogrids are used mainly for reinforcement and separation could be a function served by geogrids when soils are having very large particle sizes. Therefore, two types of geogrids were selected for the present study and the performance of the geogrid for reinforcement relies on its rigidity, strength, stiffness and aperture size, which accounts for its high capacity for interlocking with soil particles. The selection of a geosynthetic for a particular application is governed by several other factors, such as specification, durability, availability and cost (Shukla, 2016).

3.3 Experimental investigation

The standard Proctor compaction test was carried out as per IS: 2720 (Part VII-1980) to determine the maximum dry unit weight (MDU) and optimum moisture content (OMC) for the soil. The MDU and OMC of soil were found to be 18.74 kN/ m^3 and 13.91% respectively. The design method that determines the required layer thickness of the aggregate with the

reinforcement in the subgrade has been based on the *CBR* of the subgrade soil (Giroud and Noiry, 1981). If the *CBR* of the subgrade is improved by providing the reinforcement, then the required thickness of the granular subbase/base layer can be reduced for a given traffic volume or, alternatively, the traffic volume can be increased for a given thickness of granular subbase/base layer. It is not always possible to get good quality granular material as per the design specifications either because of unavailability or increase in cost because of long haulage distance. Hence there is a need of subgrade soil stabilization with geosynthetic reinforcement to increase the strength and reduce the granular layer thickness over the subgrade soil. Therefore, the unsoaked CBR tests were conducted on the subgrade soil without reinforcement and with a single layer and double layer of different types of geosynthetic reinforcement as described in IS: 2720 (Part 16) – 1979. To evaluate the effect of geosynthetic reinforcement on subgrade strength, the single layer reinforcement was placed at different positions, namely *H/2, H/3, H/*4 where *H* is the height of the soil specimen of the CBR mould from the top surface and double layer reinforcement was placed at *H/*4 from top and bottom surface of the soil specimen.

The location of single and double layers of reinforcement within the subgrade were selected based on the literature because most of the researchers believe that maximum benefit of reinforcement is obtained when the reinforcement layer is placed in the upper half portion of the CBR mould. Half of the height of CBR mould was taken to place the reinforcement layers to get the maximum benefit of reinforcement. Therefore, three positions for single layers of reinforcement and one position for double layer of reinforcement were selected.

The geosynthetic reinforcement was cut in the form of a circular disk of diameter slightly less than the diameter of CBR mould. The dry weight required for filling the mould was calculated based upon the maximum dry unit weight (MDU) and the water corresponding to OMC was added in the soil and then the soil was mixed thoroughly. The mould is filled with

this soil by placing geosynthetic reinforcement at predetermined depth as shown in Fig. 3.3. The cross section of the model along with the position of geosynthetic reinforcement is shown in Fig. 3.4. The surcharge weights were placed on the specimen to stimulate the effect of the thickness of road construction overlying the layer being tested. Load is applied to the plunger into the soil at the rate of 1.25mm/min. Readings of the load were taken at penetration of 0.5mm to until a total penetration of 12.5mm. The standard *CBR* tests were performed in the laboratory to compare the performance of various geosynthetics under the same subgarde soil condition. The soil specimen height in the *CBR* mould was taken as an equivalent to the thickness of the prepared subgrade soil in the field. Laboratory tests can be conducted more quickly and usually have more alternatives but they are only able to simulate field conditions. Further, the scaling and boundary effect can have influence on the final results, but any change in specimen size will create difficulty for comparative analysis. Thus, the measured values can be treated as relative measurements.

Figure 3.3 Orientation of reinforcement layer placed at predetermined depth in CBR mould

The improvement in *CBR* value of subgrade soil with reinforcement is measured in terms of the reinforcement ratio η, which is defined as a ratio of *CBR* value of soil with reinforcement (CBR_R) to that of original soil (*CBR*), (Koerner, 2012; Shukla, 2016).

$$\eta = \frac{CBR_R}{CBR}$$

This ratio indicates the contribution of geosynthetic reinforcement towards increasing the *CBR* value of a soil and compares the performance of geogrids and geomat reinforcement on the same soil. To quantify the role of reinforcement in increasing the strength, the reinforcement ratio is calculated for various cases and compared to distinguish the role of geosynthetic layer in improvement.
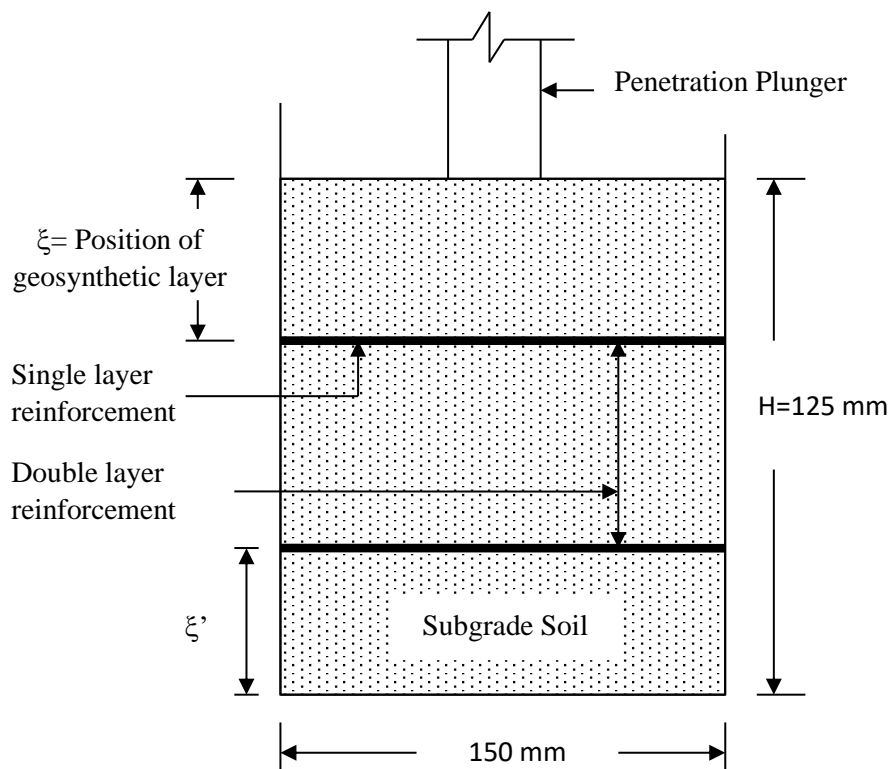
Figure 3.4 Schematic representation of the specimen in *CBR* test model, position of geosynthetic is, $\xi = H/2$, $H/3$ and $H/4$ for single layer of reinforcement and $\xi = \xi' = H/4$, for double layers of reinforcement

3.4 Results and Discussion

3.4.1 *CBR* Value

Figures 3.5 to 3.7 present the variation of the load-penetration curves obtained from the *CBR* tests for unreinforced and reinforced sections with a single layer of reinforcement. It can be observed that placing the geosynthetic reinforcement at varying depths increases the *CBR* value significantly. The amount of increase in the *CBR* value depends on the position of geosynthetic reinforcement (ξ) and type of reinforcement. The *CBR* value of the unreinforced soil specimen corresponding to 2.5 mm and 5.0 mm penetrations were found to be 1.26% and 1.66 % respectively as shown in Fig. 3.5, which were increased to 1.79 % and 2.21 % respectively, when Glasgrid reinforcement was placed at depth *H/*2. Further placing Tenax multimat reinforcement at same depth *H/*2, enhanced the *CBR* value to 2.16 % and 2.63 % respectively corresponding to 2.5 mm and 5.0 mm penetrations. When Tenax 3D grid reinforcement layer was placed at the same depth *H/*2, it decreased the *CBR* value at 2.5mm penetration to 1.19 % but increased the *CBR* at 5.0 mm penetration to 1.76 %. The maximum value of *CBR* obtained at 5.0 mm penetration is 2.63 % when Tenax multimat reinforcement layer was placed at depth *H/*2. Similar results have been observed for other geosynthetic reinforcements placed at depth *H/*3 and *H/*4 as presented in Figs. 3.6 and 3.7.

Figure 3.6 presents the variation of load-penetration curve for the soil specimen without reinforcement and soil specimen reinforced with different types of geosynthetic reinforcement layer at depth *H/*3. The increase in the *CBR* value of the Tenax 3D grid reinforced soil specimen corresponding to 2.5 mm and 5.0 mm penetrations were found to be 1.41 % and 2.08 % respectively. In case of Tenax multimat reinforcement it increased to 1.30 % and 1.74 % respectively corresponding to 2.5 mm and 5.0 mm penetrations. Only in case of Glasgrid reinforced specimen the *CBR* value decreased at 2.5 mm penetration to 1.19 % and increased at 5.0 mm penetration to 1.76 % as compared to the unreinforced specimen. The maximum

value of *CBR* obtained at 5.0 mm penetration is 2.08 % when Tenax 3D grid reinforcement was placed at depth *H/3*.
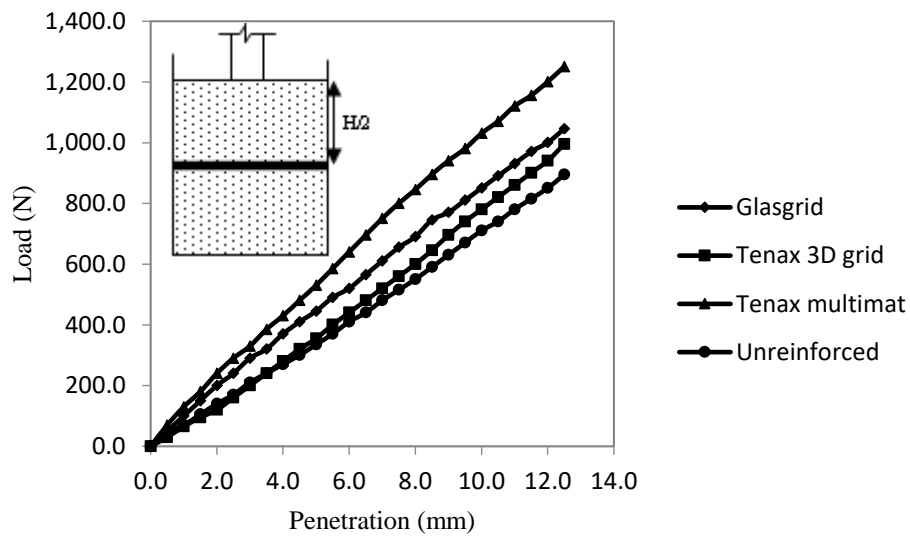
Figure 3.5 Load penetration curve with geosynthetic placed at, $\xi=H/2$
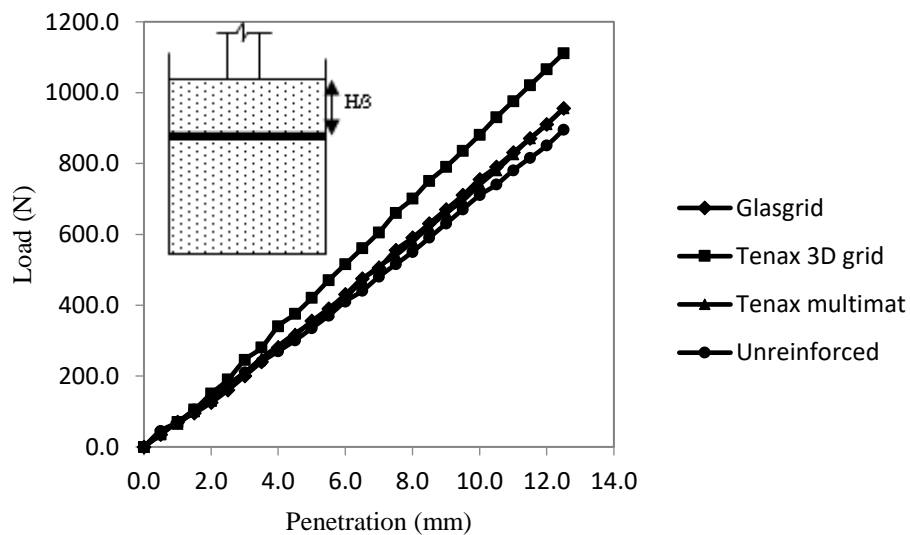
Figure 3.6 Load penetration curve with geosynthetic placed at, $\xi= H/3$

Figure 3.7 represents the influence of the position of the reinforcing layer on the load-penetration curve for both unreinforced and reinforced specimens obtained from the *CBR* tests when the reinforcement was placed at depth *H/*4. The *CBR* value of the Tenax multimat reinforced soil corresponding to 2.5 mm and 5.0 mm penetrations were found to be 1.34% and 1.94% respectively. For Glasgrid and Tenax 3D grid reinforced soil specimen, the same *CBR* value was obtained at 5.0 mm penetration is 2.03% but it decreased to 1.19% and 1.12% at 2.5 mm penetration corresponding to Glasgrid and Tenax3D grid reinforcement respectively. The results are in good agreement with data presented by (Williams, 2008) on effect of geosynthetic reinforcement on *CBR* strength of soil that leads to improve the strength of soil, resulting in a decrease in the surface penetration and deformation with stress distribution over a wider area. This means that the inclusion of single layer of geosynthetic reinforcement increases soil resistance against loading.
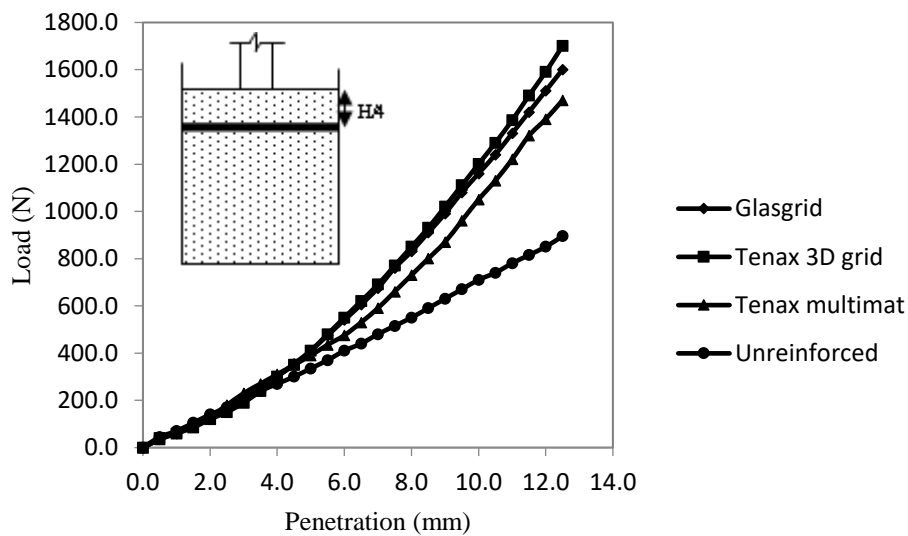
Figure 3.7 Load penetration curve with geosynthetic placed at, $\xi= H/$4

Figure 3.8 shows the variation of the load-penetration curves obtained from the *CBR* tests for unreinforced and reinforced sections with double layers of reinforcement. The *CBR* value

of the soil increased to 1.86% and 3.52% corresponding to 2.5 mm and 5.0 mm penetrations respectively when the subgrade is reinforced with double layers of Glasgrid reinforcement. The strength of the soil increased further by placing double layers of Tenax 3D grid reinforcement and Tenax multimat reinforcements. The *CBR* value of soil reinforced with double layers of Tenax 3D grid reinforcement corresponding to 2.5mm and 5.0mm penetrations were found to be 3.72% and 6.25% respectively as shown in Fig. 8, which were increased to 4.16% and 7.05% when the soil was reinforced with double layers of Tenax multimat reinforcement. It is clearly observed that Tenax multimat performs far better in terms of increase in *CBR* and load carrying capacity for double layers of reinforcement. The highest increase in *CBR* value was achieved when the subgrade soil was reinforced with double layers of reinforcement as compared to the unreinforced section and the section reinforced with a single layer of reinforcement.
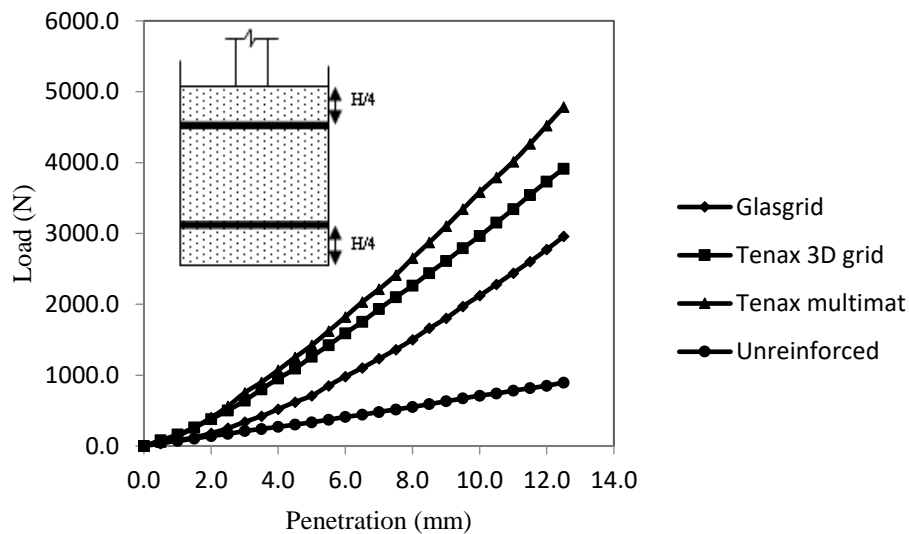
Figure 3.8 Load penetration curve with double geosynthetic layer placed at $\xi=\xi'=H/4$

The reason for the improvement in the strength of the subgrade soil reinforced with single and double layers of reinforcement is that, the geosynthetics used in the study has good interlocking and frictional capability which can provide tensile resistance to any lateral movements. Thus, it improves the strength of the soil with low *CBR*. Another reason for the

improvement in the strength of the subgrade with low *CBR* is that, through the inclusion of geosynthetic reinforcement layers the maximum vertical stress on the subgrade is reduced. The vertical stress on the subgrade is more uniformly distributed than on the absence of a geosynthetic. Therefore, reinforcement helps to improve the bearing capacity of the soil with low *CBR*. Also, the combining action of geosynthetic tension and geosynthetic improved load distribution results in vertical restraint of the subgrade.

3.4.2 Effect of multiple layer reinforcements

Table 3.3 shows the results of the *CBR* tests on soil reinforced with three different types of geosynthetics and presents the reinforcement ratio for these three types of geosynthetic reinforcement placed at depth *H/2, H/3* and *H/4* and double layers. It is clear that there is a considerable amount of increase in the *CBR* value of a soil reinforced with different types of geosynthetics at various depths. As the reinforcement ratio exceeds unity ($\eta>1$) throughout the tests for different types of geosynthetic reinforcement used in the tests as shown in Table 3.3, which indicates the beneficial effect of reinforcement at varying depth to increase the subgrade strength of geosynthetic reinforced unpaved road. The location of the geosynthetic reinforcement within the subgrade is an important factor for the performance of unpaved road. The reinforcement ratio varies from 1.05 to 1.58 for a single layer of geosynthetic reinforcement and 2.12 to 4.25 for double layers of geosynthetic reinforcement respectively. Out of three types of geosynthetic reinforcement used in the study, geogrids perform better than geomat for soil reinforced with a single layer of reinforcement. Only in one case geomat reinforcement yields the maximum strength when it is placed at $\xi=H/2$ from the top, when compared to the other two geogrids. Geomat performs best among the three types of geosynthetic when soil is reinforced with double layers of reinforcement. An increase in the number of reinforcement layers led to the further increase in strength and load carrying capacity

of soil. The reinforcement ratio lies between 2 to 5 which indicates that an introduction of geosynthetic as double layers of reinforcement offers a good resistance against the penetration.

Table 3.3 Results of *CBR* tests for different positions of geosynthetics

Type of geosynthetic	Position of geosynthetic reinforcement	*CBR* (%)	Increase in *CBR* with respect to unreinforced section (%)	Reinforcement ratio (η)
Glasgrid	*H/2*	2.21	33.13	1.33
	H/3	1.76	6.02	1.06
	H/4	2.04	22.89	1.23
	Double layers	3.52	112.05	2.12
Tenax 3D grid	*H/2*	1.76	6.02	1.06
	H/3	2.08	25.30	1.25
	H/4	2.04	22.89	1.23
	Double layers	6.25	276.51	3.77
Tenax multimat	*H/2*	2.63	58.43	1.58
	H/3	1.74	4.82	1.05
	H/4	1.94	16.87	1.17
	Double layers	7.05	324.70	4.25

3.4.3 Comparison of different types of geosynthetic reinforcement

Figure 3.9 shows the relative influence of geosynthetic reinforcement at different positions on the reinforcement ratio. Three different types of geosynthetic were used in the test and the properties of these geosynthetic materials were presented earlier in Table 3.2. The comparision of the ability of different types of geosynthetic used in this study to reinforce the weak subgarde soil can only be accomplished if the conditions between each of the individual tests are identical. The comparison between the different types of geosynthetic reinforcement, in terms of reinforcement ratio is described in Fig. 3.9 for the section with a single layer of

reinforcement placed at *H/2*, *H/3*, *H/4* and double layers of reinforcement. It can be observed

that the reinforced section with double layers of reinforcement has higher strength than the

section reinforced with a single layer of reinforcement. Comparing the performance of different

types of geosynthetic reinforcement is difficult because all three geosynthetics used are

individualy different from each other based on the properties given in Table 3.2. Imporatant

parameters which are responsible for comparing the performance of various geosynthetics to

increase the subgrade strength are (1) type of geosynthetic used, (2) properties of geosynthetic,

such as strength, stiffness, aperture size etc., (3) number of geosynthetic layers, and (4) depth

of geosynthetic reinforcement. It is hard to identify which parameter has more imporatnt effect

on the enhancement of subgrade strength reinforced with different types of geosynthetic.

Therefore, it is better to investigate and quantify the mechanism that is responsible for the

improved strength when different types of geosynthetics are used for comparision. The

performance of the subgrade soil of an unpaved road is improved through three mechanisms:

(1) impact of load distribution on subgrade soil resilient modulus, (2) subgrade soil vertical

restraint, and (3) load transfer by the tensioned membrane effect (Koerner, 2012). The presence

of geosynthetic in the subgrade soil reduces the maximum vertical stress on it and also more

uniformly distributes the vertical stress on the subgrade soil than in the absence of a

geosynthetic. Tensioned membrane effect becomes important only when large deformations

occur in subgrade soil, when it is weak/soft.

Out of three types of geosynthetics used to reinforce subgrade with a single layer of

reinforcement at varying depths, both geogrid reinforcements perform better than the geomat

reinforcement except one case when geomat reinforcement it is placed at $\xi=H/2$ which yields

the maximum strength when compared to the other two geogrids. Both geogrid reinforcements

behaived similarly and gain the similar strength when placed at $\xi=H/4$. The same order was

obtained for achieving the improvement when reinforcement layer was placed at $\xi=H/3$ and

$\xi=H/4$ where Tenax 3D grid yields the maximum improvement. The results show that the behaviour of reinforced subgrade was better than that of the unreinforced subgrade and improvement with reinforcement is more pronounced when reinforcement layer is placed near to the load.
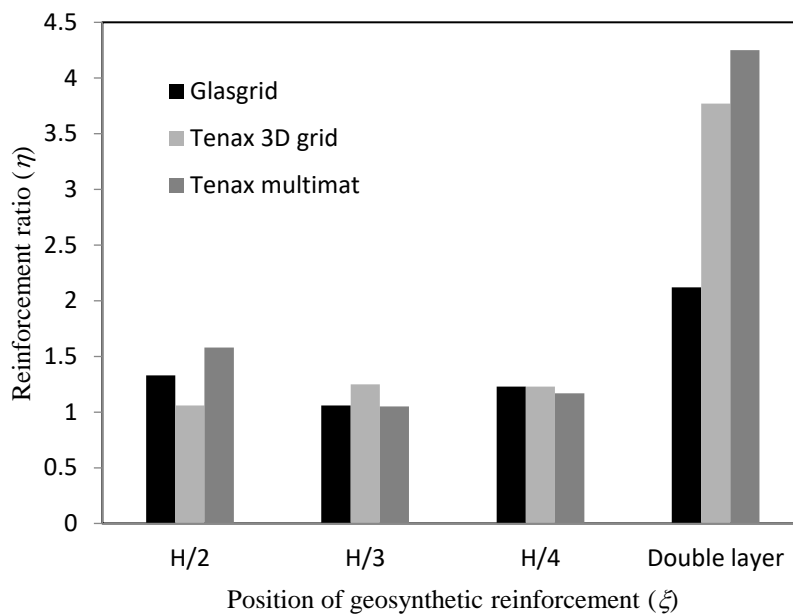
Figure 3.9 Variation in reinforcement ratio for the various positions of geosynthetic reinforcement

The overall preference of choosing reinforcement type should be given to Tenax 3D grid which performs better than other geosynthetics because of the higher tensile strength and has relatively higher stiffness. Even handiling of Tenax 3D grid over Glasgrid was easier because of the pressure sensitive adhesive provided at the back creates little inconvenience. Aperture size is different for all types of geosynthetic which governs the lateral confinement effect and justifies the selection of geogrid over geomat for subgrade reinforcement. To ensure effective interlocking between geosynthetic and soil, aperture size is a factor to be considered. The results of subgrade soil reinforced with double layers of reinforcement shows that Tenax multimat reinforcement type performs best because they offer good interlocking and frictional

resitance. Increasing the number of reinforcement layers leads to enhance the strength significantly, as compared to the single layer of reinforcement and the extent of improvement is independent of type of geosynthetic. Tenax multimat is composed of tieing three layers of extruded and bi-oriented polypropylene grids. The non-uniform texture of top and bottom layers of Tenax multimat offers good tensile resistance to the lateral movement. The relative cost of reinforcement type is also a factor which should be considered before the final selection is made.

3.4.4 Optimum position of the geosynthetic

Figure 3.10 shows the effect of placement of a single layer of geosynthetic reinforcement along the height of the specimen on *CBR*. A set of experiments were carried out to determine the optimum position of placing the geosynthetic reinforcement along the depth of the subgrade in order to produce a maximum gain in the strength. The results of CBR tests indicates that for the maximum benefit, the geosynthetic reinforcement layer should be placed either at the middle of the height of specimen or between the upper one-third layer and middle layer which yields the higher strength as compared to the other locations. The tests were conducted at three different positions of geosynthetic and the maximum value of all strength parameters was obtained in the case when Tenax multimat reinforcement layer was placed at middle half of the specimen. Based on the properties of these geosynthetics, an increase in the strength of subgrade depends on the value of ξ i.e the depth of placement of reinforcement. Placing the geosynthetic at base of the specimen is just as good as having no reinforcement in the sample. The beneficial position of the geosynthetic reinforcement was obtained by plotting the graph between *CBR* of the soil and depth of the geosynthetic placement from top as shown in Fig. 3.8. The optimum position of the geosynthetic reinforcement layer should be taken as $0.3H$ to $0.36H$ for Tenax 3D grid reinforcement and $0.41H$ to $0.62H$ for Glasgrid reinforcement and Tenax multimat reinforcement where *H* is the height of the soil specimen. Naeini and Moayed,

(2009) have also shown that the best location of geosynthetic reinforcement layer is at 30% of the thickness measured from the top of CBR mould. Reinforcement inclusion can be less effective if it is not placed at the proper location. Thus, reinforcement layer should be located at the optimal depth to improve contribution of the geosynthetic reinforcement. For field applications, the finding of optimal location of geosynthetic reinforcement for maximum enhancement in *CBR* is essential.
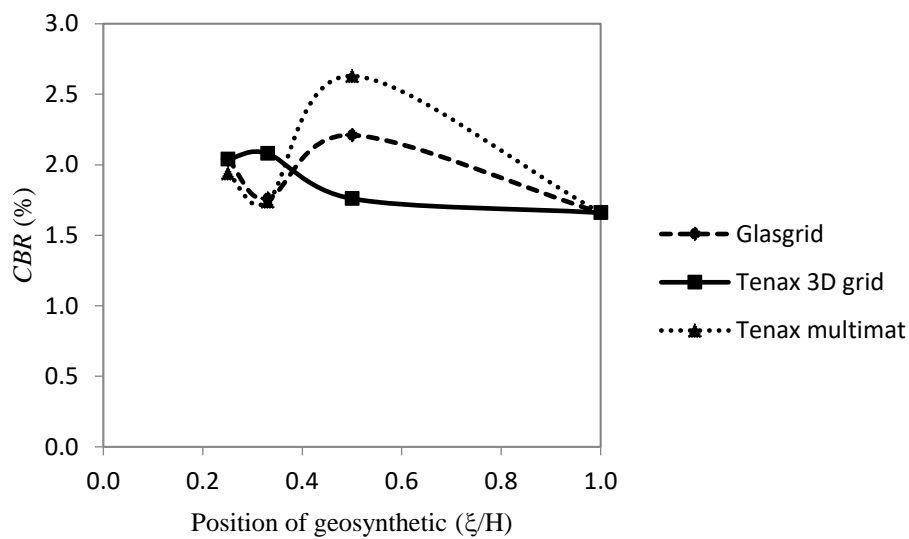
Figure 3.10 Optimum position of geosynthetic based on *CBR* value of soil reinforced with different types of geosynthetics

3.5 Conclusions

In the present chapter, reinforcement benefits of different types of geosynthetics in unpaved road have been evaluated in terms of their *CBR* value. The performance of several geosynthetics in terms of increase in CBR value of soil with reinforcement can be compared with each other because all the tests are performed under the same condition, that is, with the same subgrade soil. All these experiments can be related to an unpaved road as to whether the geosynthetic reinforcement can really improve the subgrade soil strength where the specimen height is considered as the depth of compacted subgrade soil in field. The findings indicate that

there is a considerable amount of increase in strength of subgrade soil reinforced with geosynthetics and the amount of increase depends on the properties and type of geosynthetics, depth and number of reinforcement layers, and mechanisms involved. It is important to mention here that these findings are based on the laboratory investigations carried out in this study. It is possible that these findings may vary if conducted in the field. Therefore, actual field trials must be made to have more confidence in these results.

The important findings of this research are summarized below:

1. The inclusion of a single layer and double layers of geosynthetic reinforcements at varying depths in soil enhances the strength of the subgrade soil in terms of *CBR* value

2. The *CBR* value of the soil increases by 5 to 60 % when a single layer of reinforcement is placed within the subgrade soil and strength increases by 112 to 325 % when it is reinforced with double layers of reinforcement. The amount of improvement depends upon the position of reinforcement layer and type of reinforcement.

3. Placing the geosynthetic reinforcement in the double layers yields the largest improvement regardless of the type of geosynthetic.

4. The optimum benefit of reinforcement is evident if it is placed at middle height of the CBR mould and for better improvement in strength the reinforcement layer should be placed between the upper one-third layer and middle layer.

5. Of the three geosynthetics used in the study, Tenax 3D grid performed better than other two geosynthetics for soil reinforced with a single layer of reinforcement at $\xi=H/3=H/4$ and Tenax multimat performed better than other two geosynthetics for soil reinforced with double layers of reinforcement and single layer of reinforcement at $\xi=H/2$.

6. Optimum location of reinforcement was found as $0.3H$ to $0.36H$ for Tenax 3D grid reinforcement layer and $0.41H$ to $0.62H$ for both Glasgrid reinforcement layer and Tenax multimat reinforcement layer.

References

AASTHO. Geosynthetic Materials Association 2000.

Abu-Farsakh MY, Akond I, Chen Q. Evaluating the performance of geosynthetic-reinforced unpaved roads using plate load tests. *Int J Pavement Eng* 2016; 17:901–12. doi:10.1080/10298436.2015.1031131.

Abu-Farsakh M, Hanandeh S, Mohammad L, Chen Q. Performance of geosynthetic reinforced/stabilized paved roads built over soft soil under cyclic plate loads. *Geotext Geomembranes* 2016; 44:845–53. doi: 10.1016/j.geotexmem.2016.06.009.

Abu-Farsakh M, Souci G, Voyiadjis GZ, Chen Q. Evaluation of Factors Affecting the Performance of Geogrid-Reinforced Granular Base Material Using Repeated Load Triaxial Tests. *J Mater Civ Eng* 2012; 24:72–83. doi:10.1061/(ASCE)MT.1943-5533.0000349.

Adams CA, Apraku E, Opoku-boahen R. Effect of Triaxial Geogrid Reinforcement on CBR Strength of Natural Gravel Soil for Road Pavements. *J Civ Eng Res* 2015; 5:45–51. doi: 10.5923/j.jce.20150502.05.

Al-Qadi IL, Brandon TL, Valentine RJ, Lacina BA, Smith TE. Laboratory evaluation of geosynthetic-reinforced pavement sections. *Transp Res Rec* 1994:25–31.

Choudhary A k., Gill K, J.N. J, Sk. S. Improvement in CBR of the expansive soil subgrades with a single reinforcement layer. *Proc Indian Geotech Conf* 2012:289–92.

Duncan-Williams E, Attoh-Okine NO. Effect of geogrid in granular base strength - An experimental investigation. *Constr Build Mater* 2008; 22:2180–4. doi: 10.1016/j.conbuildmat.2007.08.008.

Fannin RJ, Sigurdsson O. Field Observations on Stabilization of Unpaved Roads with Geosynthetics. *J Geotech Eng* 1996; 122:544–53. doi:10.1061/(ASCE)0733-9410(1996)122:7(544).

Giroud JP, Noiray L. Geotextile-reinforced unpaved road design. *J Geotech Eng* 1981;107(9):1233-54.

Góngora IAG, Palmeira EM. Influence of fill and geogrid characteristics on the performance of unpaved roads on weak subgrades. *Geosynth Int* 2012; 19:191–9. doi:10.1680/gein.2012.19.2.191.

Hufenus R, Rueegger R, Banjac R, Mayor P, Springman SM, Brönnimann R. Full-scale field tests on geosynthetic reinforced unpaved roads on soft subgrade. *Geotext Geomembranes* 2006; 24:21–37. doi: 10.1016/j.geotexmem.2005.06.002.

IS:2720 (Part VII-1980). Methods of Test for Soils, Determination of Water Content-Dry Density Relation using Light Compaction, Bureau of Indian Standards, New Delhi (Reaffirmed 2011). Indian Stand 2011.

Kamel MA, Chandra S, Kumar P. Behaviour of subgrade soil reinforced with geogrid. *Int J Pavement Eng* 2004; 5:201–9. doi:10.1080/1029843042000327122.

Koerner R M. Desigining with geosynthetics. 6th ed. New York: Xlibris PublishingCo.; 2012.

Kuity A, Roy TK. Utilization of Geogrid Mesh for Improving the Soft Subgrade Layer with Waste Material Mix Compositions. *Procedia - Soc Behav Sci* 2013; 104:255–63. doi: 10.1016/j.sbspro.2013.11.118.

Naeini SA, Ziaie-Moayed R. Effect of plasticity index and reinforcement on the CBR value of soft clay. *Int J Civ Eng* 2009; 7:124–30.

Palmeira EM, Antunes LGS. Large scale tests on geosynthetic reinforced unpaved roads subjected to surface maintenance. *Geotext Geomembranes* 2010; 28:547–58. doi: 10.1016/j.geotexmem.2010.03.002.

Som N, Sahu RB. Bearing capacity of a geotextile-reinforced unpaved road as a function of deformation: a model study. *Geosynthetics International* 1999; 6(1):1-7.

Rajesh U, Sajja S, Chakravarthi VK. Studies on Engineering Performance of Geogrid Reinforced Soft Subgrade. *Transp Res Procedia* 2016; 17:164–73. doi: 10.1016/j.trpro.2016.11.072.

Raymond G, Ismail I. The effects of geogrid reinforcement on unbound aggregates. *Geotext Geomembranes* 2003; 21:355–80. doi:10.1016/S0266-1144(03)00044-X.

Shukla S K. An introduction to geosynthetic engineering. London: CRC Press; 2016.

Shukla S K. Geosynthetics and their applications. London: Thomas Telford Publishing; 2002.

Subaida EA, Chandrakaran S, Sankar N. Laboratory performance of unpaved roads reinforced with woven coir geotextiles. *Geotext Geomembranes* 2009; 27:204–10. doi: 10.1016/j.geotexmem.2008.11.009.

Vinod P, Minu M. Use of coir geotextiles in unpaved road construction. *Geosynth Int* 2010; 17:220–7. doi:10.1680/gein.2010.17.4.220.

CHAPTER 4

STRENGTH BEHAVIOUR OF SUBGRADE-AGGREGATE COMPOSITE SYSTEM

This chapter is based on the paper published in Lecture Notes in Civil Engineering, Springer, as listed in Section 1.6. The details are presented here with some changes in the layout in order to maintain a consistency in the presentation throughout the thesis.

4.1 Introduction

Geosynthetics have been found as an important innovation in the field of geotechnical engineering. Geosynthetics such as geotextiles and geogrids, which have been used very commonly on various construction sites, can improve the performance and life span of unpaved road when built over weak subgrades. Soil and aggregate are the basic material required for the construction of unpaved roads. Unpaved roads are generally constructed by placing one or more layers of locally available material or good quality granular fill material over a natural subgrade. Since no asphalt or concrete surfacing is provided on the top of an unpaved roads, they are prone to problems such as excessive deformations, rutting and potholes, due to which frequent maintenance work is required. Geosynthetic reinforcement can be used to reinforce these roads where reinforcement can be placed at the interface of subgrade and granular fill, increasing its life and reducing maintenance costs (Shukla, 2016). Benefits of reducing granular subbase/base layer thickness are realized if the cost of the geosynthetic is less than the cost of the reduced granular subbase/base layer material (Subaida, et. al., 2009).

The haul roads as well as the temporary roads can be considered as an unpaved road where subbase/base layers are laid directly on in situ subgrades. These can be referred to as subgrade-aggregate composite systems. Geosynthetic reinforcement has been introduced into a pavement system by placing the geosynthetic layer directly on the unprepared subgrade and sometimes

it is laid on the prepared subgrade before the placement of the subbase/base layer. These systems are referred to as subgrade-geosynthetic-aggregate composite systems. Subgrade-aggregtae composite system requires a aggregate layer of greater thickness than subgrade-geosynthetic-aggregate composite system to carry the same traffic (Bender and Barenberg, 1978). It is also observed that the bearing resistance of these soil-aggregate systems is improved by the presence of geosynthetic reinforcement as well as with an increase in quantity or the stiffness of the reinforcement (Asha and Latha, 2011).

Several works in the literature have shown the benefits of geosynthetics in reinforcing the paved and unpaved roads by conducting the laboratory model studies and field studies (Fannin and Sigurdsson, 1996; Hufenus et. al., 2006). Some of the analytical studies on reinforced unpaved roads include the works by Giroud and Han (2004) and Giroud and Noiray (1981). Limited studies have carried out California bearing ratio (CBR) tests on unreinforced and reinforced soil-aggregate system to understand the improvement in the *CBR* value of soil or aggregate with the inclusion of reinforcement (Williams and Okine, 2008; Kamel, et al., 2004; Asha and Latha, 2010; Singh, et al., 2019). Conventional road design uses the *CBR* value of the subgrade/subbase/base course material as a measure of the load-carrying capacity of the roads and for the estimation of thickness of granular base course.

The main objective of this chapter was to conduct a series of CBR tests on unreinforced and reinforced soil–aggregate composite systems. Tests were conducted on soil alone, and unreinforced and reinforced soil–aggregate systems. Different types of geosynthetics used in this study were a geotextile, geogrid and geomat. Geosynthetic layers were placed at the interface of subgrade and aggregate layer and sometimes within aggregate layer also, and a significant improvement in the strength behavior of system was observed due to the separation and reinforcing action provided by the geosynthetic materials. Effect of various types of geosynthetic as reinforcement on the *CBR* value was also studied. The test results have been

69

analysed to understand the effect of type of reinforcement on the performance of the subgrade-aggregate composite system in terms of increase or decrease in *CBR* value. The tests performed in the present study are small-scale tests and were subjected to scale effects.

4.2 Materials

Locally available soil was collected from the campus of Delhi Technological University that has been used as a subgrade material in the experiments. The soil is classified as silty sand (SM) using the particle-size analysis and Atterberg limit tests as per the Indian Soil Classification System. Maximum dry unit weight (MDU) and optimum moisture content (OMC) of the soil were determined through the standard Proctor compaction test (IS: 2720 (Part VII-1980)), which was obtained as 18.6 kN/ m^3 and 13.9%, respectively. The properties of the soil used in the study are given in Table 4.1. The aggregates having size ranging from 4.75 mm to 12.5 mm was used as the subbase/base material in the tests. The specific gravity of the aggregates is 2.65.

Table 4.1 Properties and classification of subgrade soil

Particulars	Soil
Specific gravity	2.65
Soil classification	SM
Liquid limit and plastic limit (%)	29 & 20
Maximum dry unit weight (kN/ m^3)	18.6
Optimum moisture content (%)	13.9

The geosynthetics used in the experiments to prepare the subgrade-aggregate composite system are geotextile, geogrid and geomat. These three geosynthetics were placed at the interface of subgrade and aggregate layer. The photograph of various geosynthetic

reinforcement used in the study are shown in Fig. 4.1. Woven multifilament polypropylene geotextiles are used and theses are resistant to chemicals and micro-organism normally found in soils and resistant to short-term exposure to ultraviolet radiation. High strength geogrid was used; the geogrid is coated with a patent-pending elastomeric polymer and self-adhesive glue and had ultimate tensile strength of 115 kN/m. Three dimensional geomat used in the experiments had peak tensile strength of 3.8 kN/m and it is formed by laying extruded polypropylene grids in between the two bi-oriented polypropylene grids and tied together by black polypropylene yarn. The properties of geosynthetic materials as provided by the manufacturer are given in Table. 4.2.

| (a) | (b) | (c) |
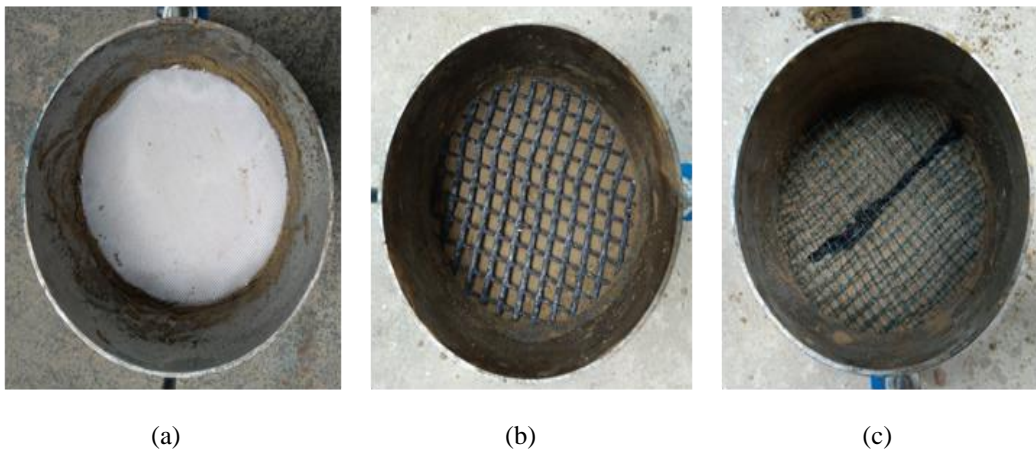
Figure 4.1 Geosynthetics used in the study (a) Geotextile (b) Geogrid (c) Geomat

Table 4.2 Properties of geosynthetics used in experiments

Property	Geotextile	Geogrid	geomat
Aperture size (mm)	-	12.5×12.5	7×9
Tensile strength in machine direction (kN/m)	45	115	3.8
Tensile strength in transverse direction (kN/m)	34	115	13
Tensile elongation in machine direction (%)	30	2.5	23
Tensile elongation in transverse direction (%)	28	2.5	23
Mass per unit area (g/m^2)	200	405	180

4.3 Experimental Studies

A series of unsoaked laboratory CBR tests were conducted on unreinforced and reinforced subgrade-aggregate composite system with a single layer and double layer of geosynthetic reinforcement, in the conventional CBR mould of 150 mm internal diameter and having the height of 175 mm. To evaluate the effect of geosynthetic reinforcement on the performance of subgrade-aggregate composite system, the single layer of reinforcement was placed at the interface of subgrade and aggregate layer and the double layer of reinforcement was laid in such a way that the first reinforcing layer is placed at the interface of the subgrade and aggregate layers and another reinforcing layer is placed at the middle half of the compacted aggregate layer. These tests were conducted as described in IS: 2720 (Part 16), with single and double layer of reinforcement in order to check the consistency of the obtained results, many of them were repeated. The details of the experiments carried out are given in Table. 4.3.

The total height of the prepared specimen was maintained to 125 mm for all the unreinforced and reinforced subgrade-aggregate composite systems. Subgrade soil was filled in the CBR mould in 2 lifts and aggregate was filled in one lift. All these layers were compacted using a rammer of 2.6 kg weight, falling from a height of 310 mm and the number of blows on each

layer was 56. Aggregates were filled in two layers; each layer compacted with 28 blows, so that the total number of blows for the aggregate layer remained 56. During the compaction of the aggregate layer, a metal plate was used to avoid jumping of the aggregate from the CBR mould. Geotextile, geogrid and geomat were cut in the form of a circular shape of diameter slightly less than the diameter of CBR mould and placed inside it at the interface of subgrade and aggregate layer and sometimes within the aggregate layer also. Figure 4.2 shows the schematic sketch of the prepared subgrade-aggregate composite systems. Hence, the present study quantifies the improvement in strength of subgrade-aggregate composite system and the beneficial effect of various reinforcing layer at different positions.
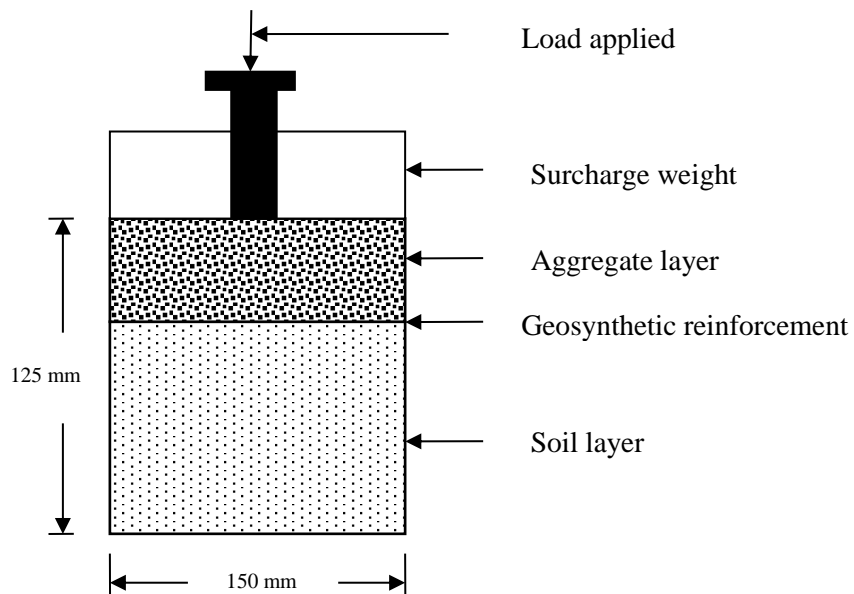
Figure 4.2 Schematic diagram of subgrade-aggregate composite system

Table 4.3 Details of the experiments carried out and results of CBR tests

Details of the test	Reinforcement	*CBR* Value (%)
Subgrade only	-	1.67
Subgrade-aggregate composite system	-	8.14
Subgrade-aggregate composite system reinforced with geotextile at the interface	Single layer of reinforcement	11.51
Subgrade-aggregate composite system reinforced with biaxial geogrid at the interface		9.13
Subgrade-aggregate composite system reinforced with geomat at the interface		4.81
Subgrade-aggregate composite system reinforced with double layer of geotextile, one at the interface and other within the aggregate layer	Double layer of reinforcement	6.35
Subgrade-aggregate composite system reinforced with double layer of biaxial geogrid, one at the interface and other within the aggregate layer		3.87
Subgrade-aggregate composite system reinforced with double layer of geomat, one at the interface and other within the aggregate layer		2.23

The load is applied through a plunger of 50 mm diameter. Before the testing, a surcharge weight of 5 kg was applied on the unreinforced and reinforced subgrade-aggregate composite system. The plunger was allowed to penetrate the prepared unreinforced and reinforced specimen at a rate of 1.25 mm/minute. Based on the load and penetration values recorded, the *CBR* values were computed from the load-penetration curves.

4.4 Results and Discussion

4.4.1 Effect of geosynthetic reinforcement

Figures 4.3 present the variation of the load-penetration curves obtained from the CBR tests conducted on unreinforced and reinforced subgrade-aggregate composite system. A clear comparison can be seen in between the unreinforced subgrade-aggregate and reinforced subgrade aggregate composite system with a single layer of reinforcement placed at the interface of subgrade and aggregate layer and double layers of reinforcement. The *CBR* values for the various composite systems are given in Table 4.3. The unreinforced and reinforced subgrade-aggregate composite system exhibited a good performance when compared to the subgrade only.

The *CBR* value of the unreinforced subgrade-aggregate composite system were found to be 8.14 %, which was increased to 11.51 % and 9.13 %, when geotextile and geogrid reinforcement was placed at the interface of subgrade and aggregate layer respectively. Further placing geomat reinforcement at same interface, reduces the *CBR* value to 4.81 %. Reduced *CBR* values were obtained as 6.35 %, 3.87 % and 2.23 %, when subgrade-aggregate composite system was reinforced with double layers of geotextile, geogrid and geomat reinforcement respectively as shown in Fig. 4.3. It was observed that an increase in the quantity of reinforcement led to degrades the performance of reinforced subgrade-aggregate composite system because placing the reinforcement layer very near to the load reduces its load carrying capacity. Only geotextile reinforcement and geogrid reinforcement, when placed at the

interface of subgrade-aggregate composite system performs better than the unreinforced subgrade-aggregate composite systems and other than these two reinforced systems, all of them performed poorly even in comparison with the unreinforced subgrade-aggregate composite system. The highest increase in *CBR* value was achieved when the subgrade-aggregate composite system was reinforced with geotextile at the interface because it prevents the intermixing of the aggregate and subgrade soil and maintaining a clean separation of the subgrade and aggregate layer. As geogrid and geomet have apertures and geotextile does not have aperture, there is a possibility of aggregates embedded into the subgrade soil during the loading.
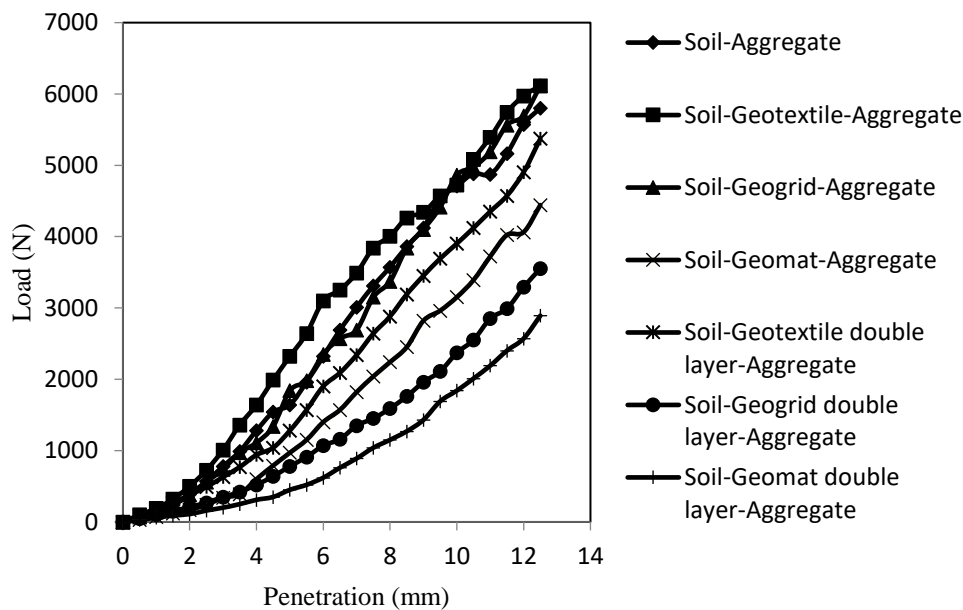
Figure 4.3 Load-penetration curve for geosynthetic reinforcement placed at different location

4.4.2 Effect of type of reinforcement

To understand the beneficial effect of using reinforcements in subgrade-aggregate composite systems, three geosynthetic materials namely, geotextile, geogrid and geomat were used at the interface of the subgrade and aggregate layers and an extra layer is place within the aggregate layer. Figure 4.4 shows the comparison of the load-penetration response for subgrade-

76

aggregate composite systems reinforced with geotextile, geogrid and geomat reinforcement at the interface of subgrade and aggregate layer over unreinforced system at optimum moisture content. The experimental results were analysed and compared to evaluate the beneficial effect of various geosynthetic reinforcement in improving the performance of the subgrade-aggregate composite system. It is clear that geotextile reinforced composite system yields the maximum strength and geomat reinforced composite system yields minimum strength even less than the unreinforced composite system. Figure 4.5 shows the comparison of the load-penetration response for subgrade-aggregate composite systems reinforced with double layer of geotextile, geogrid and geomat reinforcement, over unreinforced system at optimum moisture content. Again geotextile reinforced composite system with double layer of reinforcement yields the maximum strength but this gained strength is less than the unreinforced subgrade-aggregate composite system.
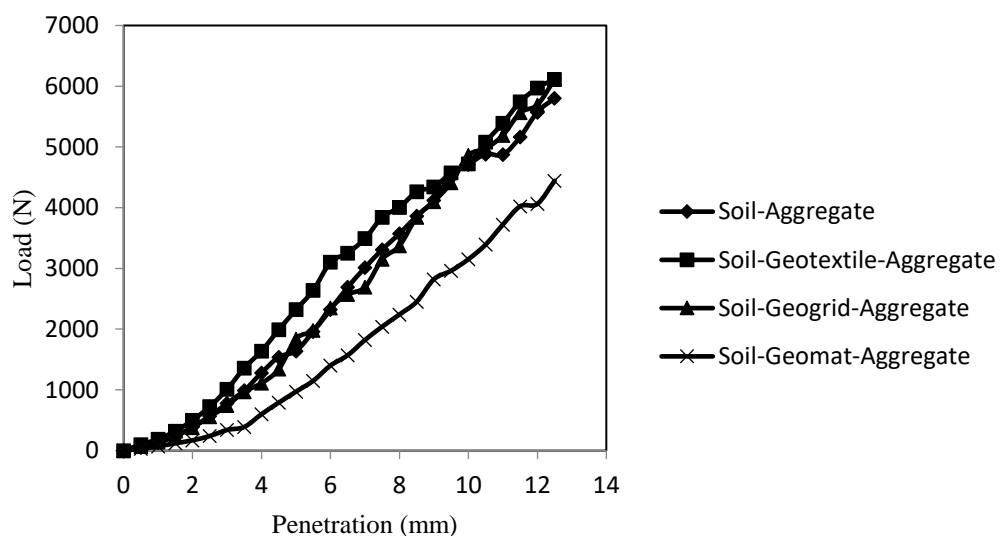
Figure 4.4 Load-penetration curve for geosynthetic reinforcement placed at the interface of subgrade and aggregate layer
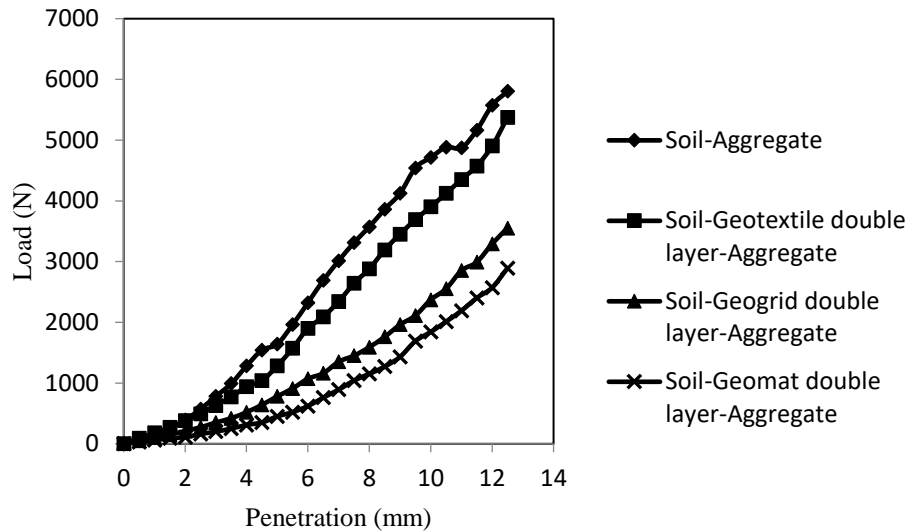
Figure 4.5 Load-penetration curve for double layer of geosynthetic reinforcement

Out of three types of geosynthetics used to reinforce the subgrade-aggregate composite system, the best performance was achieved by geotextile reinforcement. The reason for this is the separation function performed by the geotextile placed at the interface of subgrade and aggregate layer, which prevents the intermixing of both the layers. As geogrid and geomat have apertures, they may allow the intermixing of subgrade soil into aggregate layer during loading. Geogrid performance was not better than the geotextile because the few of the aggregates have size almost equal to the aperture size of the geogrid, which reduces the interlocking effect. Geomat results in low *CBR* because of its least tensile strength as compared to the other geosynthetics. The top layer of geomat was found to be partially damaged after the test. The ascending order of performance improvement was generally observed as geotextile, geogrid and geomat. This order of performance improvement was not the same as the order of increase in the tensile strength of the geosynthetic reinforcement. Though the tensile strength of geotextile is less than the geogrid but still it performs better than the geogrid because the reinforcing mechanism of geogrids and geotextiles are different. The performance of geotextile and geogrid were more effective than geomat in reinforcing the subgrade-aggregate composite system because of the high tensile strength of geogrid and good separation function served by

78

geotextile. The contribution of geomat in improving the strength/performance is least as compared to the other reinforcements.

4.5 Conclusions

Based on the results and discussion presented here, the following conclusions can be made:

1. The reinforced subgrade-aggregate composite system with reinforcement at the interface of subgrade and aggregate layer performs better than the reinforced subgrade-aggregate composite system with double layer of reinforcement.

2. Geotextile and geogrid reinforcement proved to be the most effective reinforcement and the contribution of geomat was least in improving the performance of subgrade-aggregate composite system.

3. The reinforced subgrade-aggregate composite system performs better than the unreinforced subgrade-aggregate composite system only in case of geotextile and geogrid reinforcement placed at the interface of subgrade and aggregate layer.

4. Contribution of geosynthetic reinforcement would be ineffective if it is not implemented at the suitable location.

References

Asha MN, Latha GM. Modified CBR Tests on Geosynthetic Reinforced Soil-aggregate Syatems. *Indian Geotechnical Conference*-2010, GEOtrendz, 16-18 December 2010, IGS Mumbai Chapter & IIT Bombay, pp. 297-300.

Asha MN, Latha GM. Bearing resistance of reinforced soil-aggregate systems. Proceedings of the Institution of Civil Engineers, *Ground Improvement* 2011; 164, Issue GI2, pp. 83-95. https://doi.org/10.1680/grim.2011.164.2.83.

Bender DA, Barenberg EJ. Design and behaviour of soil-fabric-aggregate systems. *Transportation Research Record* 1978; 671: 64-75.

Bureau of Indian Standards (1980). Methods of test for Soils: Determination of water content dry density relation using light compaction. IS 2720-7, New Delhi, India.

Bureau of Indian Standards (1987). Methods of test for Soils: Laboratory determination of CBR. IS 2720-16, New Delhi, India.

Duncan-Williams E, Attoh-Okine NO. Effect of geogrid in granular base strength - An experimental investigation. *Construction and Building Materials* 2008; 22:2180–4. doi: 10.1016/j.conbuildmat.2007.08.008.

Fannin RJ, Sigurdsson O. Field Observations on Stabilization of Unpaved Roads with Geosynthetics. *J Geotech Eng* 1996; 122:544–53. doi:10.1061/(ASCE)0733-9410(1996)122:7(544).

Giroud JP, Han J. Design Method for Geogrid-Reinforced Unpaved Roads. I. Development of Design Method. *Journal of Geotechnical and Geoenvironmental Engineering* 2004; 130 (8): 775–786. DOI: 10.1061/(ASCE)1090-0241(2004)130:8(775).

Giroud J P, Noiray L. Geotextile-reinforced unpaved road design. *J Geotech Eng* 1981;107(9):1233-54.

Hufenus R, Rueegger R, Banjac R, Mayor P, Springman SM, Brönnimann R. Full-scale field tests on geosynthetic reinforced unpaved roads on soft subgrade. *Geotext Geomembranes* 2006; 24:21–37. doi: 10.1016/j.geotexmem.2005.06.002.

Kamel MA, Chandra S, Kumar P. Behaviour of subgrade soil reinforced with geogrid. *Int J Pavement Eng* 2004; 5:201–9. doi:10.1080/1029843042000327122.

Shukla SK. An introduction to geosynthetic engineering 2016. CRC Press, London.

Singh M, Trivedi A, Shukla SK. Strength Enhancement of the Subgrade Soil of Unpaved Road with Geosynthetic Reinforcement Layers. *Transportation Geotechnics* 2019; 19: 54-56. https://doi.org/10.1016/j.trgeo.2019.01.007.

Subaida EA, Chandrakaran S, Sankar N. Laboratory performance of unpaved roads reinforced with woven coir geotextiles. *Geotextiles and Geomembranes* 2009; 27: 204-210. https://doi.org/10.1016/j.geotexmem.2008.11.009.

CHAPTER 5

STATIC AND DYNAMIC CONE PENETRATION TESTS ON GEOSYNTHETIC REINFORCED UNPAVED ROADS

This chapter is based on the paper published in International Journal of Geosynthetics and Ground Engineering, Springer, as listed in Section 1.6. The details are presented here with some changes in the layout in order to maintain a consistency in the presentation throughout the thesis.

5.1 Introduction

In the current road construction practice, application of geosynthetic reinforcement is a routinely used technique for stabilizing the unpaved roads. An unpaved road typically consists of an aggregate layer resting on the soil subgrade. When the unpaved roads are subjected to the traffic loads, the base course layer helps to distribute the vehicular load to the subgrade. Subgrade plays a vital role in the design of pavements. When the subgrade is weak, performance of the road can be improved by the inclusion of geosynthetic (geotextile and/or geogrid) reinforcement. The performance of geosynthetic-reinforced unpaved road is enhanced by reducing the thickness of aggregate layer required above the subgrade, reducing rut deformation, improving the durability of road, reducing construction and maintenance cost. Reinforcement also leads to reduce the time required for the construction of the roadway (Cuelho and Perkins, 2017). This chapter focuses on the use of geosynthetics, such as geotextile and geogrid, which are very commonly used for reinforcing the unpaved roads. Reinforcement and separation are the most benefited functions served by the geosynthetic in road construction. The reinforcement mechanism served by geogrid is lateral restraint and interlocking of aggregates, while the geotextile serves many functions in roadways, including separation

between the subgrade and aggregate base course, reinforcement through interaction interface friction, filtration and drainage (Shukla, 2016).

A penetrometer is a device, which is forced into the soil to quickly measure the resistance against vertical penetration. Penetrometers can be classified into two groups: static cone penetrometer (SCP) and dynamic cone penetrometer (DCP). In SCP tests, the penetrometer is pushed steadily into the soil at a constant force applied manually or with hydraulic power. It is an established routine test used for soil characterization and strength estimation (Schnaid et al., 2017). Hand-pushed SCP is economical to fabricate, easy to use and transport to the field site. However, it is difficult to maintain a constant force applied manually on the device which may produce variable results, especially when used by different users (Sun et al., 2011). Alternatively, in a DCP test, the penetrometer is driven into the soil by a hammer or falling weight. The DCP has been widely used for the pavement evaluation and in-situ strength of pavement layers and subgrade. Most common applications of DCP in pavement engineering is to measure the layer thickness of existing pavements, layer stiffness, resilient modulus, in-situ strength, pavement condition, and variation of granular bases and subgrade soil of existing pavement (Amadi et al., 2018; Chao et al., 2017; Chen et al., 2001; Chen et al., 1999; Gabr et al., 2000; Mohammad et al., 2007). DCP has been demonstrated as an excellent device because it is simple to operate on any pavement layer, portable, fast, quick measurements, and there is no need to excavate the subgrade or pavement layer before the test as required in the in-situ *CBR* tests, plate load tests, and sand cone tests. In-situ determination of *CBR* by the conventional method is time-consuming and requires costly equipment. To overcome this disadvantage, it is necessary to have an accurate, economical and reliable method for in-situ determination of *CBR* of subgrade soil and pavements. In the past, many correlations were developed by the researchers for prediction of commonly used design parameters in pavement design (*CBR* and subgrade modulus) from the DCP test results (Boutet et al., 2011; George et

al., 2009; Mousavi et al., 2018; Nguyen and Mohajerani, 2015). Such empirical relationships can be effectively used for highway projects. Design approach for low volume roads adopts in-situ strength of subgrade, and pavement layer thickness is calculated from the DCP device, rather than the soaked *CBR* value (Rolt and Pinard, 2016). However, the DCP device has also been used to provide compaction quality control and prediction of the effectiveness of rolling dynamic compaction (Ampadu et al., 2017; Kessler, 2009; Ranasinghe et al., 2017; Yang et al., 2015). Mo et al., (2017) discussed the mechanisms of soil displacement that occurs around a penetrometer while pushing its cone into the layered soils. Ma et al., (2015) proposed an approach for interpreting cone penetrometer data by identifying the layer boundaries and undrained shear strength in clay deposits using large deformation finite-element analyses.

Kwon and Tutumluer (2009) discuss the benefits of using geogrid for improving the performance of pavement by using DCP equipment for in-situ evaluation of unreinforced and geogrid-reinforced pavements. Shoulder performance was evaluated over for 10 months using a DCP device, whose subgrade was stabilized with three biaxial geogrids, which caused the improvement in the strength properties of the shoulder section (Mekkawy et al., 2011). DCP was also used for estimating the strength and elastic modulus of the multiple material layers of the Macadam stone base section reinforced with geotextile and geogrid (Li et al., 2017). Since limited studies are available on the use of DCP and digital SCP devices for performance evaluation of geosynthetic-reinforced pavements, this study focuses on the use of these devices for evaluating the benefits of geosynthetic reinforcement in unpaved roads. Laboratory and field tests were performed on the unreinforced, geotextile-reinforced and geogrid-reinforced unpaved test sections at the optimum moisture content for investigating the mechanism responsible for the improvement in the performance of reinforced test sections.

5.2 Materials

5.2.1 Subgrade

Locally available soil was used as the subgrade soil for field experiments. Representative samples of subgrade soil were obtained from the campus of Delhi Technological University to represent the subgrade material for unpaved test section and the physical properties of the soils were determined in the laboratory. The subgrade soil is classified as silty sand (SM) according to the Unified Soil Classification System with a liquid limit of 29% and a plastic limit of 20%. The soil has a maximum dry unit weight of 18.6kN/m^3 and an optimum moisture content of 13.9%, as determined by the standard Proctor compaction tests. The grain size distribution curve for the subgrade soil is shown in Fig. 5.1. California Bearing Ratio (*CBR*) of the soil used for the preparation of subgrade is 1.9%. Strength of subgrade soil can be improved through the inclusion of geosynthetic reinforcement.

5.2.2 Base course material

The stone aggregates were used to represent the base course material for unpaved test section and they are designated as well-graded gravel (GW) as per the Unified Soil Classification System. The aggregates used in the study were obtained from the nearby quarry site. The size of the aggregate varies from 4.75mm to 12.5 mm. The base course material has a specific gravity of 2.65. The particle size distribution curve for aggregate is shown in Fig. 5.1. The granular material of various sizes was collected and then sampled such that the sample belongs to the grade-III of the base course material as per MORTH (Ministry of Road Transport and highways), New Delhi, India. The maximum dry unit weight obtained was 20.3kN/m^3 at a water content of 5.2%.
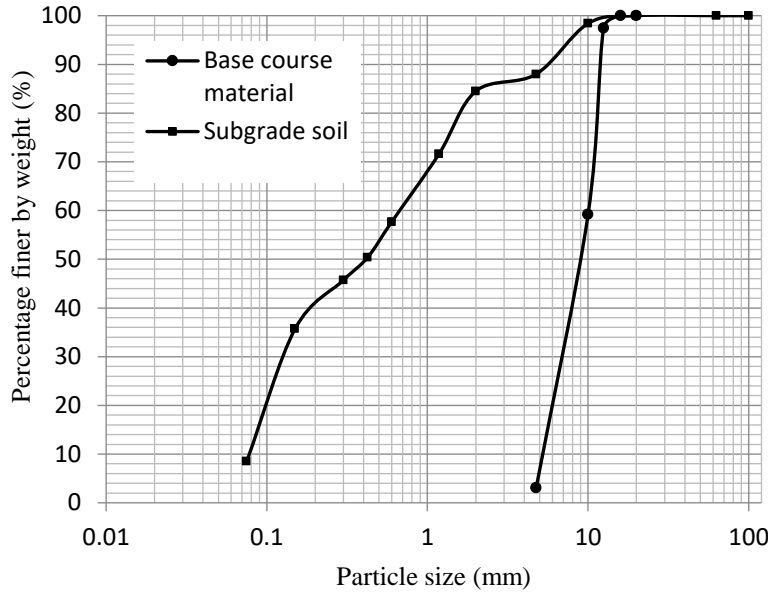
Figure 5.1 Particle size distribution curve of base course material and subgrade soil

5.2.3 Geosynthetics

Geosynthetic reinforcement used in this study to prepare the reinforced unpaved test sections were geotextile and geogrid. Both geotextile and geogrid were placed at the interface of the subgrade and aggregate layer for all the field tests. Geotextile used in the experiments is a polypropylene multifilament woven fabric, and it is resistant to chemicals and micro-organisms found in soil. Geotextile has a tensile strength of 45kN/m in the machine direction and 34kN/m in the cross-machine direction. Puncture strength of geotextile is 480 N, and tensile elongations in the machine direction and cross-machine direction are 30% and 28%, respectively. The properties of geotextile are presented in Table 5.1.

Geogrid is made of perforated polypropylene sheet with ribs, which are capable to provide best possible mechanism between geogrid and granular particles by preventing the horizontal movements of granular particles and displacements. Geogrid properties are illustrated in Table 5.2. Geogrid has an aperture size of 30mm × 30mm and the stiffness at 0.5% strain in the machine direction is 550-kN/m and 350-kN/m in the cross-machine direction. The ability of

geogrid to restrict the horizontal movement of soil particles when placed at the interface of the subgrade and aggregate layer depends on the coefficient of interface friction between the soil and geosynthetics. The interface coefficient of friction (soil/geosynthetic) was determined as 1.78 by measuring the force required for pulling out a geogrid that is fully embedded in the standard soil as provided by the manufacturer. Fig. 5.2 shows the photographs of these two types of geosynthetics used in the present study.

Table 5.1 Properties of geotextile used in the study

Property	Value	Test method
Tensile strength (kN/m)	45×34 (MD $\times$ CMD)[a]	ASTM D4595
Punture strength (N)	480	ASTM D4833
Apparent opening size (mm)	0.075	ASTM D4751
Mass per unit area of fabric (g/m^2)	200	ASTM D5261

[a] MD: Machine direction; CMD: Cross-machine direction
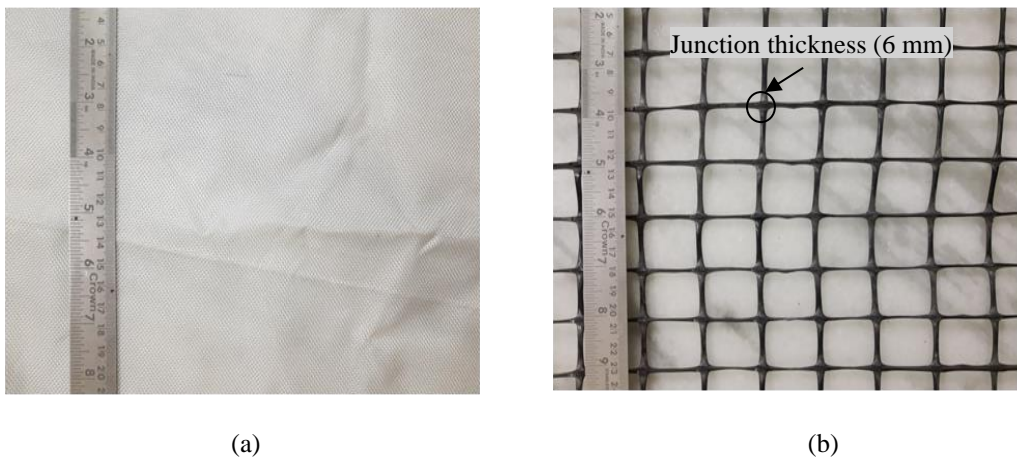
Figure 5.2 Geosynthetics used in the study: (a) Geotextile; (b) Geogrid

Geosynthetics, mainly woven geotextile and geogrid, are used to reinforce the weak soil subgrade. In the present study, the selection of geotextile and geogrid as different types of

geosynthetics have been done in view of the local availability as well as aiming at investigating their effectiveness through the variation in reinforcing mechanisms. Geotextile interacts with soil mainly through interface shear resistance while the geogrid significantly contributes to reinforcement through passive resistance to soil particles against the ribs as a result of interlocking (Shukla, 2016; Koerner, 2012).

Table 5.2 Properties of geogrid used in the study

Characteristics	Property	Value	Test method
Physical characteristics	Structure	Bi-axial geogrid	–
	Color	Black	–
	Aperture shape	Quadrangular	–
	Polymer type	Polypropylene	–
Technical characteristics	Aperture size (mm)	30×30 (MD $\times$ CMD)[a]	–
	Stiffness at 0.5 % strain(kN/m)	550×350 (MD $\times$ CMD)[a]	ISO 10319[c]
	Transversal rib width (mm)	2.6	–
	Longitudinal rib thickness (mm)	3.8	–
	Junction thickness (mm)	6	–
Performance characteristics	Aperture coefficient of friction (soil/geosynthetics)	1.78 at 10 kPa and 1.14 at 20 kPa	EN 13738[b]
	Installation damage factor	1	ASTM D5818

[a] MD: Machine direction; CMD: Cross-machine direction
[b] Pullout testing in accordance to EN 13738 using special apparatus that measures the force required to pull-out a geogrid that is fully embedded in soil. Test with a sample of length of 400mm.
[c] Tests performed using extensometers

5.3 Field investigation

5.3.1 Dynamic cone penetrometer device

The characteristics of the DCP equipment used in this study are shown in Fig. 5.3 meet the specifications of ASTM D6951-03. The equipment consists of a 60^0 cone with a 20-mm base diameter connected at the end of a 16-mm diameter rod. The rod was held vertical during testing and the 8 kg hammer was raised over the full height of 575-mm and allowed to fall freely over the surface of the test section to drive the cone through the compacted subgrade and aggregate layer. It is necessary to ensure that while raising the hammer upward, it was allowed to touch the bottom of the handle but not lifting the cone before it was allowed to drop. Improper raising and dropping of the hammer could be a source of error in DCP data. The penetration for the first blow was discounted because the imprint area of the cone tip for the first blow is smaller than that of the subsequent blows. The diameter of the cone is slightly greater than the diameter of the rod, just to ensure that the resistance to penetration offered by the soil is exerted on the cone (George et al., 2012). The penetration depth is recorded for each blow. The dynamic cone penetration index (*DCPI*) is defined as the penetration depth per blow of the hammer (mm/blow). The results are expressed in terms of *DCPI,* and it is calculated using Eq. (1) (Chennarapu et al., 2018). Alternatively, the penetration was plotted against the cumulative number of blows to obtain the gradient as the *DCPI* (slope of the line of best fit is defined as the *DCPI*, expressed in mm/blow) (Ampadu and Fiadjoe, 2015).

$$DCPI = \frac{P_{(i+1)} - P_{(i)}}{N_{(i+1)} - N_{(i)}} \tag{1}$$

where *DCPI*=dynamic cone penetration index (mm/blow); $P_{(i)}$ and $P_{(i+1)}$ are cone penetration values at i and i+1 hammer drops (mm); and $N_{(i)}$ and $N_{(i+1)}$ are blow counts corresponding to $P_{(i)}$ and $P_{(i+1)}$, respectively. The data obtained from the DCP testing were interpreted to obtain a representative *DCPI* value of the subgrade and base course layer by a relationship described

in Eq. (2) (Chennarapu et al., 2018). DCP test data were used to establish the boundaries between the layers, which were identifiable by sudden changes in the slope of the cumulative number of blows versus the penetration depth profile.

$$DCPI_{avg} = \frac{\Sigma_i^N DCPI}{N}$$ (2)

Where N= total number of $DCPI$ values recorded in a given depth of penetration.
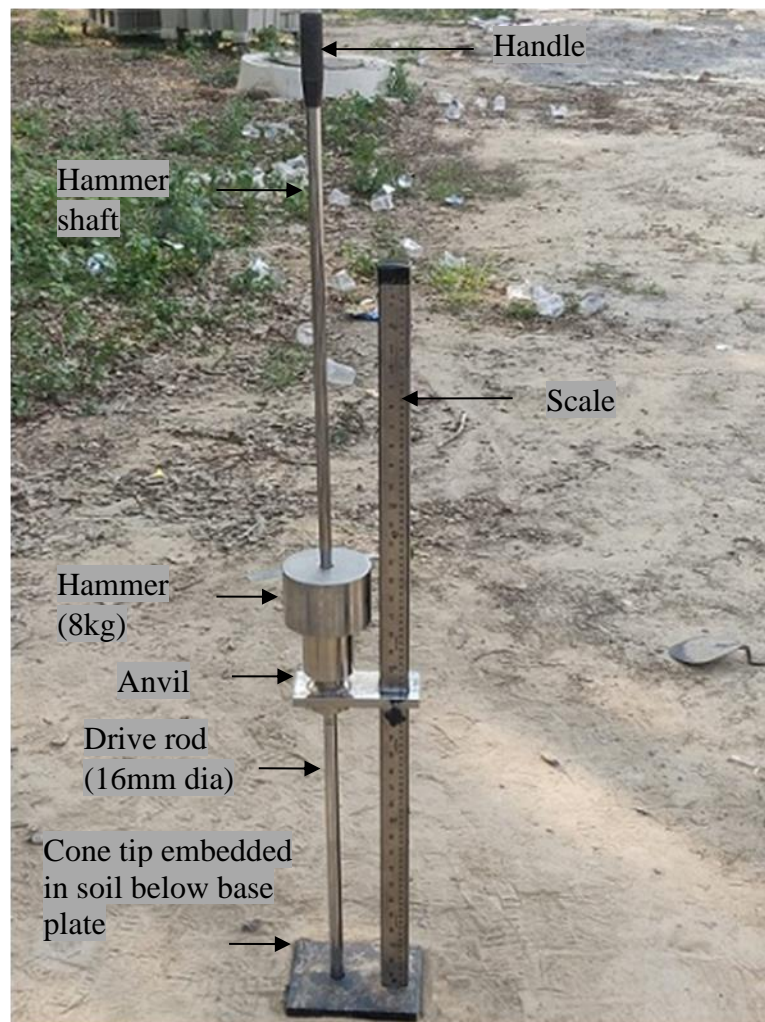
Figure 5.3 Dynamic Cone Penetrometer device in the field

5.3.2 Digital static cone penetrometer device

A standard static cone penetrometer (SCP) test is a cost-effective test used for site exploration, determining layer thickness of pavement and its strength properties. In SCP test, the cone tip was hydraulically pushed into the soil at a constant rate of penetration, and the cone tip resistance and sleeve friction resistance were recorded. In the present study, digital SCP was used which consists of a measuring body with two push handles, a drive rod of 16-mm diameter and 498-mm long, 60°cone assemble at the bottom of drive rod, LVDT ranged from 0 to 200-mm, data acquisition system with USB output device and one load cell with a capacity of 300 kg, as shown in Fig. 5.4.
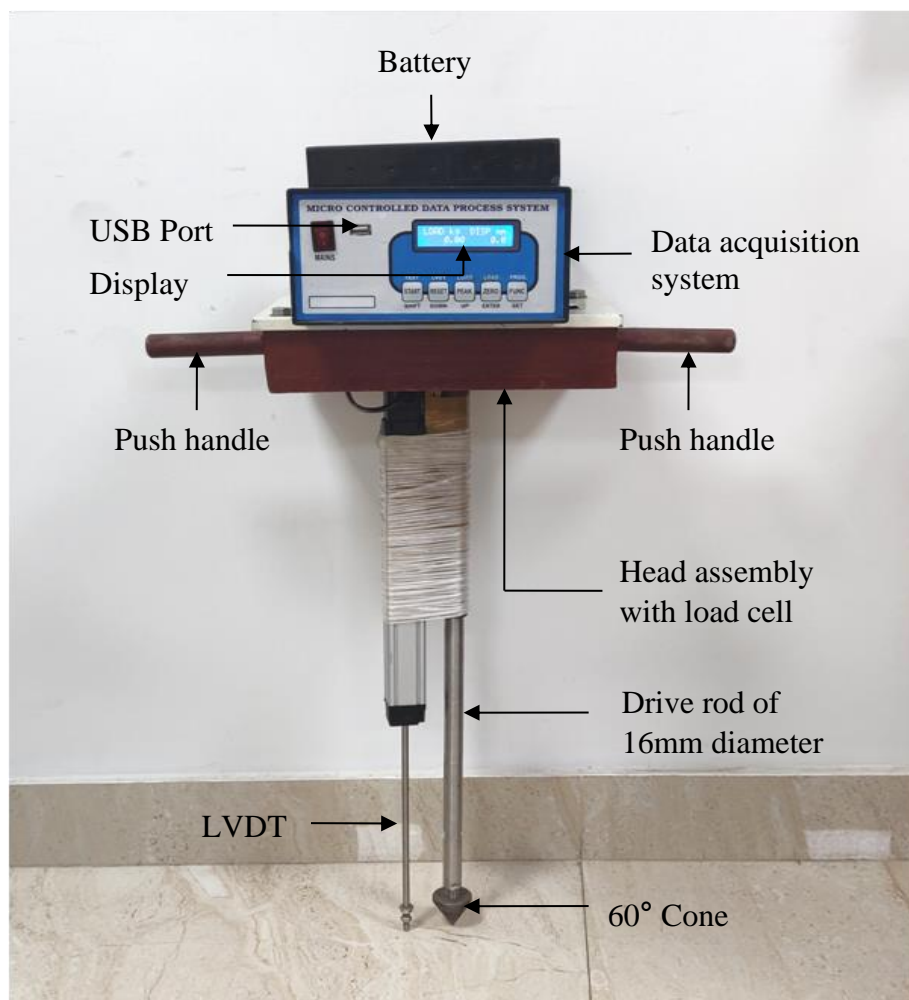
Figure 5.4 Digital static cone penetrometer

The digital SCP is a hand-held instrument that can easily penetrate to sub-base and subgrade soils. A consistent load was applied with the help of body weight by pushing the push handles provided at the head assembly of the digital SCP, which penetrates the cone connected to the drive rod into the soil. During the testing, both the load cell and LVDT work simultaneously. The Load cell helps to measure the applied load and LVDT measures the penetration of the digital SCP. Both of them send the electrical signal to the data acquisition system which converts the analog signal to digital. The digital SCP was held vertical to the ground level. While pushing the handles of digital SCP, jerks were avoided because it could have affected the output data. The data obtained from the load cell and LVDT were stored automatically in the USB output device in a tabular format comprises of two columns: load and displacement. Once, the applied force results in a negligible change in the magnitude of penetration then stop penetrating the device into the soil. Because it could result in inaccurate readings and damage the cone, drive rod or load cell.

5.3.3 Field location description and construction of test section

A total of three unpaved test sections were constructed in the field for evaluating the performance of geosynthetic-reinforced test section using DCP and digital SCP tests at the campus of Delhi Technological University. Fig. 5.5 illustrates the typical cross-section of the unpaved test section which consists of a 120-mm thick base course, 280-mm thick prepared soil subgrade and geosynthetic placed at the interface of base course and subgrade for reinforcement. To conduct the field study, one unreinforced and two geosynthetic-reinforced test sections were constructed with dimensions of 500-mm long, 500-mm wide and 400-mm deep. Fig. 5.6 shows the dimensions of the test section and the construction process for preparing it.
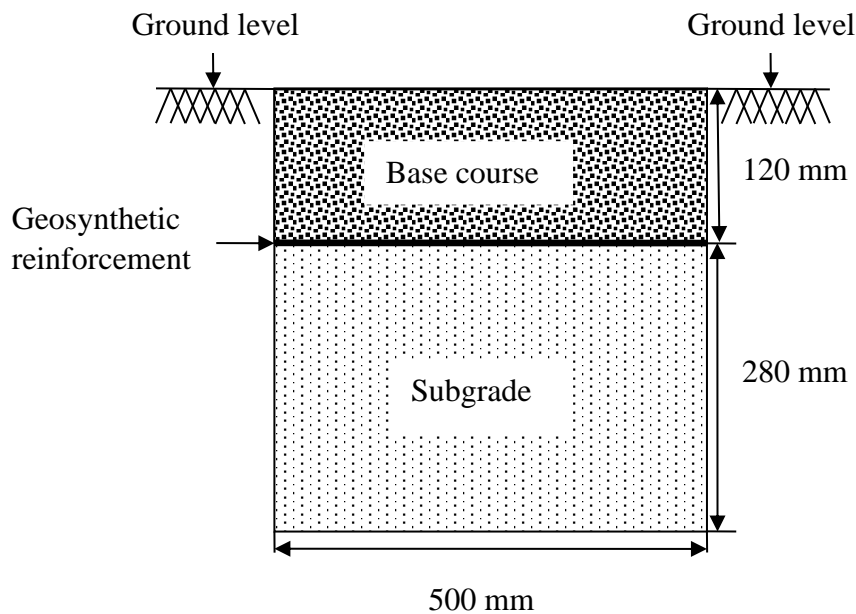
Figure 5.5 Typical cross-section of the geosynthetic-reinforced unpaved test section

The soil subgrade was prepared by compacting soil in two equal lifts at 13.9 % moisture content. After preparing the subgrade at this optimum moisture content, a geosynthetic reinforcement layer was placed on the top of the subgrade in the reinforced unpaved test section. Geotextile and geogrid were used as geosynthetic reinforcement to prepare reinforced test section. After placing the geosynthetic reinforcement layer, the aggregate layer was laid over it and compacted. Subgrade and base course layer were prepared by manual compaction. For compaction, a rammer of weight 8 kg is used and a free fall of 50 cm was considered. Base course was compacted in a single lift of 120 mm thickness using the rammer to achieve 91% of the maximum dry density at the optimum moisture content. The surface dressing was on the finished top of the aggregate layer. For each unpaved road test section, the tests were performed at five distinct points named 'A', 'B', 'C', 'D', and 'E'. The DCP tests were performed at the centre of the unpaved test section named as 'A' and digital SCP tests were performed at four locations around the centre point named as 'B', 'C', 'D' and 'E'. The detailed layout of the field testing locations of DCP tests and digital SCP tests are illustrated in Fig. 5.7. The DCP

tests were conducted to measure the in-situ strength of base course and subgrade material in terms of *DCPI* in mm/blow.
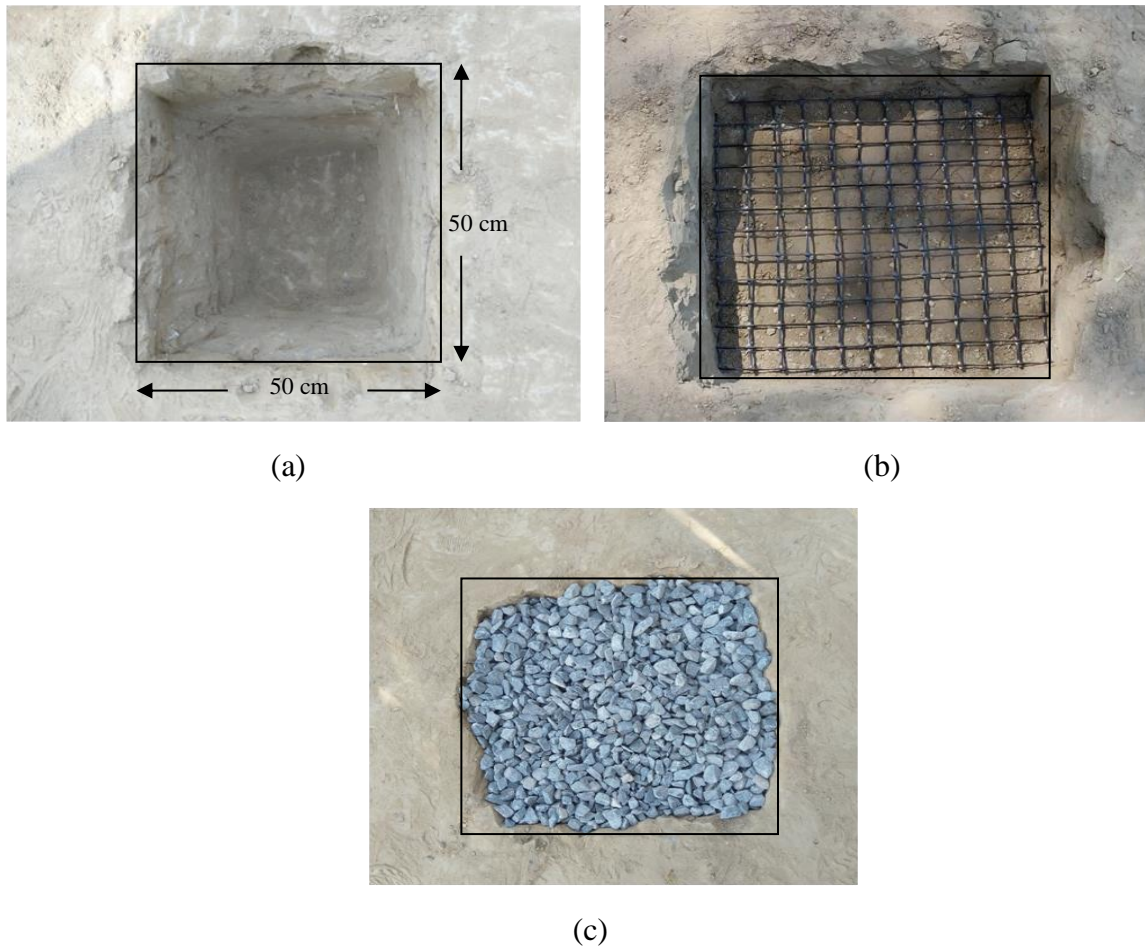
Figure 5.6 Construction details of geosynthetic-reinforced unpaved test section: (a) Construction of test section with dimension 500-mm × 500-mm; (b) 280-mm thick compacted subgrade soil with geogrid reinforcement layer on top; (c) 120-mm thick compacted aggregate layer on the reinforcement layer.

The strength and stiffness of the individual layer of the unpaved test section significantly influence the performance and durability of the overall test section. All the field tests on the unpaved test section were conducted with and without geosynthetic reinforcement. To study

the influence of geosynthetic reinforcement on *DCPI* measured by DCP test, geotextile and geogrid were used as reinforcement layers at the interface of the subgrade and aggregate layer. The maximum number of blows in this study was chosen as 153. During the DCP testing on both the geosynthetic-reinforced test sections, number of blows versus penetration is recorded. It was found that for maximum number of blows, maximum penetration depths of 545 mm and 350 mm are obtained for geogrid-reinforced test section and geotextile-reinforced test section, respectively. Maximum penetration depth is greater than the depth of test section. But in case of unreinforced test section, the cone reaches to the maximum penetration depth of 545 mm corresponding to 79 number of blows only. Hence, the number of blows and the corresponding penetrations was recorded up to a depth of penetration of 545-mm for unreinforced and geogrid-reinforced test sections and 350-mm for geotextile-reinforced test section.
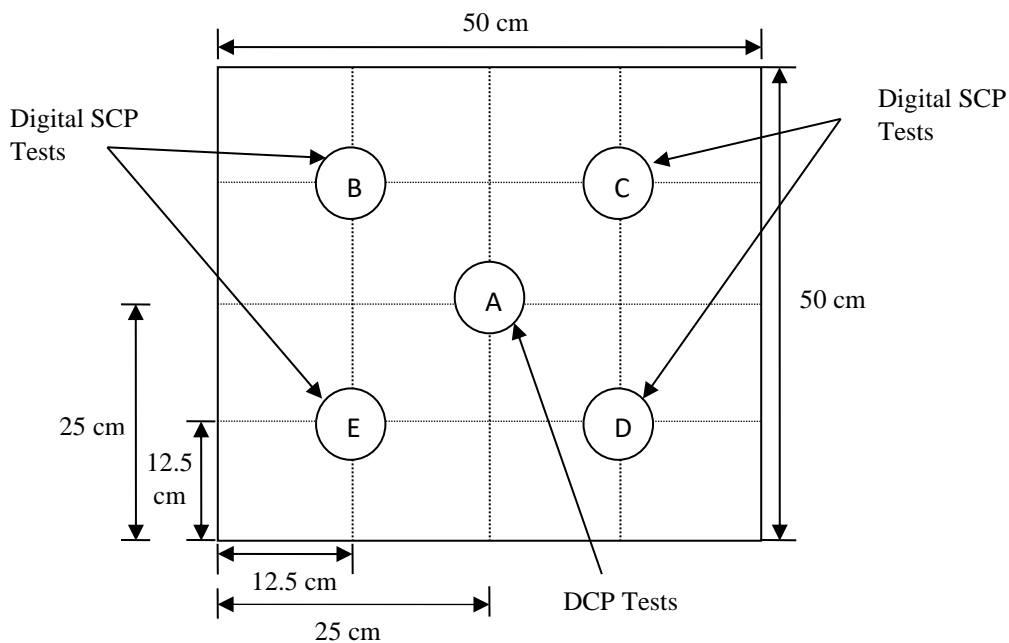
Figure 5.7 Layout of the unpaved test section measurements and testing locations of DCP and digital SCP tests

5.4 Results and discussion

5.4.1 Analysis of DCP data along depth of penetration

Dynamic cone penetrometer tests were performed at location 'A' in both reinforced and unreinforced road test sections of this study. The DCP test results were used in distinguishing the base course and subgrade layer, which mark the boundaries between the subgrade and aggregate layer due to the presence of geosynthetic reinforcement. Fig. 5.8 shows the DCP blow counts versus the penetration depth of the cone into the unpaved test section reinforced with geotextile, geogrid, and unreinforced test section. DCP device is placed on the surface of test section to be tested and the penetration depth for the first two blows was recorded as a reference reading called the initial reading. Initial reading is the point from where the subsequent penetration depth is recorded. The test section consisted of two distinct layers along with the reinforcement layer. The graph plotted between the number of blows versus depth helps to observe the change in slope for each layer. It is difficult to find the exact position of the interface because a transition zone exists between the base course and subgrade layer. This transition zone is more visible in the plots due to the presence of the geosynthetic reinforcement layer.

Figure. 5.9 and 5.10 presents the variations in the DCP blow counts with penetration depth for aggregate layer and subgrade layer individually to identify the transition zone. Fig. 5.9 shows a clear distinction between the aggregate layer and subgrade when geotextile is used as reinforcement layer as compared to the geogrid-reinforced and unreinforced test sections. Fig. 5.10 depicts that it is difficult to identify the transition zone between the subgrade and the natural ground surface, especially for unreinforced test section and cannot be observed for geotextile-reinforced test section because the cone penetrates only up to 350-mm depth which is less than the depth of test section. The DCP test results were recorded for 153 number of blows for each geosynthetic-reinforced test section. It was observed that for the same number

of blows the cone penetrates to the depth of 350-mm and 545-mm for geotextile-reinforced and geogrid-reinforced test sections, respectively. For unreinforced test section, cone reaches to the penetration depth of 545-mm corresponding to 79 number of blows. The cone reaches to a maximum penetration depth of 545 mm, which is greater than the depth of test section; hence the soil surface below the test section is represented as the natural ground. Since the thickness values of the aggregate layer and subgrade layer are 120-mm and 280-mm, respectively, the subsequent calculation of *DCPI* is based on the DCP data along the depth of test section. The *DCPI* values range from 3 mm/blow to 8.5 mm/blow for the aggregate layer and 1 mm/blow to 7 mm/blow for the subgrade layer. Overall *DCPI* values obtained for geogrid-reinforced, geotextile-reinforced and unreinforced test sections are 4.38 mm/blow, 2.04 mm/blow and 6.33 mm/blow, respectively.
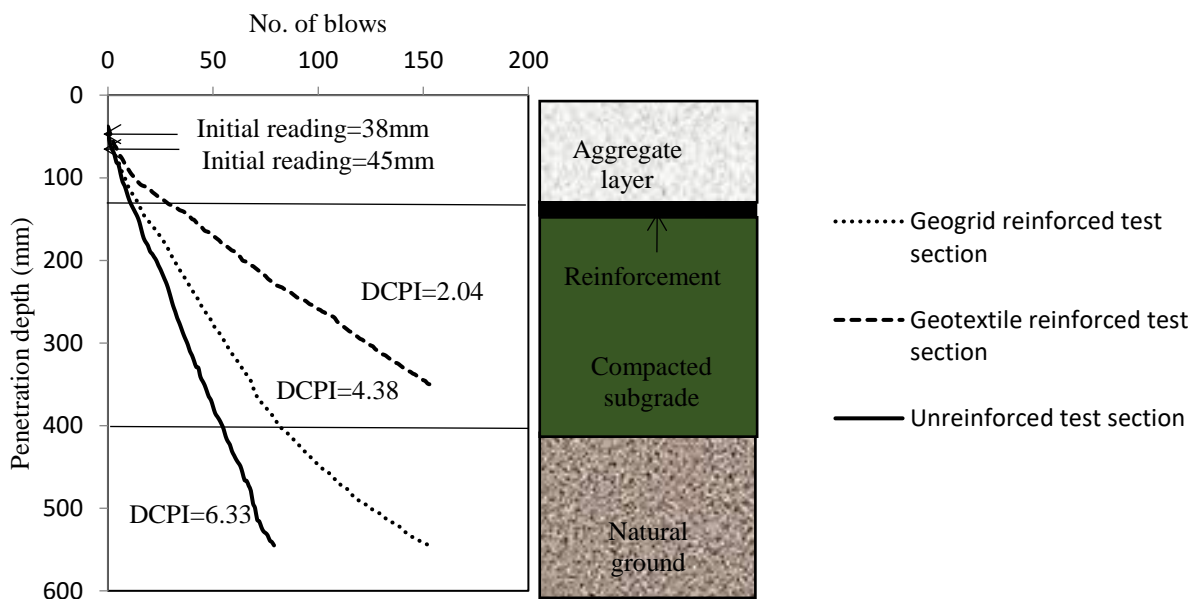
Figure 5.8 DCP test data for unreinforced and geosynthetic-reinforced test sections
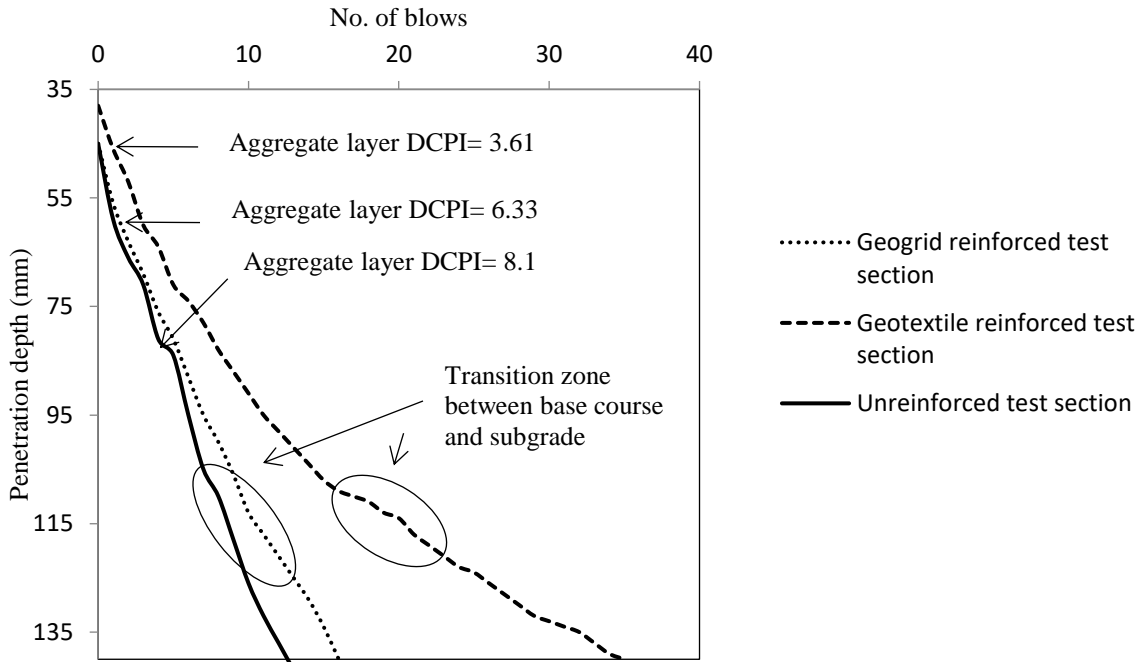
Figure 5.9 DCP test data for aggregate layer of unreinforced and geosynthetic-reinforced test sections
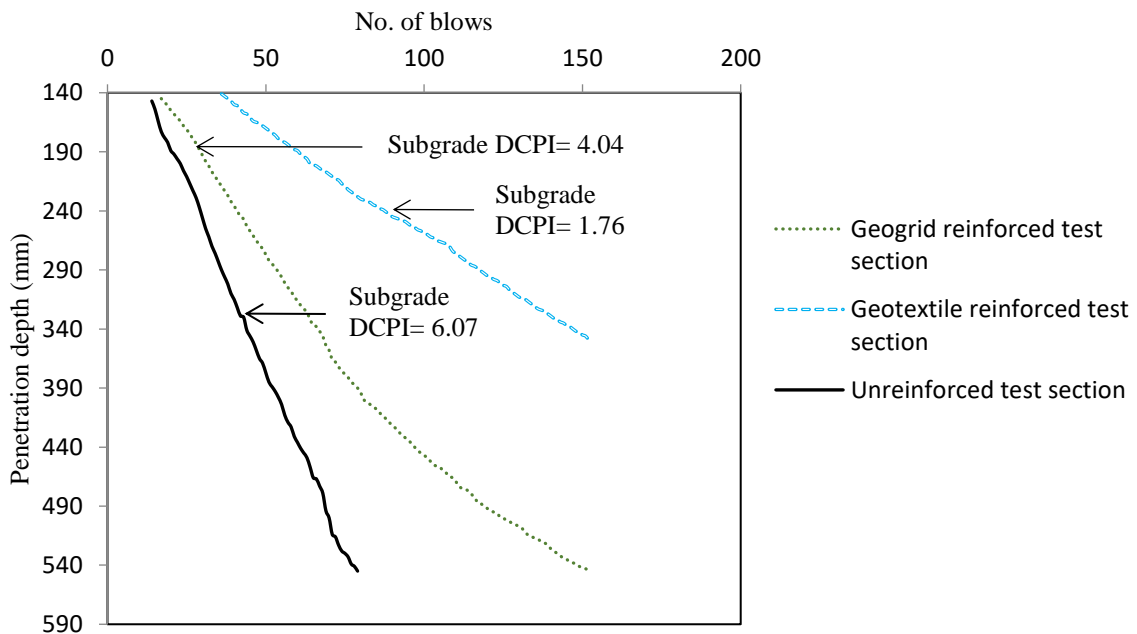
Figure 5.10 DCP test data for subgrade layer of unreinforced and geosynthetic-reinforced test sections

The subgrade has lower *DCPI* value than the granular layer because of better particles frictional interaction and interlocking mechanism. A decrease in *DCPI* value was observed for both geotextile and geogrid reinforced test sections as compared to the unreinforced test section. Sayida et al., (2019) also reported that a decrease in *DCPI* value was obtained for the reinforced one as compared to the unreinforced one. These values of *DCPI* indicate that the resistance to penetration is more in the reinforced test section as compared to the unreinforced test section. The percentage decrease in *DCPI* value of the geotextile-reinforced test section is 67.8 % and 30.8% for the geogrid-reinforced test section.

The typical *DCPI* results obtained for geotextile-reinforced, geogrid-reinforced and, unreinforced test sections are shown in Fig. 5.11. The profile of the graph plotted between the *DCPI* and penetration depth shows the change in the strength of the unpaved test section along with the depth. The *DCPI* profile moves towards the left as the strength is improved. *DCPI* profile for the geotextile-reinforced test section is on the extreme left and for the unreinforced test section; it is on the extreme right. The *DCPI* values signify that the geotextile-reinforced test section has the greatest resistance to penetration. Both, geotextile and geogrid help to improve the performance of the reinforced test sections as compared to the unreinforced test section. Among both the geosynthetics, geotextile has more benefits in improving the performance of the test section in terms of *DCPI* as compared to the geogrid. Difficulty was faced in removing the instrument after completing the DCP tests as it was penetrated to a certain depth and inappropriate way of applying load to get the device out of the test section may cause damage to the device. Fig. 5.12 shows the condition of geotextile and geogrid after the completion of DCP tests. It has been observed that the ribs of geogrid and nearby area of geotextile around the DCP rod got damaged.
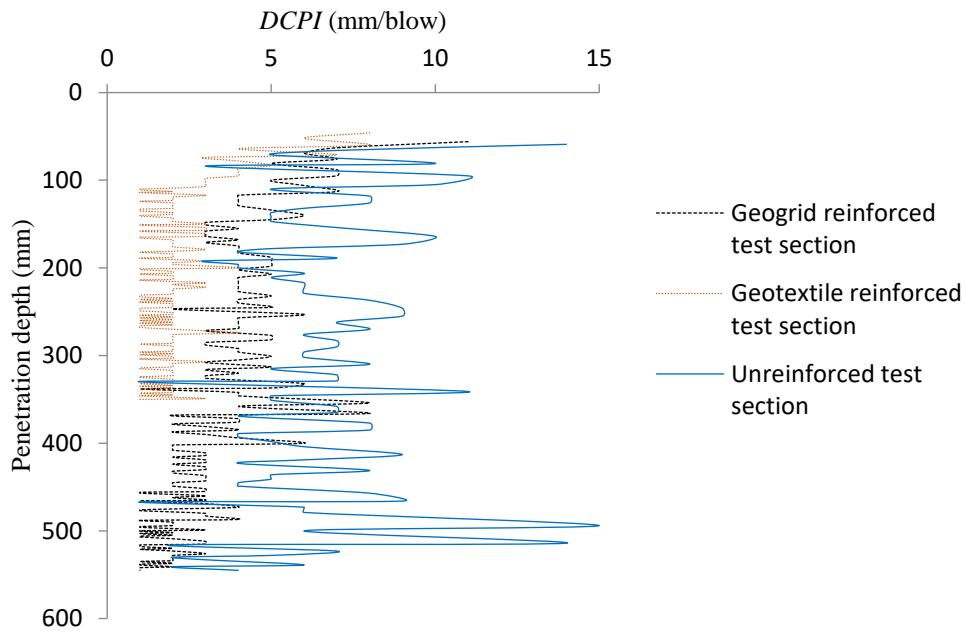
Figure 5.11 The profile representing the change in strength for unreinforced and geosynthetic-reinforced test sections along the penetration depth

| (a) | (b) | (c) |

Figure 5.12 Condition of geosynthetics after DCP test: (a) Deformed shape of geogrid; (b) easy to separate aggregates due to the presence of geotextile for the removal of DCP rod after test; (c) deformed shape of geotextile.

5.4.2 Digital static cone penetrometer resistance

Figure 5.13 presents the load-displacement behaviour of geotextile-reinforced and geogrid-reinforced test section. Digital SCP tests were performed at location 'B', 'C', 'D' and 'E' in both the geosynthetic-reinforced test sections. Almost the same results were obtained at two test locations 'B' and 'E' out of four testing locations in both the geosynthetic-reinforced test sections. Due to this reason, only three testing location results were illustrated in Fig. 5.13 for geotextile and geogrid-reinforced test sections. Digital SCP results are not identical at all the testing locations but they follow a similar pattern for each reinforced test section. Load-displacement results clearly show that the geotextile-reinforced test section has greater resistance against applied load as compared to the geogrid-reinforced section. Digital SCP can be used for estimating the strength characteristics of fine-grained soils used for pavement subgrade. This device is used on granular layer of the test section to find out its usefulness. The presence of granular material will either stop penetration or may deflect the cone. However, this device is used on granular material to evaluate the penetration resistance even for a smaller depth. It was not capable of penetrating up to a depth of 120-mm with an application of consistent load, where a geosynthetic reinforcement layer is located. Hence, it should not be used in granular materials. This attempt was made to utilize the benefits of digital SCP like, automatic data storage, low cost, only one person can operate the device and easy to handle.
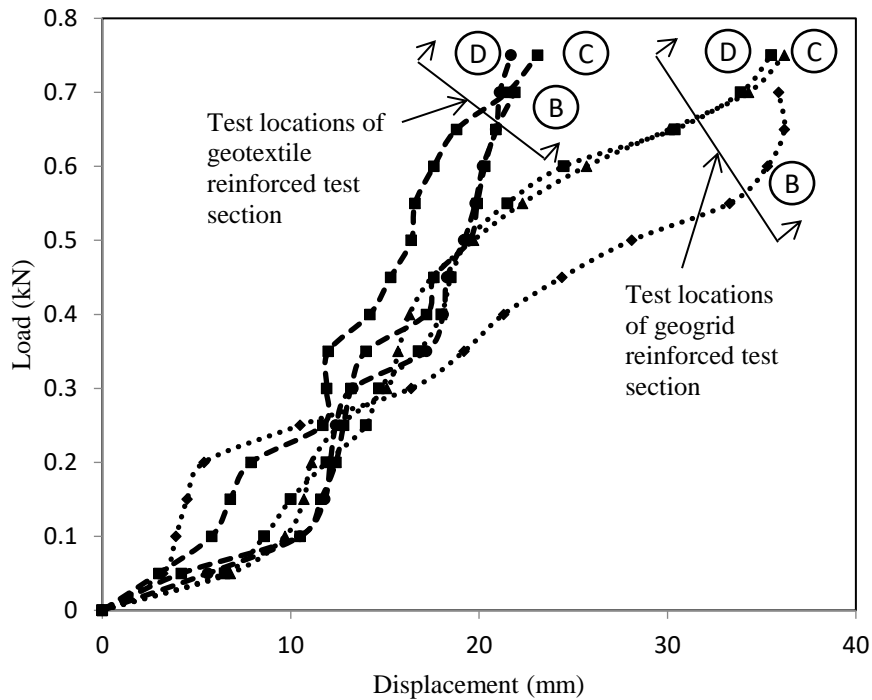
Figure 5.13 Load-displacement curve obtained from digital SCP data for geotextile and geogrid-reinforced test sections.

5.4.3 Influence of geosynthetic reinforcement

To investigate the effect of different types of geosynthetic reinforcement, geotextile and geogrid were used to reinforce the unpaved test section. The performance of the unpaved test section reinforced with geosynthetic at the interface of subgrade-base course depends on various factors such as strength and stiffness of subgrade and base course, type of geosynthetic, properties and characteristics of geosynthetics, location of geosynthetic reinforcement, the thickness of base course and relative contribution of the various reinforcing mechanism. In the present study, some factors were kept the same for all the laboratory and field test sections, such as; same subgrade and base course material; same base layer thickness, and same location of reinforcement. Keeping these parameters identical for all the test sections, the comparison will be easier between the geotextile and geogrid reinforcement in improving the performance. Both the geosynthetic-reinforced test sections behave differently because of the different

properties of geosynthetics and reinforcing mechanisms. Geotextiles are typically used to perform the separation and reinforcement functions (Tingle and Jersey, 2005). Geotextile prevents the intermixing of subgrade soil and base course material. The inclusion of geogrid provides lateral restraint to the base course material, which significantly reduced the lateral movement of the aggregate layer and helps to enhance the performance. However, a geogrid can also provide some degree of subgrade-base separation as a secondary function because of its adequate aperture size. If fine particles of the subgrade soil intrude into the base course, the effectiveness of the interlocking action between the base course material and geogrid is likely to be reduced. Incorporation of geosynthetic reinforcement at the interface of subgrade-aggregate section leads to improve the strength in both laboratory and field tests. Geogrid has higher strength and stiffness than geotextile but the geotextile-reinforced test section performed better than the geogrid-reinforced test section. The beneficial and contributing factor responsible for the improvement in overall performance of reinforced test section over unreinforced test section is increased resistance to penetration offered by a geotextile. Both, properties of geosynthetics and reinforcing mechanisms have some degree of contribution to the performance improvement of the test section. The mechanisms that govern the test section performance are complex. The improvement by the geosynthetic reinforcement layer was found to be more pronounced in the field tests rather than the laboratory tests.

5.5 Conclusions

This chapter presents the field studies evaluating the performance of the geosynthetic-reinforced test section using dynamic cone penetrometer and digital static cone penetrometer. To investigate the benefits of geosynthetic reinforcement, geotextile and geogrid were placed at the interface of the subgrade and base course layer in test section. Unreinforced test section results were compared with the results of geosynthetic-reinforced test sections. Based on the results and discussion, as presented earlier, the following conclusions can be made:

1. The DCP test results were found to be influenced by the inclusion of geosynthetic reinforcement. The lowest *DCPI* value was obtained for the geotextile-reinforced test section. *DCPI* indicates the resistance to penetration; a greater penetration resistance is observed for reinforced test section as compared to the unreinforced test section.

2. The behavior of the reinforced test section was significantly better than that of the unreinforced test section, with the best performance served by the geotextile-reinforced test section.

3. The results demonstrated that DCP was able to detect significant changes in the strength of base and subgrade layers through the profile of the test section along with the depth. It can also be used to delineate the transition zone of the base course and subgrade layer. However, the digital SCP results did not reflect changes in layer because the device was not able to penetrate up to the depth of the reinforcement layer with the application of load.

4. The geogrid has higher strength and stiffness than the geotextile, but the better performance was observed when the geotextile reinforcement layer was placed at the base-subgrade interface than that of the geogrid reinforcement layer placed at the same location. Higher resistance to penetration offered by the geotextile had more contribution in improving the performance of the test section.

References

Amadi AA, Sadiku S, Abdullahi M, Danyaya HA. Case study of construction quality control monitoring and strength evaluation of a lateritic pavement using the dynamic cone penetrometer. *International Journal of Pavement Research and Technology* 2018; 11(5):530-539. https://doi.org/10.1016/j.ijprt.2018.07.001.

Ampadu SIK, Ackah P, Nimo FO, Boadu F. A laboratory study of horizontal confinement effect on the dynamic cone penetration index of a lateritic soil. *Transportation Geotechnics* 2017; 10: 47–61. http://dx.doi.org/10.1016/j.trgeo.2016.12.002.

Ampadu SIK, Fiadjoe GJY. The influence of water content on the Dynamic Cone Penetration Index of a lateritic soil stabilized with various percentages of a quarry by-product. *Transportation Geotechnics* 2015; 5:68–85.

Boutet M, Dore G, Bilodeau J, Pierre P. Development of models for the interpretation of the dynamic cone penetrometer data. *International Journal of Pavement Engineering* 2011; 12(3):201–214. http://dx.doi.org/10.1080/10298436.2010.488727

Chao C, Lin D, Luo H, Wang Y, Lo W. Non-destructive evaluation of a city roadway for pavement rehabilitation: A case study. *International Journal of Pavement Research and Technology* 2017. https://doi.org/10.1016/j.ijprt.2017.12.002.

Chen D, Wang J, Bilyeu J. Application of Dynamic Cone Penetrometer in Evaluation of Base and Subgrade Layers. *Transportation Research Record* 2001; 1764(1):1–10.

Chen J, Hossain M, Latorella TM. Use of Falling Weight Deflectometer and Dynamic Cone Penetrometer in Pavement Evaluation. *Transportation Research Record* 1999; 1655(1):145–51.

Chennarapu H, Garala TK, Chennareddy R, Balunaini U, Reddy GVN. Compaction Quality Control of Earth Fills Using Dynamic Cone Penetrometer. *Journal of Construction Engineering and Management* 2018; 144(9):1–10.

Cuelho EV, Perkins SW. Geosynthetic subgrade stabilization – Field testing and design method calibration. Transportation Geotechnics 2017; 10: 22–34. http://dx.doi.org/10.1016/j.trgeo.2016.10.002

Gabr BMA, Hopkins K, Coonse J, Hearne T. DCP Criteria for Performance Evaluation of

Pavement Layers. *Journal of Performance of Constructed Facilities* 2000; 14:141–148.

George V, Rao NC, Shivashankar R. PFWD , DCP and CBR correlations for evaluation of lateritic subgrades. *International Journal of Pavement Engineering* 2009; 10(3):189-199. http://dx.doi.org/10.1080/10298430802342765.

Kessler K. Use of DCP (Dynamic Cone Penetrometer) and LWD (Light Weight Deflectometer) for QC/QA on Subgrade and Aggregate Base. Material Design, Construction, Maintenance, and Testing of Pavements 2012; GeoHunan International Conference 62–67.

Koerner RM. Designing with Geosynthetics 2012, 6th Edition, Xlibris, Bloomington, India, USA.

Kwon J, Tutumluer E. Geogrid Base Reinforcement with Aggregate Interlock and Modeling of Associated Stiffness Enhancement in Mechanistic Pavement Analysis. *Transportation Research Record* 2009; 2116:85–95.

Li C, Ashlock JC, White DJ, Vennapusa PKR. Mechanistic-based comparisons of stabilised base and granular surface layers of low-volume roads. *International Journalof Pavement Engineering* 2017. DOI:10.1080/10298436.2017.1321417.

Ma H, Zhou M, Hu Y, Hossain MS. Interpretation of Layer Boundaries and Shear Strengths for Soft-Stiff-Soft Clays Using CPT Data: LDFE Analyses. *Journal of Geotechnical and Geoenvironmental Engineering* 2015. DOI: 10.1061/(ASCE)GT.1943-5606.0001370.

Mekkawy M, White DJ, Suleiman MT, Jahren CT. Mechanically reinforced granular shoulders on soft subgrade: Laboratory and full scale studies. *Geotextiles and Geomembranes* 2011; 29:149-160.

Mo P, Marshall AM, Yu H. Layered effects on soil displacement around a penetrometer. *Soils and Foundation* 2017; 57:669–678.

Mohammad LN, Herath A, Abu-farsakh MY, Gaspard K, Gudishala R. Prediction of Resilient Modulus of Cohesive Subgrade Soils from Dynamic Cone Penetrometer Test Parameters. *Journalof Materials in Civil Engineering* 2007; 19:986–992.

Mousavi SH, Gabr MA, Borden RH. Resilient modulus prediction of soft low-plasticity Piedmont residual soil using dynamic cone penetrometer. *Journal of Rock Mechanics and Geotechnical Engineering* 2018; 10:323-332.

Nguyen BT, Mohajerani A. Determination of CBR for fine-grained soils using a dynamic lightweight cone penetrometer. *International Journal of Pavement Engineering* 2015; 16(2):180-189. http://dx.doi.org/10.1080/10298436.2014.937807.

Ranasinghe RATM, Jaksa MB, Kuo YL, Nejad FP. Applications of artificial neural networks for predicting the impact of rolling dynamic compaction using dynamic cone penetrometer test results. Journal of Rock Mechanics and Geotechnical Engineering 2017; 9:340-349.

Rolt J, Pinard MI. Designing low-volume roads using the dynamic cone penetrometer. *Transportation* 2016;169:163-172.

Sayida MK, Evangeline SY, Girish MS. Coir Geotextiles for Paved Roads : A Laboratory and Field Study Using Non-Plastic Soil as Subgrade. *Journal of NaturalFibers* 2019. https://doi.org/10.1080/15440478.2019.1568344.

Schnaid F, Lourenço D, Odebrecht E. Interpretation of static and dynamic penetration tests in coarse-grained soils. *Geotechnique Letters* 2017; 7:1–6.http://dx.doi.org/10.1680/jgele.16.00170.

Shukla SK. An Introduction to Geosynthetic Engineering 2016, CRC Press, London.

Sun Y, Cheng Q, Lin J, Lammers PS, Berg A, Meng F, Zeng Q, Li L. Energy-based comparison between a dynamic cone penetrometer and a motor-operated static cone penetrometer. *Soil

and Tillage Research 2011; 116:105–109. doi:10.1016/j.still.2011.06.005.

Tingle JS, Jersey SR. Cyclic Plate Load Testing of Geosynthetic-Reinforced Unbound Aggregate Roads. *Transportation Research Record* 2005; 1936:60–69.

Yang B, Zhang R, Zha X, Liu C, Pan Q. Improved testing method of dynamic cone penetrometer in laboratory for evaluating compaction properties of soil subgrade. Road *Materials and Pavement Designs* 2015. http://dx.doi.org/10.1080/14680629.2015.1091375.

CHAPTER 6

FUZZY-BASED MODEL FOR PREDICTING STRENGTH OF GEOGRID-REINFORCED SUBGRADE SOIL

This chapter is based on the paper published in Transportation Infrastructure Geotechnology, Springer, as listed in Section 1.6. The details are presented here with some changes in the layout in order to maintain a consistency in the presentation throughout the thesis.

6.1 Introduction

The use of geosynthetic reinforcement is one of the well-established techniques for subgrade soil improvement and road base reinforcement for over four decades. This technique has been developed extensively to improve the performance of both paved and unpaved roads. Geogrid is a major type of geosynthetic that is commonly used in unpaved roads for soil reinforcement to achieve the technical benefits and also for speeding the construction of roads over weak subgrade soils. This improvement is attributed to a set of mechanisms: improvement in load distribution through the base course, prevention of local shearing of the soil, reduction in shear stresses on the subgrade, and tensioned membrane effect (Giroud and Han, 2004). In unpaved roads, the geogrid layers are mainly used as the reinforcement for granular layer and subgrade soil although it may play the role of a separator to some extent (Shukla, 2016).

The California bearing ratio (*CBR)* of the subgrade soil is considered as a key parameter in the design of flexible pavements of paved and unpaved roads. The subgrade plays a vital role in conveying the structural load to the pavement structure as it is subjected to the moving traffic load on roads. The load has to be transferred in such a way that the shear stresses and deformation developed in the subgrade soil is within the safe limits under adverse climatic and loading conditions. Under repeated/cyclic loading due to traffic, the deformation in the successive number of load cycles is controlled by a hardening parameter which is dependent

on confining pressure and plasticity (Trivedi, 2013). The effect of hardening parameter is such that it increases the elastic modulus in successive cycles and there is a diminishing settlement for the increasing number of cycles, which improves the strength of the soil. Hence, the subgrade soil may safely withstand the stress due to traffic loads. Analyzing and designing of unpaved roads with and without reinforcement layers is generally based on the bearing capacity of the subgrade (Perkins et al., 2012). The CBR test is one of the methods to determine the bearing capacity of the subgrade soil. When soft soils are used as a road subgrade, it undergoes excessive consolidation, settlement and bearing capacity failure because of their low shear strength. Many experimental and numerical studies have been performed to investigate the reinforcing effect of geosynthetic on the pavement structures (Negi and Singh, 2019; Cuelho and Perkins, 2017; Rashidian et al., 2016; Moghaddas-Nejad and Small, 1996; Suku et al., 2017; Wu et al., 2015; Palmeira and Antunes, 2010; Ibrahim, 2017). The results of such studies indicate that the incorporation of geogrid can improves the performance of paved/unpaved roads, increases the service life and reduces the maintenance cost. Thus, it is necessary to understand the influence of geogrid on the engineering properties of subgrade soil and to identify the optimum location of geogrid reinforcement within a subgrade soil to get maximum benefit in terms of the increased strength of subgrade soil.

Soft computing techniques have been widely used in many areas of science and engineering applications for solving complex real-life problems. One of the soft computing techniques namely, fuzzy logic deals with the concept of partial truth theory to provide a methodology to model uncertainty and the human way of thinking, reasoning, and perception (Taghavifar and Mardani, 2014). The Neuro-Fuzzy model has been applied in the application of geotechnical engineering and fuzzy logic in pavement engineering applications (Bagdatli, 2018; Lee and Donnell, 2007; Cabalar, 2012; Sandra and Sarkar, 2015; Zehtabchi, 2018). Yet no major attempt has been made to apply the fuzzy logic to model the effect of geogrid reinforcement

on the strength behavior of subgrade soil. The literature review reveals that most research works focus on developing a prediction model to get the output. It has been investigated that the strength of subgrade soil is affected by the basic properties of the soil (Black, 1962; Taskiran, 2010; Venkatasubramanian and Dhinakaran; 2011). Several researchers have shown the use of soft computing systems as an application to estimate the *CBR* value from the physical and compaction properties of the soil (Günaydin, 2009; Gurtug and Sridharan, 2002; Yildirim and Gunaydin, 2011; Bhatt et al., 2014). Investigations were carried out on natal soils and the relationship between various parameters and *CBR* was predicted. Unfortunately, these models were found to be unsatisfactory (Stephens, 1990). The prediction of *CBR* of subgrade soil by using genetic expression programming and artificial neural network was studied recently by Tenpe and Patel (2018). Still, no major effort has been made in the past to utilize the fuzzy logic for the estimation of *CBR* of reinforced subgrade soil with geogrid. CBR tests are routinely carried out to identify the *CBR* value of subgrade soil, which relates the stiffness modulus and strength parameter of subgrade soil. The results of CBR test are very important in geotechnical engineering but many times engineers are facing difficulties in obtaining the desired *CBR* value for the design of pavements. Conducting this test either in the field or in the laboratory are laborious, tedious and time consuming. Inaccurate results may be obtained due to the sample disturbance in the field and poor testing conditions in laboratory. Hence, it is advantageous to develop a fuzzy logic prediction model for *CBR* of subgrade soil reinforced with geogrid using the soil parameters and conditions. Moreover, considering the data used in subgrade soil strength modeling are associated with some error, which makes the fuzzy logic approach more suitable. The relationship between the strength of geogrid-reinforced subgrade soil and the various input parameters used in this study are not continuously increasing or decreasing. For example, depth of geogrid reinforcement has an important design parameter for the reinforced subgrade at which maximum strength can be obtained. For the geosynthetic

reinforcement placed at depth below and above the optimal depth, strength of the subgrade soil may be lower than the maximum possible value. In such cases, the trend cannot be established easily and fuzzy logic can be applied to get the more realistic solution.

6.2 Objectives of the present chapter

The objective of the present chapter is to develop a model for predicting the California bearing ratio (*CBR)* value of subgrade soil reinforced with the geogrid layers at various depths using a fuzzy logic approach. This fuzzy logic model evaluates the effect of the location of geogrid reinforcement and the properties of subgrade soil on the *CBR* value of geogrid-reinforced subgrade. Laboratory tests have also been carried out on reinforced and unreinforced subgrade soil. The model has the ability to predict the *CBR* value of the geogrid-reinforced subgrade without any laboratory tests. The database for developing the model was gathered from the literature and laboratory experimentations. The fuzzy logic approach has been used for the first time in this study for the estimation of the strength of geogrid-reinforced subgrade soil with optimal depth of geogrid reinforcement. The developed models also suggest the range of optimal depth of geogrid reinforcement at which the maximum strength can be obtained. The relative importance of model input parameters for affecting the output (*CBR* value) was also evaluated.

6.3 Database development and laboratory testing

6.3.1 Database

To establish a fuzzy logic model for predicting the *CBR* value of subgrade soil, the database of number of CBR tests as performed on geogrid-reinforced subgrade soil is employed. The data used in this research were obtained from the literature (Williams and Okine, 2008; Rajesh et al., 2016; Singh and Gill, 2012; Nagrale et al., 2010) and also considering the CBR test results that were conducted in this study. Success of models in predicting the strength of geogrid-reinforced subgrade soil depends on the comprehensiveness of the training data. Factors to be

considered for the identification of data are availability of experimental data, selection of variables which affect the subgrade soil strength, properties of geosynthetic and the ambiguity in testing methods. To maintain the uniformity in database, similar compaction tests were adopted for establishing the model. The standard Proctor compaction tests were carried out as per IS: 2720 (Part VII-1980) and AASHTO T-99 for determining the maximum dry unit weight and optimum moisture content for the subgrade soil. The samples were compacted with optimum moisture content for determination of *CBR* value of geogrid-reinforced subgrade soil at maximum dry unit weight. For determining the soaked *CBR* value, the soil samples were soaked for 4 days before testing. The improvement in the *CBR* value of weak subgrade soil is expected to be greater than the strong subgrade soil by the inclusion of geosynthetic reinforcement. Therefore, laboratory tests were conducted on weak subgrade soil in the present study. In fact, in real-life projects, engineers rarely recommend the use of geosynthetic reinforcement if the subgrade soil is strong. Geosynthetic properties are excluded from the database because of the inadequate information available in the selected studies. However, the depth of geogrid reinforcement, which controls the effect of reinforcement in pavement layers significantly, has been included. It has been assumed that the geogrid used in this study meets the basic survivability and strength requirements. Depth of reinforcement is an important parameter for the development of model because the improvement in the strength of subgrade soil depends on the location of geosynthetic placement within the subgrade soil. Determining the optimal depth of geogrid reinforcement helps achieve the maximum gain in strength of subgrade soil. To better understand the effect of geogrid reinforcement on the subgrade strength a wide range of variation in depth of geogrid reinforcement is considered for the development of model such as $H/2$, $H/3$, $H/4$, $H/5$, $2H/5$, $3H/5$, $4H/5$, where H is the height of the specimen in the CBR mould. As shown in the Table 6.1, several parameters, such as depth of geogrid reinforcement, unreinforced/reinforced section, unsoaked/soaked condition, and soil properties

are considered as datasets that were used to propose a prediction model for strength of subgrade soil reinforced with geogrid. Database used for the construction of the model consists of some important geotechnical and geosynthetic parameters which are presented in Table 6.1.

6.3.2 Laboratory tests

The database consists of 7 *CBR* test results conducted on the soil which was excavated from the area closer to the Civil Engineering Department of Delhi Technological University, Delhi, India. The characterization of the excavated soil was done by the standard laboratory tests. The soil was classified as silty sand (SM) as per the Indian Soil Classification System (IS: 2720). The standard Proctor compaction test was carried out as per IS: 2720 (Part VII) to determine the maximum dry unit weight (*MDU*) and optimum moisture content (*OMC*) for the excavated soil. The *MDU* and *OMC* of soil were found to be 18.74 kN/ m^3 and 13.91% respectively. Geogrid used in this study is composed of polypropylene materials with square aperture of 12.5 mm × 12.5 mm. The ultimate tensile strength of geogrid in machine direction and cross-machine direction is 115-kN/m, while the mass per unit area of the geogrid is 405 g/m^2.

CBR tests were carried out to investigate the influence of geogrid reinforcement on penetration resistance of the soil sample, at its maximum dry unit weight obtained from the compaction test. The CBR test was performed in accordance with IS: 2720 (Part 16)-1979 as shown in Fig. 6.1. Laboratory tests were conducted on both unreinforced and geogrid-reinforced soil samples to observe the strength improvement. CBR mould was filled with subgrade soil mixed thoroughly with water corresponding to *OMC* and compacted to the maximum dry unit weight. Soil samples for unreinforced and geogrid-reinforced soil were prepared to investigate the effect of geogrid reinforcement on the strength of subgrade. For preparing geogrid-reinforced soil specimens, the mould was filled with the soil by placing a layer of geogrid reinforcement which was cut in the circular shape of diameter slightly less than the mould diameter. Geogrid reinforcement layer was laid at different depths of 62.5 mm,

41.67 mm and 31.25 mm from the top surface of the specimen. Both the unreinforced and geogrid-reinforced soil samples were compacted in three layers with the help of a 2.6 kg rammer falling from a height of 310 mm and each layer was compacted with 56 number of blows. *CBR* value is defined as the ratio of load corresponding to 2.5 mm or 5 mm penetration into the soil with a 50 mm diameter penetration plunger at a constant rate of 1.25 mm/min to that of the standard unit load. The load corresponding to the penetration ranging from 0 to 12.5 mm is measured in the experiment. *CBR* value was calculated by measuring the load corresponding to 2.5 mm and 5.0 mm penetration and maximum value was considered as the *CBR* value, as recommended in the relevant standard.

Figure 6.1 CBR test apparatus

**Table 6.1** The database used for the development of models

Soil parameters	Depth of reinforcement (mm)	Section	Condition	*CBR* (%)
LL (%) = 21, *PL* (%) = 18, *PI* (%) = 3, *OMC* (%) = 12.8 and *MDU* (kN/m³) = 18.93	-	Unreinforced	Soaked	4.6[a]
	-	Unreinforced	Unsoaked	6.9[a]
	62.5	Reinforced	Soaked	5.51[a]
	62.5	Reinforced	Unsoaked	7.97[a]
LL (%) = 45.5, *PL* (%) = 22.15, *PI* (%) = 23.35, *OMC* (%) = 16.1 and *MDU* (kN/m³) = 17.9	-	Unreinforced	Soaked	1.82[b]
	-	Unreinforced	Unsoaked	3.37[b]
	62.5	Reinforced	Unsoaked	6.11[b]
	62.5	Reinforced	Unsoaked	5.38[b]
	62.5	Reinforced	Soaked	3.92[b]
	62.5	Reinforced	Soaked	3.46[b]
LL (%) = 36.9, *PL* (%) = 18.4, *PI* (%) = 18.76, *OMC* (%) = 13.21 and *MDU* (kN/m³) = 17.36	-	Unreinforced	Soaked	1.91[b]
	-	Unreinforced	Unsoaked	4.83[b]
	62.5	Reinforced	Unsoaked	8.76[b]
	62.5	Reinforced	Unsoaked	8.57[b]
	62.5	Reinforced	Soaked	5.01[b]
	62.5	Reinforced	Soaked	4.28[b]
LL (%) = 28, *PL* (%) = 15, *PI* (%) = 13, *OMC* (%) = 16 and *MDU* (kN/m³) = 16.67	-	Unreinforced	Soaked	2.9[c]
	-	Unreinforced	Unsoaked	6.5[c]
	25	Reinforced	Unsoaked	16[c]
	50	Reinforced	Unsoaked	13.8[c]
	75	Reinforced	Unsoaked	10.9[c]
	100	Reinforced	Unsoaked	7.2[c]
	25	Reinforced	Soaked	9.4[c]
	50	Reinforced	Soaked	7.2[c]
	75	Reinforced	Soaked	5.8[c]
	100	Reinforced	Soaked	3.16[c]
LL (%) = 34, *PL* (%) = 22, *PI* (%) = 12, *OMC* (%) = 17 and *MDU* (kN/m³) = 16.9	-	Unreinforced	Soaked	1.1[d]
	25	Reinforced	Soaked	1.52[d]
	50	Reinforced	Soaked	1.84[d]
	75	Reinforced	Soaked	2.24[d]
	100	Reinforced	Soaked	2.52[d]
LL (%) = 29, *PL* (%) = 20, *PI* (%) = 9, *OMC* (%) = 13.91 and *MDU* (kN/m³) = 18.74	-	Unreinforced	Unsoaked	1.66[e]
	62.5	Reinforced	Unsoaked	2.21[e]
	62.5	Reinforced	Unsoaked	1.76[e]
	41.67	Reinforced	Unsoaked	1.76[e]
	41.67	Reinforced	Unsoaked	2.08[e]
	31.25	Reinforced	Unsoaked	2.04[e]
	31.25	Reinforced	Unsoaked	2.04[e]

[a]Williams and Okine (2008), [b]Rajesh et al. (2016), [c]Singh and Gill (2012), [d]Nagrale et al. (2010), [e]CBR test results of present study.

116

6.4 Development of fuzzy logic prediction model

6.4.1 Fuzzy logic approach

The fuzzy logic approach deals with vagueness and imprecision. Fuzzy logic has the potential to generate solution when the available data are imprecise, ambiguous, incomplete or not correct. Fig. 6.2 illustrates the basic concept of FL model with input variables and output. The fuzzy logic system consists of four sections (Zedeh and Kacprzyk, 1992; Gopal, 2009; Hossain et al., 2012): fuzzification, rule base, fuzzy inference unit and defuzzification. Fuzzification component represents the process of taking the crisp inputs and converts them into a linguistic variable with the help of membership functions that were stored in the fuzzy knowledge base. Fuzzy membership functions are available in many forms, but the preference of choosing the type of membership function for any practical application is provided in the form of simple linear functions, namely Triangular and Gaussian membership functions. The rule base defines a set of fuzzy if-then rules representing the relationship between inputs variables and output.
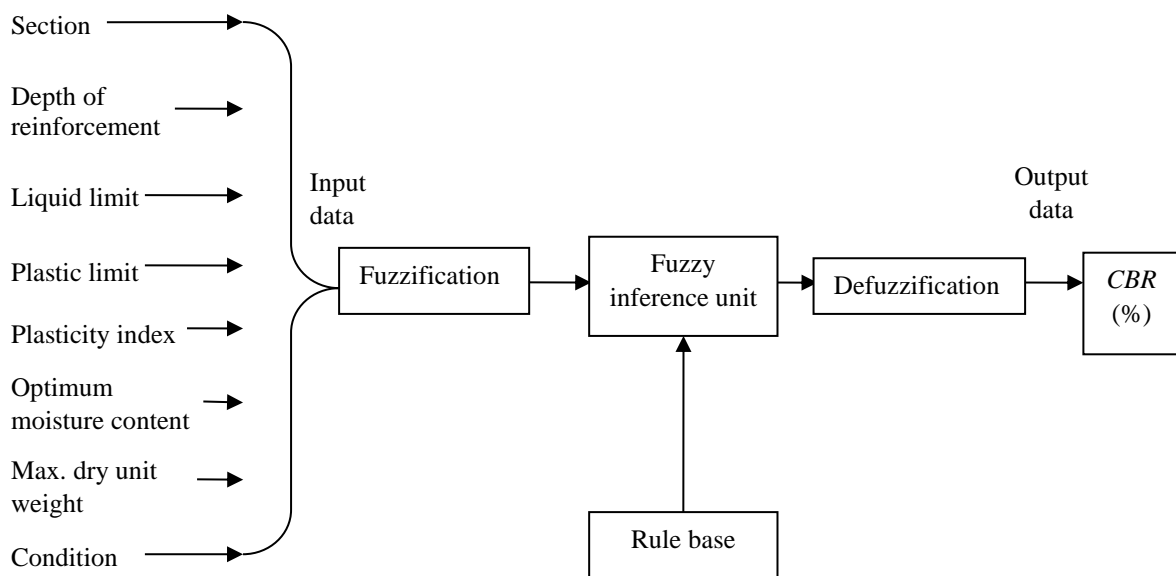
Figure 6.2 Schematic representation of activity units in the fuzzy model with input variables and *CBR* as output
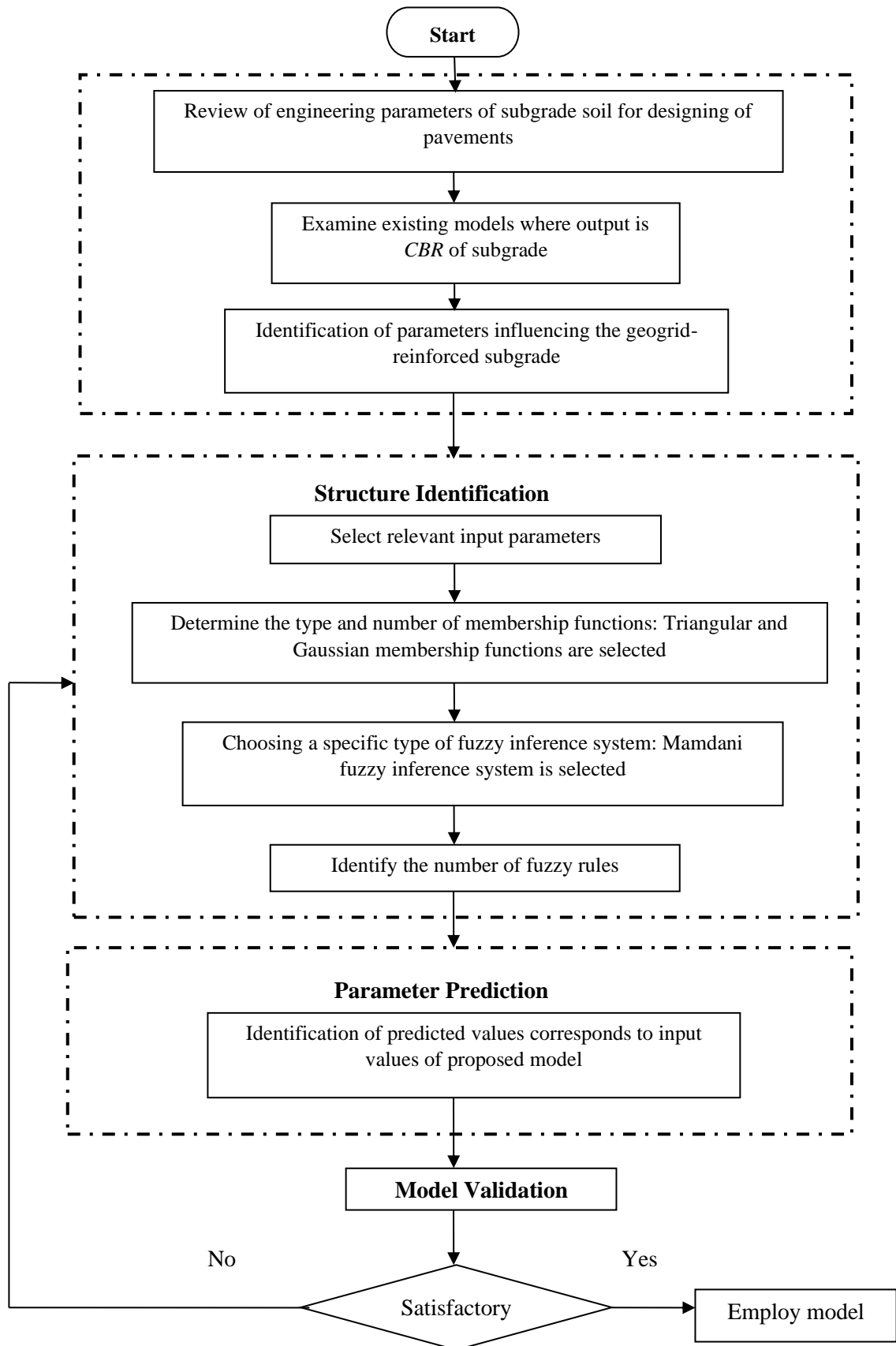
Figure 6.3 Flow chart for the methodology adopted for the development of models

Two types of fuzzy rule systems are available, namely Mamdani and Sugeno. Selection of an appropriate rule system is totally dependent on the users' problem. The fuzzy inference system consists of membership functions, operators and number of If-Then rules that transforms the available inputs to the output. Defuzzification is the process to convert the resulting output fuzzy variables from the fuzzy inference unit into a crisp value (numerical value). Structure identification and parameter prediction are the two phases of fuzzy modeling (Topçu and Saridemir, 2008). The components of structure identification includes appropriate selection of input parameters, selection of particular type of fuzzy inference system, assigning a type and number of membership function, defines rules and determine their number. Parameter prediction determines the value of output parameter corresponding to the input values of the proposed model. The methodology used to develop the fuzzy model is described in a flow chart as shown in Fig. 6.3.

6.4.2 Model construction

Fuzzy logic approach has been used in the present study to establish a relationship between the *CBR* of geogrid-reinforced subgrade soil with the engineering properties of subgrade soil and depth of geogrid reinforcement. Mamdani-type fuzzy inference system was selected to develop the model using the results of experimental tests. Mamdani fuzzy inference system is the most commonly used inference engine in developing fuzzy models. Wide range and varieties of geosynthetics are available in the market namely geotextile, geogrids, geomats, geocomposite, geomembrane. Out of these, geogrid was selected for the development of prediction model because geogrid has been widely used in unpaved roads with various applications. The fuzzy logic model was developed with eight input parameters and the *CBR* value of reinforced subgrade soil as the model single output parameter in MATLAB software. The input parameters are reinforced/unreinforced section (*R/UR*), depth of reinforcement (*DOR*), liquid limit (*LL*), plastic limit (*PL*), plasticity index (*PI*), optimum moisture content (*OMC*),

maximum dry unit weight (*MDU*), and soaked/unsoaked condition (*S/US*). No data was available in the literature where the fuzzy model was developed to know the effect of geogrid reinforcement on the reinforced subgrade soil. However, it was available in the literature that the strength of subgrade depends on the properties of geogrid, location of reinforcement and basic properties of soil such as liquid limit, moisture content, maximum dry density, plastic limit, *CBR* and compaction. Hence, based on the literature review, the input parameters were selected which significantly affects the reinforced subgrade soil to establish the fuzzy model for predicting the subgrade soil strength. The selection of realistic input parameters is essential for a successful prediction model. The statistical parameters for the input variables and output were calculated as summarized in Table 6.2.

Table 6.2 Statistical parameters of variables used for the development of fuzzy model

Variables	Statistical parameters			
	minimum	maximum	mean	Standard deviation
Section (reinforced/unreinforced)	0	1	0.5	0.707
Depth of reinforcement (mm)	20	110	65	63.639
Liquid limit (%)	20	50	35	21.213
Plastic limit (%)	10	25	17.5	10.606
Plasticity index (%)	1	25	13	16.970
Optimum moisture content (%)	11	20	15.5	6.363
Maximum dry unit weight (kN/m^3)	16	19	17.5	2.121
Condition (soaked/unsoaked)	0	1	0.5	0.707
CBR (%)	1	17	9	11.313

6.4.3 Membership functions

Membership functions of the model map an input value to its appropriate membership value which lies in between 0 and 1. Selection of membership functions, as well as the number of membership function, is dependent on system knowledge, experience gained and research

conditions. Initially, fuzzification of all input parameters and output parameter of the proposed model with the help of membership function. After defining the range of values to all the input variables and output, assign appropriate membership functions to fuzzy variables. Triangular shaped membership functions and Gaussian shaped membership functions were used in the investigation for input and output variables as shown in Fig. 6.4. Membership value defines the degree an object belongs to a fuzzy set between 0 and 1, where 1 represents full membership and 0 expresses non-membership even it allows to have partial membership. Two fuzzy logic models were developed, one with Triangular membership function and other with Gaussian membership function. The Triangular membership functions are formed with the help of a straight line and to understand the straight lines is simpler. The Triangular membership function is defined by a lower limit 'a', an upper limit 'b', and a value 'm', where $a < m < b$ as shown in Eq. (1). The Gaussian memberships functions are also popular because of the pattern so formed are smooth and nonzero at all points. Gaussian membership function is defined by a central value 'm' and a standard deviation $\sigma > 0$ as shown in Eq. (2).

$$f(x; a, m, b) = \begin{cases} 0, & x \leq a \\ \frac{x-a}{m-a}, & a < x \leq m \\ \frac{b-x}{b-m} & m < x < b \\ 0, & x \geq b \end{cases} \tag{1}$$

$$f(x; \sigma, m) = e^{\frac{-(x-m)^2}{2\sigma^2}} \tag{2}$$

6.4.4 Rule base

Fuzzy rule base consists of an entire group of if-then rules that incorporate fuzzy relations between input variables and output. Fuzzy sets and fuzzy operators are necessary to form rules to perform the fuzzy logic prediction model. If-then rules are used in developing the model to create the conditional statements that resembles with human thinking rather than any

Fuzzy Triangular MF
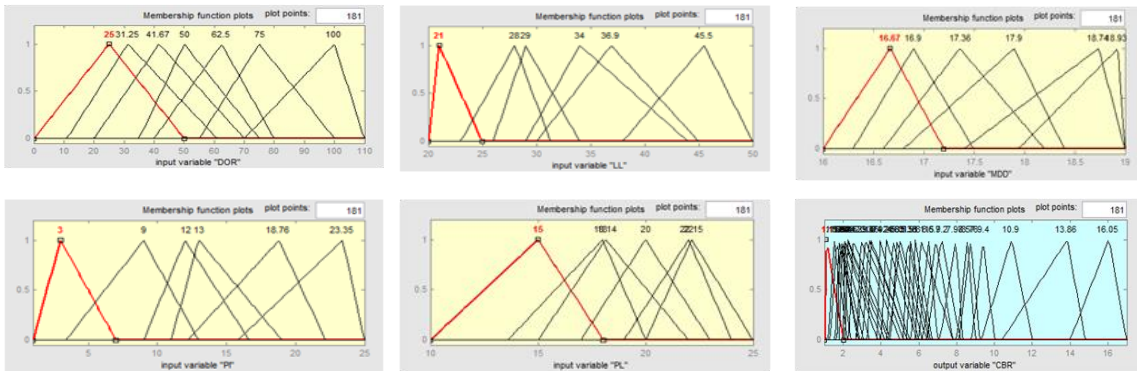
Fuzzy Gaussian MF
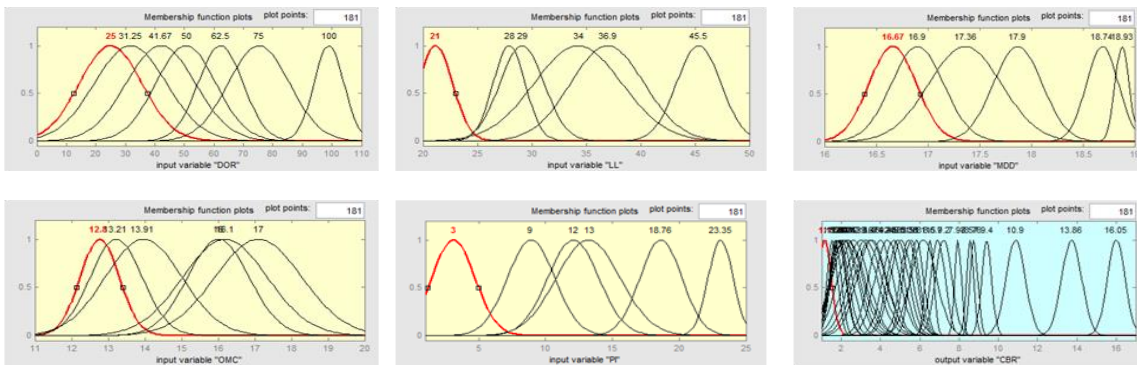
(a)
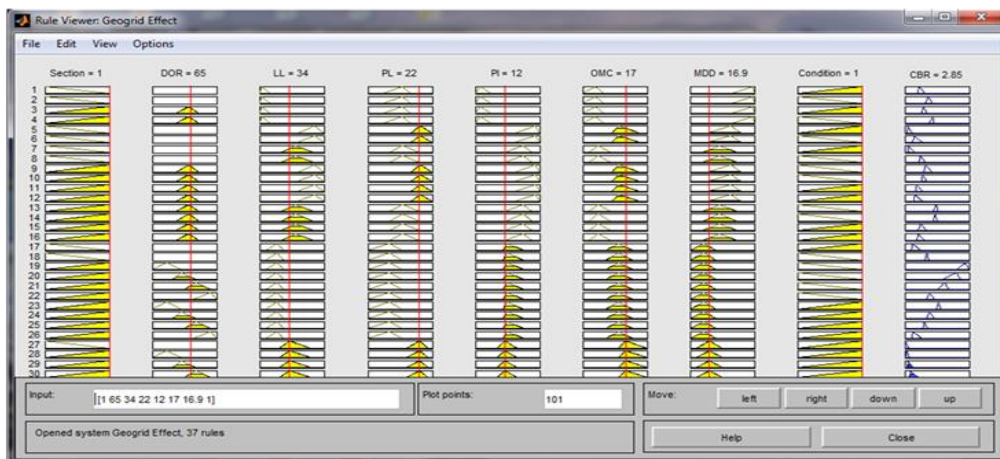
(b)

Figure 6.4 (a) Few fuzzy Triangular and Gaussian membership functions for input variables (yellow background) and output variables (blue background) (b) Typical rule viewer window for the fuzzy logic model

mathematical rules. The general form of a fuzzy if-then rule statement is 'if x is A then y is B' where A and B, are linguistic variables respectively. If-part of the rule statement "x is A" is defined as the antecedent and then-part of the rule statement "y is B" is defined as the consequent. The rules are responsible for determining the input and output membership functions; hence 37 fuzzy rules were generated for implementation of the prediction model. The rules viewer of the geogrid-reinforced prediction model is shown in Fig. 6.4. Rules viewer can be shown after the assessment of the applied if-then rules in the fuzzy model and then the output can be computed. Generally, more the number of rules, greater would be the accuracy but dealing with a larger rule base would be time-consuming. More the numbers of subsets, fuzzy logic system would work best when the set of rules are derived from the actual experimental results which help a lot in precise linking of various input parameters to the output. The fuzzy inference unit extracts the entire group of rules from the rule base and gains an understanding of converting inputs to the corresponding output. Centre of gravity method was applied for converting linguistic output into a numerical value during the defuzzification process. Center of gravity method is mostly adopted for defuzzification process.

6.5 Results and discussion

6.5.1 Evaluation of model performance

The performance of both the models developed for the estimation of the strength of geogrid-reinforced subgrade soil was evaluated through the statistical criteria for performance measures, which include mean absolute error (*MAE*), root mean square error (*RMSE*), correlation coefficient (*r*) and coefficient of determination (R^2). These performance indicators are used for comparing the output results obtained from the established models with the actual outputs. These statistical performance measures are selected to evaluate the accuracy of the results obtained from the developed models and are summarized in Table 6.3.

Table 6.3 Statistical performance of the fuzzy models with varied membership functions

Developed models	Performance measures			
	Root mean square error (*RMSE*)	Mean absolute error (*MAE*)	Coefficient of determination (R^2)	Correlation coefficient (*r*)
Fuzzy model with Triangular membership function	0.4705	0.3897	0.9927	0.9963
Fuzzy model with Gaussian membership function	0.6207	0.4913	0.9773	0.9886

It can be observed that the satisfactory agreement between the models predicted values and experimental data are found. If the value of correlation coefficient is more than 0.8, then it represents a strong correlation between the predicted and measured values of database (Smith, 1986). Based on the values of performance indicators, it can be concluded that the model with Triangular membership function performs better than the model with Gaussian membership function, in terms of a higher value of the coefficient of determination (R^2) and correlation coefficient (*r*) and lower value of errors. A prediction model with a higher coefficient of determination and lower error indicates good consent with laboratory test data. By the way, the magnitudes of errors are in the reasonable range for both the models and even very close to each other to use them for the prediction of geogrid-reinforced subgrade strength. The database of experimental results were used for the calibration of models and the same database has been used for the validation. Experimental values are compared with the predicted *CBR* values obtained from the models with Triangular and Gaussian membership functions are shown in Fig. 6.6. It concludes that fuzzy models are highly reliable to forecast the strength of geogrid-reinforced subgrade. The correlation coefficients between the predicted and experimental *CBR* values computed for geogrid-reinforced subgrade soil from both the models were found very close to unity as illustrated in Fig. 6.5. It can be observed that almost all the points were around the equality line. The results of the statistical indicators demonstrate that the fuzzy logic is a

powerful tool for predicting the strength of geogrid-reinforced subgrade soil and models predicted values are near to the experimental values.
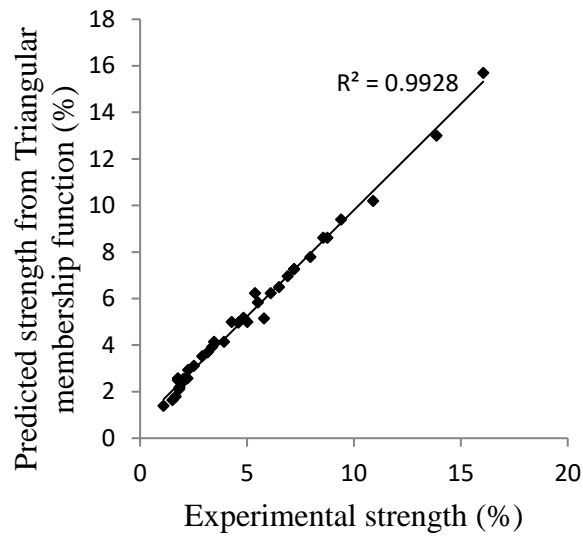
(a)
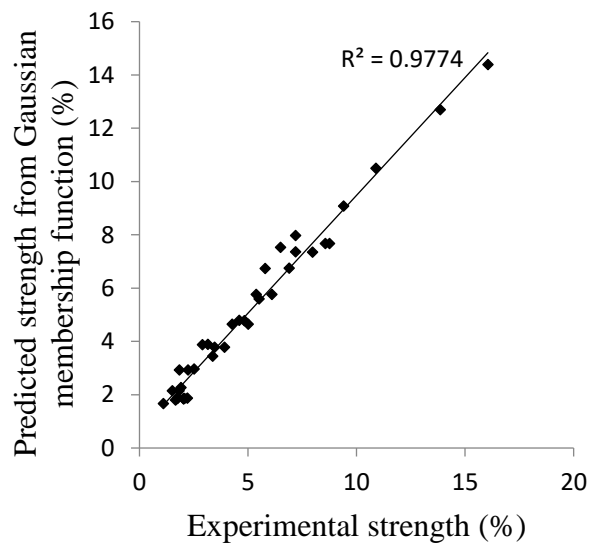
(b)

Figure 6.5 Correlation between experimental and predicted values of *CBR* by (a) Model with Triangular membership function (b) Model with Gaussian membership function
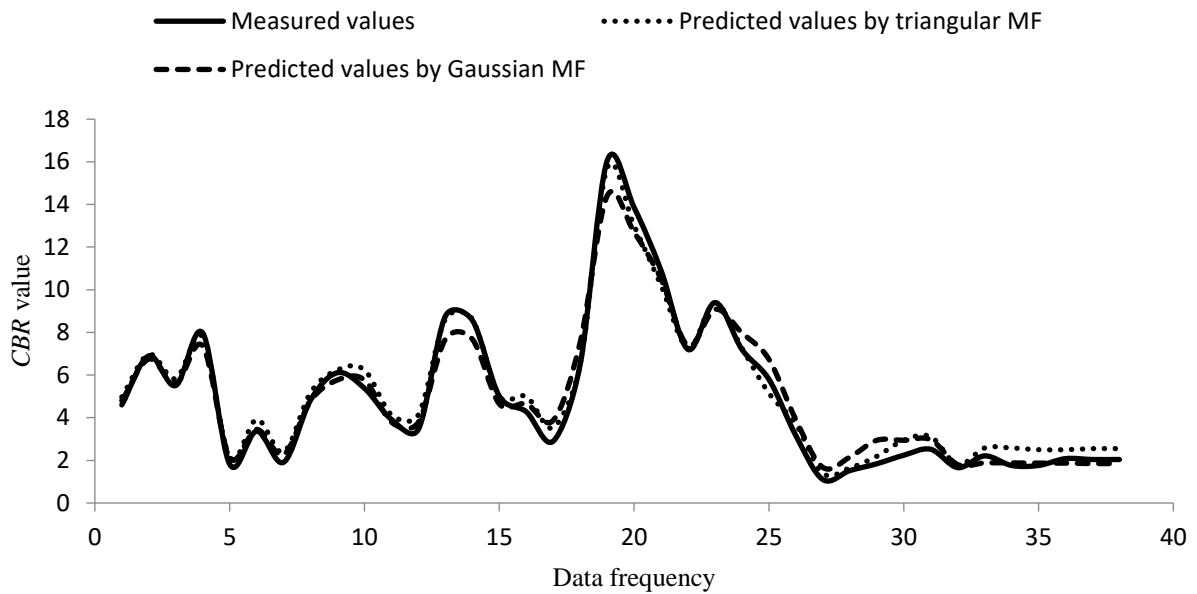
Figure 6.6 Comparison between *CBR* value predicted by fuzzy model with Triangular membership function and Gaussian membership function with actual experimental values.

6.5.2 Control surfaces and optimal depth of reinforcement

Figure 6.7 to 6.8 presents the control surface diagrams for both the models with Triangular and Gaussian membership functions representing the interdependency of input parameters and output. It can be observed that each surface plot is showing the effect of two parameters at a time on the output. Surface diagrams are limited to only two input parameters because the visualization of figures will become more difficult if we increase the number of input variables by more than two. Fig. 6.7 shows the three-dimensional description of model with Triangular membership function which takes the combined effect of two input parameters on the strength of geogrid-reinforced subgrade soil.

There is a particular range of possible defuzified values for the depth of geogrid reinforcement in which the *CBR* increases gradually and beyond that range it gradually decreases. Therefore, it is important to place the reinforcement layer at the optimal depth of
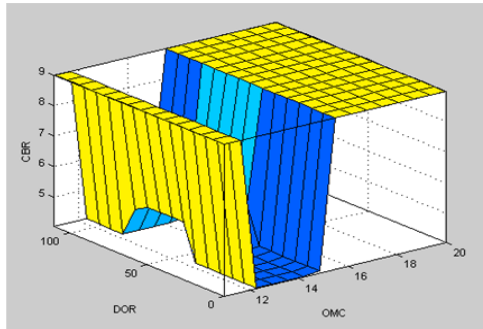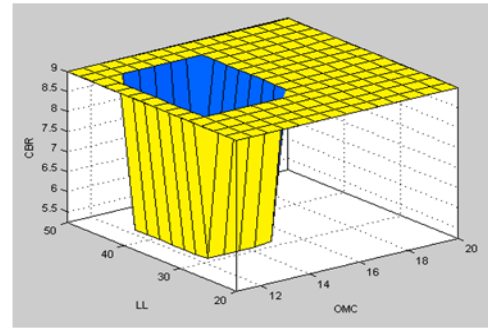
Figure 6.7 Few control surfaces of the fuzzy model with Triangular membership function on *CBR* with combined effect of (a) *DOR* and *OMC* (b) *LL* and *OMC* (c) *OMC* and section (d) *OMC* and condition.

geogrid reinforcement to get the maximum strength of the geogrid-reinforced subgrade. For finding the optimal location of geogrid reinforcement the predicted values of *CBR* are obtained from the proposed model for the given database by varying the depth of the reinforcement parameter in a range of 20 to 80 mm. Variation in the strength was observed at an interval of 10 mm from 20 to 80 mm. While calculating the optimal depth of geogrid reinforcement only the parameter 'depth of reinforcement' is varied and remaining all other parameters is kept constant as per the database. Optimal depth of geogrid reinforcement was found as 36 to 60 % of the height of the subgrade soil specimen hence, maximum strength can be gained if the geogrid is placed at a depth in between 45 to 75 mm from the top surface of soil specimen. As

the optimum moisture content and liquid limit increases, initially the strength reduces then remains constant and then reaches to its respective maximum value. The *CBR* reaches the peak when the section is reinforced and the least value is obtained when the section in unreinforced. Fig. 6.8 shows the three-dimensional description of model with Gaussian membership function which shows the strength of the reinforced soil is maximum at the maximum value of optimum moisture content then reduces suddenly as the optimum moisture content reduces. Similarly, the maximum value of strength can be obtained if the reinforcement layer is placed within an optimal range, beyond which the effect is insignificant.

(a)   (b)
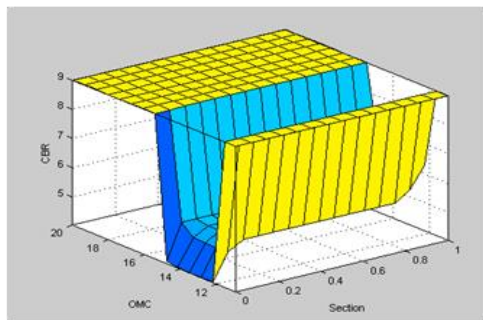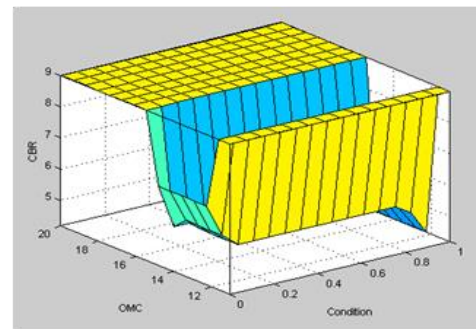
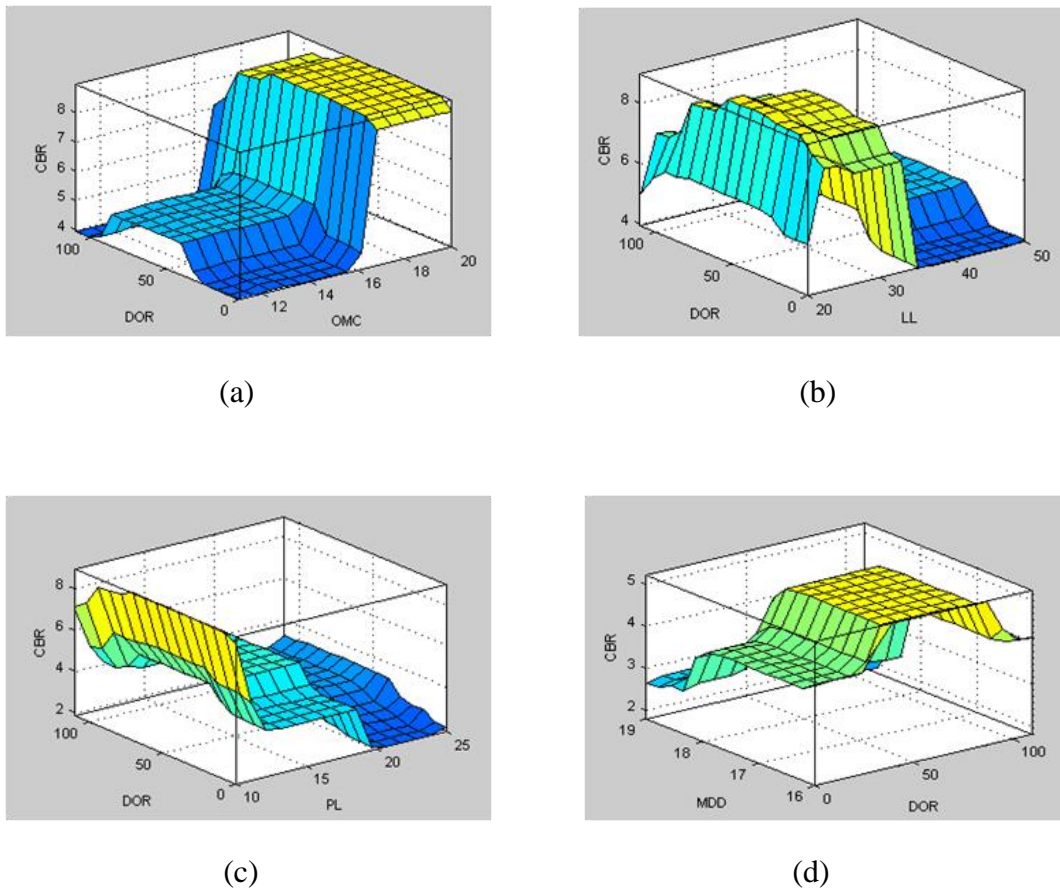(c)   (d)

Figure 6.8 Few control surfaces of the fuzzy model with Gaussian membership function on *CBR* with combined effect of (a) *DOR* and *OMC* (b) *DOR* and *LL* (c) *DOR* and *PL* (d) *MDD* and *DOR*.

For the design of pavements, subgrade strength plays an important role which needs to be evaluated in terms of *CBR* value. The range considered for the *CBR* value of subgrade varies from 1% to 16% for the development of fuzzy logic model. Subgrade strength can be classified into various classes based on the *CBR* value as shown in Table 6.4. The strength of unreinforced subgrade lies under class S1 has been improved to lies in class S2 and S3 due to the presence of geogrid reinforcement at depth $H/5$ to $4H/5$ and $H/2$ respectively. When the strength of unreinforced subgrade lies under class S2 has been improved to lies in class S3 and S4 due to the presence of geogrid reinforcement at depth $H/2$ and $H/5$ to $4H/5$ respectively. Similarly, the strength of unreinforced subgrade which lies in class S3 and S4 has been improved to lies in class S4 and S5 respectively. It is clear from the results that inclusion of geogrid reinforcement to the subgrade improves its *CBR* value. The strength of geogrid-reinforced subgrade is improved due to good interlocking and frictional capability of geogrid against lateral movement. But the dominating mechanism responsible for the enhancement in the *CBR* value of geogrid-reinforced subgrade is the maximum stresses in the subgrade is reduced because of the presence of geogrid reinforcement layer within the subgrade (Cuelho and Perkins, 2017; Singh et al., 2019). Geogrid reinforcement will help to distribute the vertical stresses more uniformly. As per IRC: 37-2012 as the *CBR* value of subgrade soil increases, it will decrease the thickness of granular base course required for the pavement design. Ultimately it will reduce the construction cost and helps economy.

Table 6.4 Subgrade soil strength as classified into the classes

Quality of subgrade	Range of *CBR* value (%)	Class
Very low	< 2	S1
Low	3–4	S2
Average	5–6	S3
Good	7–9	S4
Very good	10–15	S5

6.5.3 Sensitivity Analysis

Sensitivity analysis was conducted to investigate the effectiveness of the input parameters on the strength of geogrid-reinforced subgrade soil. The cosine amplitude method was implemented to evaluate the sensitivity of each input parameter on the *CBR* of geogrid-reinforced subgrade and to recognize the most sensitive factor affecting the performance. Assign a degree of sensitivity to each input parameter during the sensitivity analysis by establishing the strength of the relationship (r_{ij}) between the input parameters and *CBR* of geogrid-reinforced subgrade soil. The strength of the relationship between various input parameters and output can be estimated from Eq. (3).

$$r_{ij} = \frac{\sum_{k=1}^{m} x_{ik} x_{jk}}{\sqrt{\sum_{k=1}^{m} x_{ik}^2 \sum_{k=1}^{m} x_{jk}^2}} \quad , \quad 0 < r_{ij} < 1 \tag{3}$$

where, r_{ij} = strength of the correlation between input parameter and output; x_i = input parameter; x_j = output parameter; and m = number of input variables.

Figure 6.9 presents sensitivity analysis for different input parameter used in the proposed fuzzy model on the output results. The value of r_{ij} for each input parameter is an indicator of the effect of that parameter on the output results. A higher value of r_{ij} represents a greater effect of that parameter on the output. According to the sensitivity analysis results, maximum dry density and optimum moisture content of subgrade soil have the most significant effect on strength of reinforced subgrade, whereas the soaked/unsoaked condition has a marginal effect only. Liquid limit, depth of geogrid reinforcement, plasticity index, plastic limit, and reinforced/unreinforced section were also found to have a good contribution to the strength of reinforced subgrade. Very low difference is observed between the values of r_{ij} for seven input parameters except for one input i.e 'soaked/unsoaked condition'. Depth of reinforcement has a high influence on the reinforced subgrade strength because by providing a reinforcement layer

within the subgrade soil increases the stiffness of the soil which further increases the strength of the reinforced subgrade.
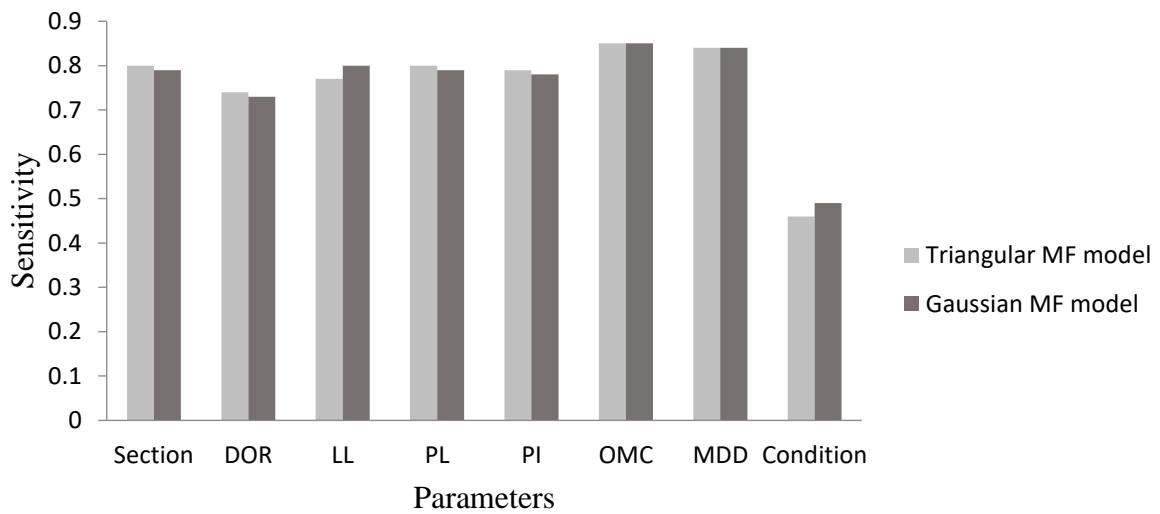
Figure 6.9 Sensitivity analysis for various input parameters used in the model

6.6 Conclusions

The present study is likely to be one of the very first research which aims at investigating the applicability of fuzzy logic model for estimating the geogrid-reinforced subgrade soil strength. To achieve this, two models were developed with Triangular and Gaussian membership functions with eight input parameters and one output parameter. Output results were obtained from the proposed model, and they were compares with the laboratory test results. The correlation coefficients of models were found to be 0.996 and 0.988, suggesting a good correlation between predicted *CBR* values and laboratory *CBR* values. Therefore, the strength of subgrade soil reinforced with geogrid can be estimated through fuzzy logic model depending on the subgrade soil properties and depth of geogrid reinforcement, thus saving the cost and time. This study as presented also reveals that there is an improvement in the *CBR* value of subgrade soil by stabilizing it with geogrid. The potentialities of fuzzy logic were found to be satisfactory in predicting the behavior of geogrid-reinforced subgrade soil subjected to traffic

loads. Based on the results and discussion presented earlier, the following conclusions can be drawn:

a) Fuzzy logic modeling is a convenient approach for predicting the strength of geogrid-reinforced subgrade soil, thus saving time and resources in real-life projects.

b) The correlation coefficient is found to be closer to unity for both the developed models having Triangular membership function and Gaussian membership function, thus validating the results.

c) Sensitivity analysis evaluated the contribution of individual input parameters on the *CBR* value of geogrid-reinforced subgrade soil and it reveals that, $r_{ij} > 0.7$ for all the input parameters except for 'soaked/unsoaked condition'. This demonstrates the good selection of input parameters for the development of models.

d) As the availability of data on geogrid-reinforced subgrade soil increases in the literature, more accurate prediction model can be proposed for a wider range.

e) The range of the optimal depth of geogrid reinforcement is found as 36% to 60% of the thickness of the subgrade soil layer.

References

Bagdatli MEC. Fuzzy logic-based life-cycle cost analysis of road pavements. *J. Transp. Eng., Part B: Pavaments* 2018; 144 (4): 04018050. DOI: 10.1061/JPEODX.0000081.

Bhatt S, Jain PK, Pradesh M. Prediction of California Bearing Ratio of Soils Using Artificial Neural Network. *American International Journal of Research in Science, Technology, Engineering & Mathematics* 2014; 8 (2): 156–161.

Black WPM. A method of estimating the CBR of cohesive soils from plasticity data. *Geotechnique* 1962; 12: 271-2.

Cabalar AF, Cevik A, Gokceoglu C. Some applications of Adaptive Neuro-Fuzzy Inference System (ANFIS) in geotechnical engineering. *Computers and Geotechnics* 2012; 40: 14–33. doi: 10.1016/j.compgeo.2011.09.008.

Cuelho EV, Perkins SW. Geosynthetic subgrade stabilization – Field testing and design method calibration. *Transportation Geotechnics* 2017; 10: 22–34. doi.org/10.1016/j.trgeo.2016.10.002.

Duncan-Williams E, Attoh-Okine NO. Effect of geogrid in granular base strength - An experimental investigation. *Construction and Building Materials* 2008; 22 (11): 2180–2184. doi: 10.1016/j.conbuildmat.2007.08.008.

Giroud JP, Han J. Design Method for Geogrid-Reinforced Unpaved Roads. I. Development of Design Method. *Journal of Geotechnical and Geoenvironmental Engineering* 2004; 130 (8): 775–786. DOI: 10.1061/(ASCE)1090-0241(2004)130:8(775).

Gopal M. Digital control and state variable methods: conventional and intelligent control systems. 3rd ed. Singapore; Tata McGraw-Hill Education Pvt. Ltd: 2009.

Günaydin O. Estimation of soil compaction parameters by using statistical analyses and artificial neural networks. *Environmental Geology* 2009; 57 (1): 203–215.

Gurtug Y, Sridharan A. Prediction of compaction characteristics of fine-grained soils. Géotechnique 2002; 52 (10): 761–763.

Hossain A, Rahman A, Mohiuddin AKM. Fuzzy evaluation for an intelligent air-cushion tracked vehicle performance investigation. *Journal of Terramechanics* 2012; 49 (2): 73–80. doi: 10.1016/j.jterra.2011.08.002.

Ibrahim EM, El-Badawy SM, Ibrahim MH, Gabr A, Azam A. Effect of geogrid reinforcement on flexible pavements. *Innovative Infrastructure Solutions* 2017; 2 (1): 54. DOI: 10.1007/s41062-017-0102-7.

Lee D, Donnell ET. Analysis of nighttime driver behavior and pavement marking effects using fuzzy inference system. *Journal of Computing in Civil Engineering* 2007; 21: 200–210. doi: 10.1061/ASCE0887-3801200721:3200.

Moghaddas-Nejad F, Small JC. Effect of Geogrid Reinforcement in Model Track Tests on Pavements. *Journal of Transportation Engineering* 1996; 122 (6): 468–474.

Nagrale PP, Sawant PH, Pusadkar SS. Laboratory investigation of reinforced sub grade soils. Indian Geotechnical Conference, GEOtrendz 2010; 637−640.

Negi MS, Singh SK. Experimental and numerical studies on geotextile reinforced subgrade soil. *International Journal of Geotechnical Engineering* 2019. DOI: 10.1080/19386362.2019.1684654.

Palmeira EM, Antunes LGS. Large scale tests on geosynthetic reinforced unpaved roads subjected to surface maintenance. *Geotextiles and Geomembranes* 2010; 28 (6): 547–558. doi: 10.1016/j.geotexmem.2010.03.002.

Perkins SW, Christopher BR, Lacina BA, Klompmaker J. Mechanistic-Empirical Modeling of Geosynthetic-Reinforced Unpaved Roads. *International Journal of Geomechanics* 2012; 12 (4): 370–380. DOI: 10.1061/(ASCE)GM.1943-5622.0000184.

Rashidian V, Naeini SA, Mirzakhanlari M. Laboratory testing and numerical modeling on bearing capacity of geotextile reinforced granular soils. *International Journal of Geotechnical Engineering* 2016. DOI: 10.1080/19386362.2016.1269042.

Rajesh U, Sajja S, Chakravarthi VK. Studies on Engineering Performance of Geogrid Reinforced Soft Subgrade. *Transportation Research Procedia* 2016; 17: 164–173. doi: 10.1016/j.trpro.2016.11.072.

Sandra AK, Sarkar AK. Application of fuzzy logic and clustering techniques for pavement maintenance. *Transp. Infrastruct. Geotech.* 2015; 2: 103−119. DOI 10.1007/s40515-015-0021-z.

Singh M, Trivedi A, Shukla SK. Strength enhancement of the subgrade soil of unpaved road with geosynthetic reinforcement layers. *Transportation Geotechnics* 2019; 19: 54–60. doi.org/10.1016/j.trgeo.2019.01.007.

Singh P, Gill KS. CBR Improvement of Clayey Soil with Geo-grid Reinforcement. *International Journal of Emerging Technology and Advanced Engineering* 2012; 2 (6): 315–318.

Shukla SK. An introduction to geosynthetic engineering. CRC Press: London; 2016.

Smith GN. Probability and statistics of civil engineering. Collins; London: 1986.

Stephens DJ. Prediction of the California bearing ratio. *The Journal of the South African Institution of Civil Engineering* 1990; 32 (12): 523–527.

Suku L, Prabhu SS, Babu GLS. Effect of geogrid-reinforcement in granular bases under repeated loading. *Geotextiles and Geomembranes* 2017; 45 (4): 377–389. doi.org/10.1016/j.geotexmem.2017.04.008.

Taghavifar H, Mardani A. Fuzzy logic system based prediction effort: A case study on the effects of tire parameters on contact area and contact pressure. *Applied Soft Computing* 2014; 14: 390–396. doi.org/10.1016/j.asoc.2013.10.005.

Taskiran T. Prediction of California bearing ratio (CBR) of fine grained soils by AI methods. *Advances in Engineering Software* 2010; 41(6): 886-892. doi: 10.1016/j.advengsoft.2010.01.003.

Tenpe AR, Patel A. Application of genetic expression programming and artificial neural network for prediction of CBR. *Road Materials and Pavement Design* 2018; 1–18. doi.org/10.1080/14680629.2018.1544924.

Topçu IB, Saridemir M. Prediction of mechanical properties of recycled aggregate concretes containing silica fume using artificial neural networks and fuzzy logic. *Computational Materials Science* 2008; 42 (1): 74–82. doi: 10.1016/j.commatsci.2007.06.011.

Trivedi A. Estimating In Situ Deformation of Rock Masses Using a Hardening Parameter and RQD. *International Journal of Geomechanics* 2013; 13(4): 348–364.

Venkatasubramanian C, Dhinakaran G. ANN model for predicting CBR from index properties of soils. *International Journal of Civil and Structural Engineering* 2011; 2 (2): 605–611.

Wu H, Huang B, Shu X, Zhao S. Evaluation of geogrid reinforcement effects on unbound granular pavement base courses using loaded wheel tester. *Geotextiles and Geomembranes* 2015; 43 (5): 462–469. doi.org/10.1016/j.geotexmem.2015.04.014.

Yildirim B, Gunaydin O. Expert Systems with Applications Estimation of California bearing ratio by using soft computing systems. *Expert Systems with Applications* 2011; 38 (5): 6381–6391.

Zedeh L, Kacprzyk J. Fuzzy logic for the management of uncertainty. Johnwiley and Sons, Inc. New York; USA: 1992.

Zehtabchi A, Hashemi SAH, Asadi S. Predicting the strength of polymer-modified thin-layer asphalt with fuzzy logic. *Construction and Building Materials* 2018; 169: 826–834. doi.org/10.1016/j.conbuildmat.2018.02.002.

CHAPTER 7

MOVING WHEEL LOAD TESTS ON GEOSYNTHETIC REINFORCED UNPAVED ROADS

This chapter is being prepared for submission to Journal of Transportation Engineering, ASCE, as listed in Section 1.6. The details presented here are the same, except some changes in the layout in order to maintain a consistency in the presentation throughout the thesis.

7.1 Introduction

The economic development of any country is dependent on its transportation infrastructure. The total road length in India has been increased significantly and growing at a compound annual growth rate of 4.2%. Along with the increase in total road network, the paved and unpaved road length has also been increased (MORTH, 2017). Unpaved roads receive less attention because they are designed to support small amount of traffic. The availability of good quality pavement materials for the construction of roads is getting depleted rapidly but their demand increases at an accelerated rate. This scarcity of good quality pavement materials may harm the environment in future. So, there is a need to adopt some alternative measures like, stabilization of locally available materials, use of recycled pavement materials and use of geosynthetic reinforced pavements. Geosynthetics have been used successfully for reinforcing paved/unpaved roads. These roads can be stabilized with geosynthetic reinforcement either by placing them at the base-subgrade interface or within the granular base layer. Field application of geosynthetic as reinforcement in unpaved roads clearly shows the evidence of improvement in the performance of these roads by enhancing the service life of roads durability and reducing the thickness of base course which ultimately leads to saving of granular material (Al-Qadi et al., 1994; Tingle and Jersey, 2005; Hufenus, et al., 2006; Chen et al., 2018; Abu-Farsakh and Chen, 2011). The mechanisms responsible for these advantages of geosynthetic reinforcement

in pavement to carry higher traffic volumes are separation between base and subgrade, tensioned membrane effect, vertical restraint of the subgrade soil, lateral restraint of the base course and improved load distribution to the subgrade layer (Perkins and Ismeik, 1997; Giroud and Noiray, 1981; Giroud and Han 2004; Hufenus et al. 2006; Maxwell et al. 2005).

Geogrid and geotextile are major type of geosynthetics which are commonly used in pavement construction. Various laboratory studies are available in the literature to understand the benefits of geosynthetic but full-scale field studies conducted on unreinforced and reinforced unpaved roads are limited. Hence, more full-scale moving wheel load field tests are required to be carried out to investigate the contribution of geosynthetic reinforcement in pavement because in actual practice it is used throughout the width of the pavement. Field test results are more reliable than laboratory test results to use them in actual pavement construction practice. Yang et al. (2012) constructed four unpaved road sections reinforced with geocell to measure rut depth under accelerated pavement testing. Their test results demonstrated that the geocell improve the stability of unpaved roads and reduces the permanent deformation significantly. Ingle and Bhosale (2017) tested unpaved road section under accelerated pavement testing and found 22% reduction in the thickness of granular base layer due to the inclusion of geotextile reinforcement. Imjai et al. (2019) investigated the effect of geosynthetic as reinforcement in flexible pavements where it was placed at different depths to measure the structural response under a series of full-scale field trials. Their result show 66% reduction in vertical static stresses developed at the base of the pavement and dynamic stresses were reduced by 72%. Hufenus et al. (2006) carried out field tests on geosynthetic reinforced unpaved road on soft subgrade to evaluate its bearing capacity and performance in the presence or absence of geosynthetic reinforcement. Biaxial geogrids were used for stabilizing granular shoulder supported on clayey subgrade layer to eliminate severe rutting (Mekkawy et a. 2011). Wu et al. 2015 proposed the use of loaded wheel tester to investigate the influence of geogrid

reinforcement on unbound granular pavement base materials. Improvement in the rutting resistance was observed in the reinforced base course under loaded wheel tester comparing to the unreinforced base courses. Large scale laboratory tests were performed on unbound aggregate pavement section to investigate geogrid and geotextile reinforcement in the aggregate bases (Tingle and Jersey 2005). Their results indicate that geosynthetic can improve the performance in terms of better load distribution and reduced rutting. Field observations were reported by Fannin and Sigurdsson (1996) on five test sections of unpaved road through a vehicle of standard axle loading. The information discovered from these findings encourages the use of geogrid and geotextile at the base-subgrade interface or within base layer in unpaved road construction. Geosynthetic reinforcement has been placed at the base-subgrade interface for thinner granular layer to get the better results. But for thicker granular layer, geosynthetic reinforcement has been placed in the upper one-third of the granular layer to get good results (Abu-Farsakh and Chen, 2011; Haas et al., 1988; Al-Qadi et al., 2008). The benefit of a geosynthetic becomes insignificant if the base course layer is very thick (Collin et al., 1996).

The objective of this chapter is to evaluate the performance of unreinforced and geosynthetic reinforced unpaved test sections in terms of rutting under moving wheel load tests. In order to achieve this objective, three unpaved road test sections were constructed in the field and geogrid and geotextile were installed at base-subgrade interface for evaluating the influence of geosynthetic reinforcement. Moving wheel load test results of reinforced unpaved test sections were compared with the unreinforced unpaved test section. Traffic benefit ratio was used to identify the efficiency of geosynthetic reinforcement in unpaved test sections.

## 7.2 Materials Characterization

7.2.1 Subgrade and Base Course

The subgrade soil used in this study for the preparation of subgrade is classified as silty sand according to the Unified Soil Classification System. Standard proctor compaction and

California Bearing Ratio tests on the subgrade soil were carried out in the laboratory. The subgrade soil has an optimum moisture content of 13.9 % and a maximum dry unit weight of 18.6kN/m^3 according to the standard proctor test. California Bearing Ratio of the subgrade soil measured in the laboratory was approximately equal to 1.7%. Greater benefits can be obtained by the inclusion of geosynthetic reinforcement for the subgrade with lower *CBR* values. Holtz et al. (2008) proposed that the optimum use of geosynthetics in pavement construction is when the CBR value of the subgrade soil is less than 3%. Therefore, geosynthetics were selected to reinforce the weak subgrade in field tests.

Well graded aggregates were used as a base course material in all the unpaved road test sections. Base course material is classified as GW according to the Unified Soil Classification System. The optimum moisture content and maximum dry unit weight of the base material was 22kN/m^3 at a water content of 6.8%. The grain size distribution curve for the subgrade soil and base course material is shown in Fig. 7.1.
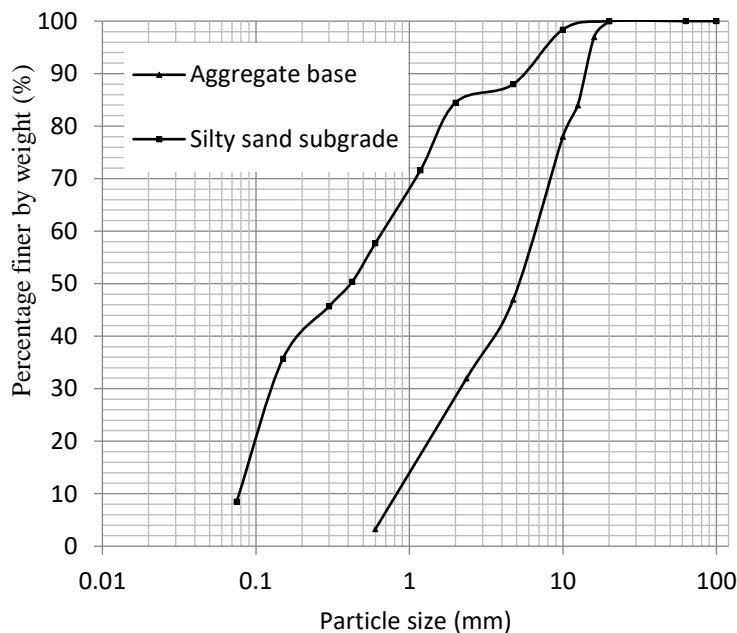
Figure 7.1 Particle size distribution curve of base course material and subgrade soil

7.2.2 Geotextile and Geogrid

In this study, two geosynthetic reinforcement materials were employed in between the subgrade and base course for the reinforced unpaved road test sections in the field. The properties of geotextile and geogrid, as provided by the manufacturer are summarized in Table 7.1. Geogrid is made up of polypropylene with transverse and longitudinal ribs which is obtained from the manufacturer, H.M.B.S Textiles Pvt. Ltd, New Delhi, India. These ribs are capable to provide the best possible interaction mechanism between geogrid and granular soils by restricting the horizontal movement of soil particles and preventing further displacements.

The geotextile used in this study was woven geotextile. It is also made up of polypropylene, with a tensile strength of 45kN/m in the machine direction and 34kN/m in the cross-machine direction. The material properties of the geotextile are provided in Table 7.1. For conducting moving wheel load tests, geosynthetic reinforcement layer was positioned at the interface of subgrade-base course layer.

Table 7.1 Properties of geotextile and geogrid used in the study

Geosynthetics	Properties	Value	Unit	Test method
Geogrid	Polymer type	polypropylene	-	-
	Carbon black content	2	%	ASTM D4218
	Structure	Bi-oriented geogrids	-	-
	Stiffness at 0.5% strain			
	Machine direction	550	kN/m	ISO 10319
	Cross-machine direction	350	kN/m	ISO 10319
	Aperture size			-
	Machine direction	30	mm	
	Cross-machine direction	30	mm	-
	Residual resistance to chemical degradation	100	%	EN 14030

	Residual resistance to weathering	100	%	EN 12224
	Installation damage factor	1	-	ASTM D5818
	Apparent coefficient of friction			
	soil/geosynthetics at 10 kPa	1.78	-	EN 13738
	soil/geosynthetics at 20 kPa	1.14		
	Tensile strength			
	Machine direction	45	kN/m	IS 1969
	Cross-machine direction	34	kN/m	
	Elongation at break			
Geotextile	Machine direction	30	%	IS 1969
	Cross-machine direction	28	%	
	Puncture resistance	700	N	ASTM D4833
	Apparent opening size	0.075	mm	ASTM D4751
	Weight of fabric	200	g/m^2	ASTM D5261

## 7.3 Field Testing Program

7.3.1 Unpaved Test Sections

In this study, three unpaved road test sections were constructed in a test pit of dimension 9m long, 2.7m wide, and 0.8m deep to evaluate the performance of geosynthetic reinforced unpaved roads. A cross-sectional view of a typical unpaved road test section is shown in Fig. 7.2. The dimension of each test section is 3m long and 2.7 m wide and overall dimension of test pit is 9m long and 2.7 m wide. Section 1 is an unreinforced section and section 2 is reinforced with geotextile reinforcement, whereas section 3 is reinforced with geogrid reinforcement. The unreinforced and geosynthetic-reinforced test sections were constructed as per IRC-SP-72 guidelines. To evaluate the influence of geosynthetic reinforcement on the unpaved test section, a geosynthetic reinforcement layer is laid at the interface of base-subgrade layer. All the unpaved test sections (section 1, section 2 and section 3) have the same aggregate layer thickness of 200mm. Unreinforced and geosynthetic-reinforced unpaved test section

consisted of a 200mm thick base course over a 500mm subgrade along with 100mm of modified subgrade.

Major steps involved in the construction of geosynthetic-reinforced unpaved test sections were: excavation and leveling of test pit, preparation of subgrade, preparing and placing the modified subgrade, installation of geogrid and geotextile over the modified subgrade, and placing and spreading granular layer over geosynthetic reinforcement. To construct this unpaved test section, a test pit was excavated on an existing ground in the campus of Delhi Technological University. Bottom of the excavated test pit was leveled. This test pit excavation was 9000mm long, 3000mm wide and 800mm deep to accommodate the unreinforced and geosynthetic-reinforced test sections. The subgrade of 500 mm thick was compacted in three layers by using electric operated vibratory plate compactor. The unit weight and water content of prepared subgrade was determined by core cutter method by considering three random soil samples. It can be observed that 91% compaction was achieved. When the CBR of subgrade soil is less than 2, a capping layer of thickness not less than 100mm of modified soil with CBR not less than 10 should be provided and the granular base layer thickness required is designed as per the design catalogue of IRC: SP:72-2007. In the present study, lime stabilization technique has been used for improving the subgrade. Quantity of lime to be added is 3% by weight of the dry soil and it is spread all over the prepared subgrade in test pit and mixed with the soil manually. Capping layer was compacted and allowed for curing of this layer to 7 days. Field CBR value of capping layer was found to be 12.8% as per IS 2720 Part-16. The geotextile and geogrid were rolled over the prepared modified subgrade and the granular material then spread and compacted. During the installation of geotextile, wrinkles were removed by pulling the fabric on the ends. The geosynthetic reinforcement layer was covered with a layer of 200mm thick aggregate base layer and compacted by 10-ton three-wheeled road roller. Surface course of 50mm thickness was placed over granular layer. Figure 7.3 illustrate the construction

procedure adopted for the geosynthetic-reinforced unpaved test section at the field for moving wheel load tests. The unreinforced unpaved test section was also constructed in the same manner without the geosynthetic at subgrade-base interface.
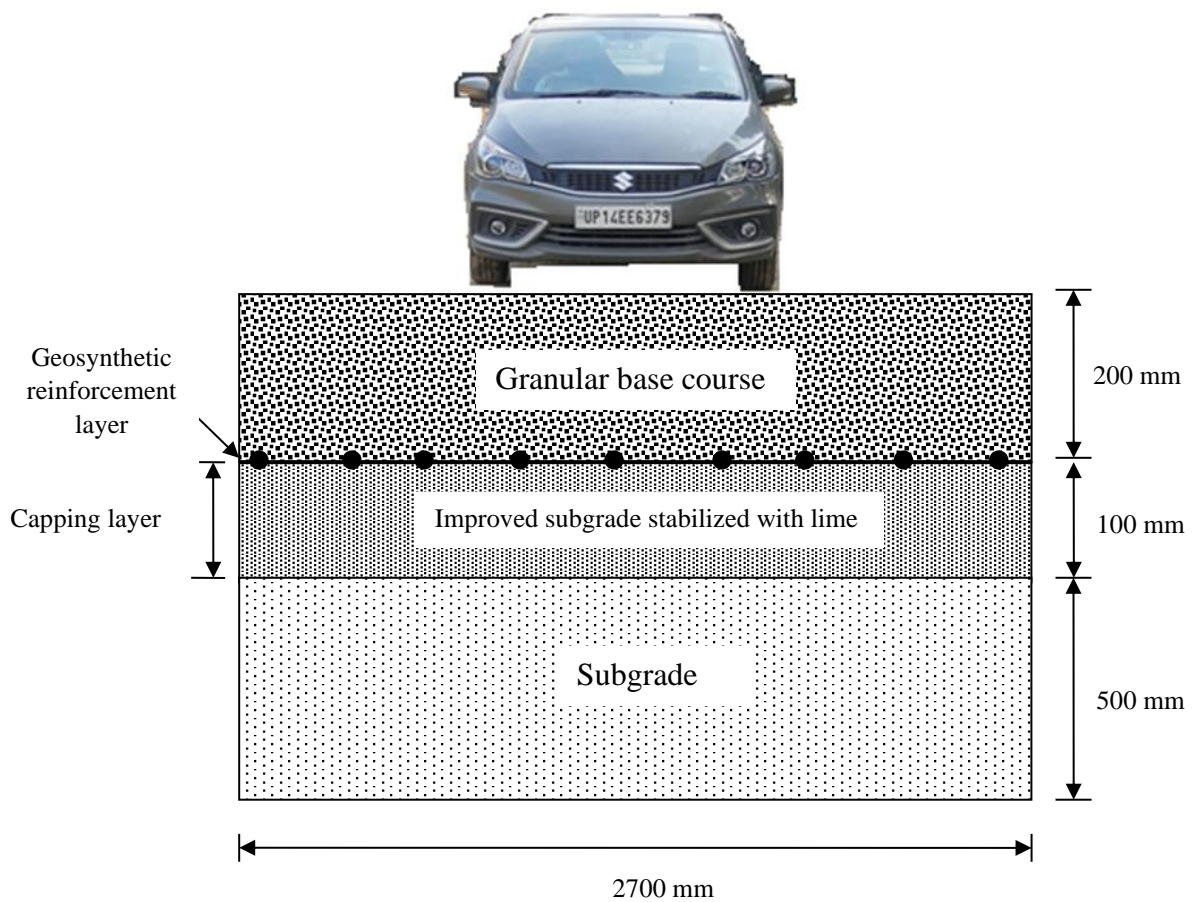
Figure 7.2 A cross-sectional view of geosynthetic-reinforced unpaved road test section.

Figure 7.3 Overview of construction procedure of unpaved test section: (a) excavation of test pit; (b) leveling of bottom of test pit; (c) placing and spreading subgrade soil and compaction of the subgrade in 3 layers; (d) manual mixing of lime with subgrade soil for modified subgrade; (e) 100mm capping layer after curing of 7 days; (f) placing the geogrid and geotextile over the modified subgrade; (g) placing and spreading granular layer over geosynthetic reinforcement and compacting by 10-ton three wheeled roller; (h) surface course of 50 mm and compaction with 10-ton three wheeled roller; (i) geosynthetic-reinforced unpaved test section

7.3.2 Moving Wheel Load Tests

A single-axle testing vehicle was used to conduct the moving wheel load tests on unreinforced and geosynthetic-reinforced unpaved test sections. The test vehicle of weight 1530 kg was used to traffic each unpaved test section as shown in Fig. 7.2. The trafficking was conducted in one direction from one end to another end of the test pit such that the testing vehicle passes through the test sections at a speed of 15 km/hr. A total of 350 passes of wheel load were applied to the unpaved test sections. Rut measurements were made along the three grid lines for each unpaved test section and there were 17 grid points on each grid line for rut measurement. G1, G2, and G3 are grid lines presented on unreinforced test section and the distance between these grid lines is 0.75 m. During testing, the testing vehicle was steered to move along the same wheel path for each vehicle pass. The testing arrangement and the layout of unpaved test section indicating the grid points marked on it for measuring rut under moving wheel load tests is shown in Fig. 7.4. Rut depth was measured by using an aluminum reference bar placed across the test section surface on predetermined locations. Wooden pegs were driven on each side of the unpaved test section to the same elevation at every grid line. The reference bar rests on the left and right measuring pegs driven on both sides of the test section. After certain numbers of vehicle passes, elevation of the wooden pegs was checked to make sure that they were not disturbed by trafficking. The reference bar was marked with 17 grid points and each grid point is 150 mm apart from each other. A laser meter with accuracy of ± 0.1 mm was used to measure the rut depth at 17 grid points by placing this device on the reference bar. The reference bar was moved from grid line G1 to G9 for measuring the rut after vehicle passes of 3, 5, 10, 20, 40, 80, 150, 200, 250, 300, and 350. Rut depth is defined as the distance between the initial elevation of the surface before trafficking and the lower point in the rut beneath the wheel under the channelized traffic (Fannin and Sigurdsson, 1996). In the present study, rut depth was measured after certain numbers of vehicle passes of the testing vehicle as the difference
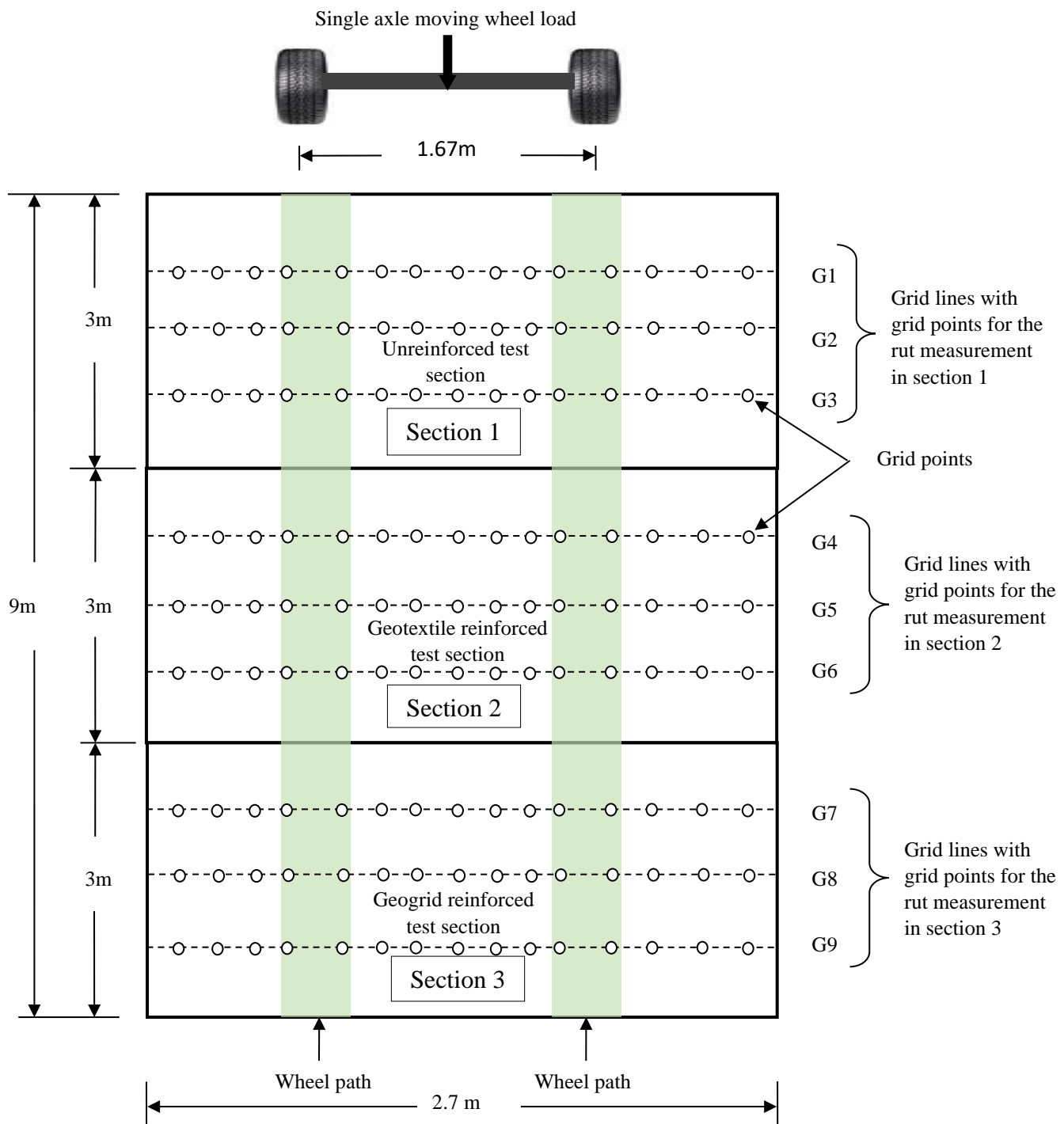
Figure 7.4 layout of unpaved test section indicating grid points for measuring rut under moving wheel load tests

between the distance from a reference bar to the surface of test section and that before the testing vehicle had passed over. Rut depth measurements were recorded throughout the three grid lines for each unreinforced and geosynthetic-reinforced unpaved test sections. Dynamic Cone Penetrometer (DCP) tests were also performed on the section-1, section-2, and section-3 for determining the strength of the unpaved road in terms of CBR value after completing the moving wheel load tests.

7.4 Results and Discussion

7.4.1 Transverse rut surface profile

The performance of unreinforced and geosynthetic-reinforced unpaved test sections was analyzed based on the rut depth measurements. Figure 7.5 – 7.7 shows the transverse rut surface profiles for the unreinforced, geotextile-reinforced and geogrid-reinforced test sections, respectively. These surface profiles were taken at 9 grid lines along the 9m long unpaved test section. Transverse rut surface profiles at middle grid line (G2, G5, G8) of each unpaved test sections were plotted in Fig. 7.5–7.7. Initial road surface measurements were taken at 17 grid points along the 9 grid lines by determining the distance of road surface from reference bar before trafficking. Rut depth was measured in each of the test sections after vehicle passes of 3, 5, 10, 20, 40, 80, 150, 200, 250, 300, and 350 during trafficking. All the measurements were taken in the transverse direction along the 17 grid points marked on the reference bar. Transverse direction is defined as the direction perpendicular to the direction of testing vehicle. Transverse rut surface profile was determined for all the unpaved test sections by comparing the current measurements for particular numbers of vehicle passes to the initial road surface measurements which was made before trafficking. Figure 7.5 shows the transverse rut surface profile for the unreinforced test section at each vehicle passes.
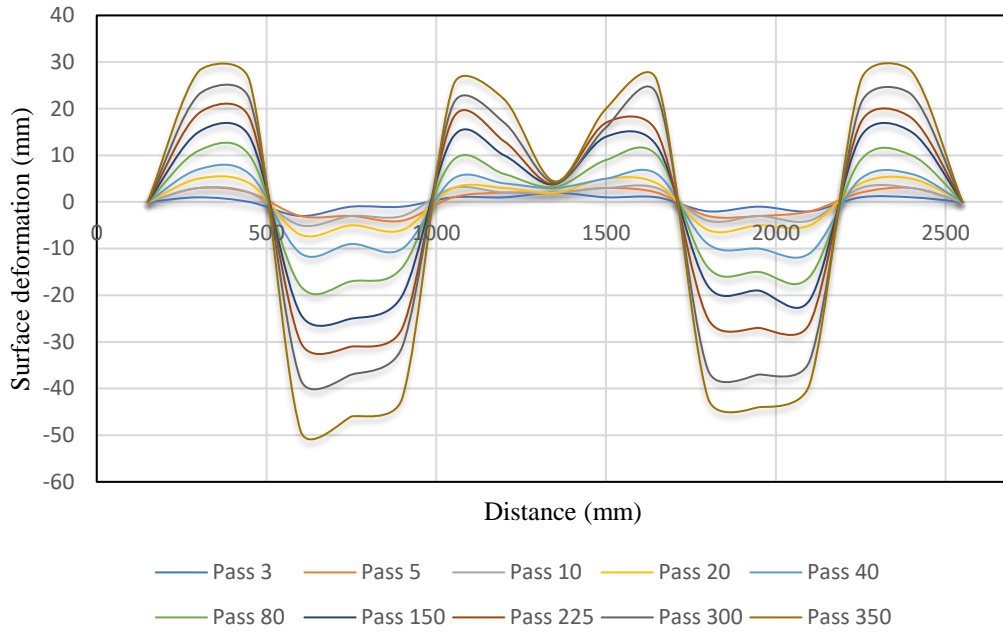
Figure 7.5 Transverse rut surface profile of unreinforced test section during trafficking

Trafficking was conducted for maximum of 350 vehicle passes. Almost similar rut surface profiles were observed for section 1, section 2, and section 3 up to 20 vehicle passes. Figure 7.6 and 7.7 shows the change in transverse rut surface profiles of section 2 and section 3 with an increasing number of testing vehicle passes. Section 1, section 2, and section 3 exhibits a rut depth of 18mm, 11mm, and 15mm, respectively at 80 vehicle passes. The rut development increases with the continued trafficking and geotextile-reinforced test section exhibits smaller rut as compared to the geogrid-reinforced test section. Hence, it indicates that the role of separation is more important than the tensile stiffness of the geosynthetic.
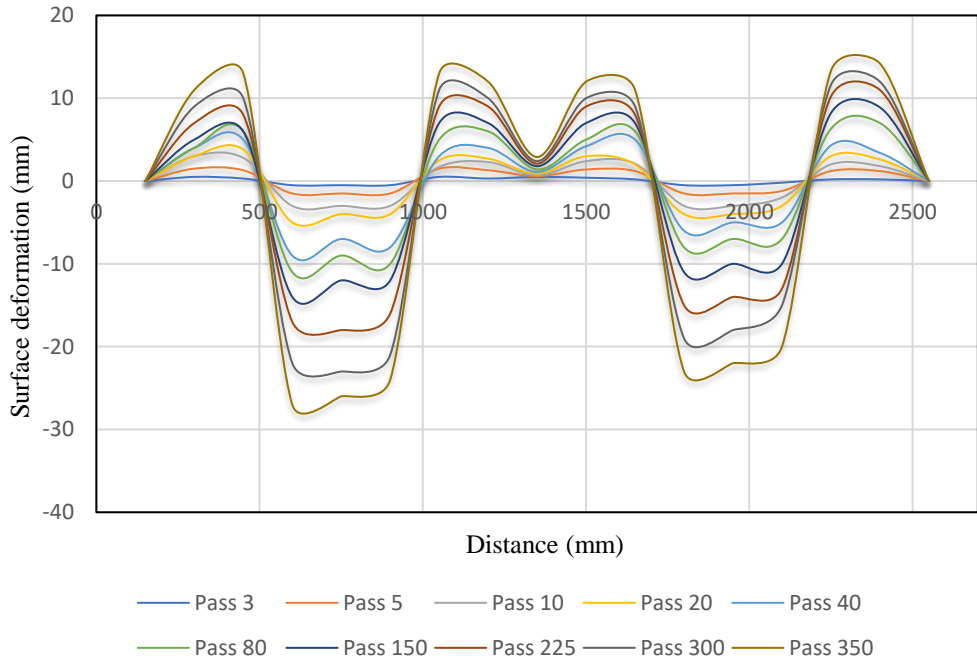
Figure 7.6 Transverse rut surface profile of geotextile-reinforced test section during trafficking
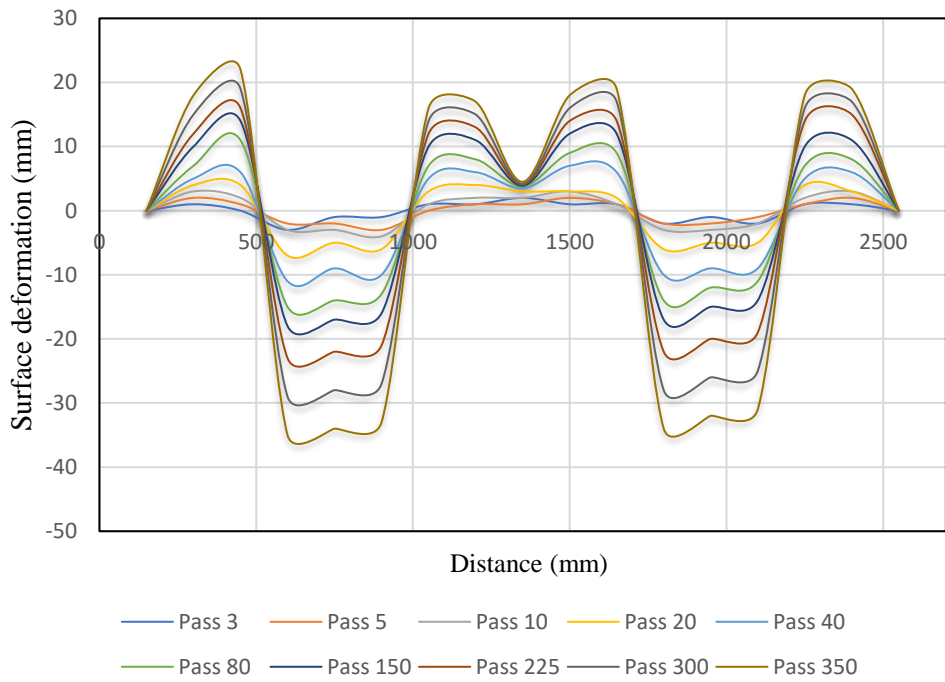

Figure 7.7 Transverse rut surface profile of geogrid-reinforced test section during trafficking

150

7.4.2 Rut depth

Three test sections were subjected to the same moving wheel load. Rut depth measured at three grid lines of each test section was averaged for each vehicle pass and plotted against the numbers of vehicle passes as shown in Fig. 7.8. After 350 vehicle passes, the rut depth developed in section 1, section 2, and section-3 were 49mm, 27mm, and 35mm, respectively. Among the three unpaved test sections, unreinforced test section developed more rut than geosynthetic-reinforced test section. Whereas, geotextile-reinforced test section performed better than geogrid-reinforced test section in terms of rutting. Test results showed that rut depth increases in unreinforced and geosynthetic-reinforced unpaved test sections as vehicle passes increase. This indicates the benefit of geosynthetic reinforcement in reducing surface deformation in unpaved roads. The traffic benefit ratio (TBR) was calculated to evaluate the contribution of geosynthetic reinforcement in performance evaluation of unpaved test sections. TBR is defined as the ratio of the numbers of vehicle passes to reach a certain rut depth between the geosynthetic-reinforced to the unreinforced test section. TBR value indicates that the geosynthetic-reinforced test sections can bear additional amount of traffic load. TBR values obtained for geotextile-reinforced and geogrid -reinforced test sections was 3 and 1.86 respectively, corresponding to 18mm rut depth. For a rut depth of 27mm, a TBR value of 1.92 and 1.51 was obtained for section 2 and section 3, respectively. After 350 vehicle passes, the geotextile-reinforced and geogrid -reinforced test sections reduced rutting by 44.89% and 28.57%, respectively. Overall, it can be suggested that geosynthetic-reinforced test sections performed better than unreinforced test section.
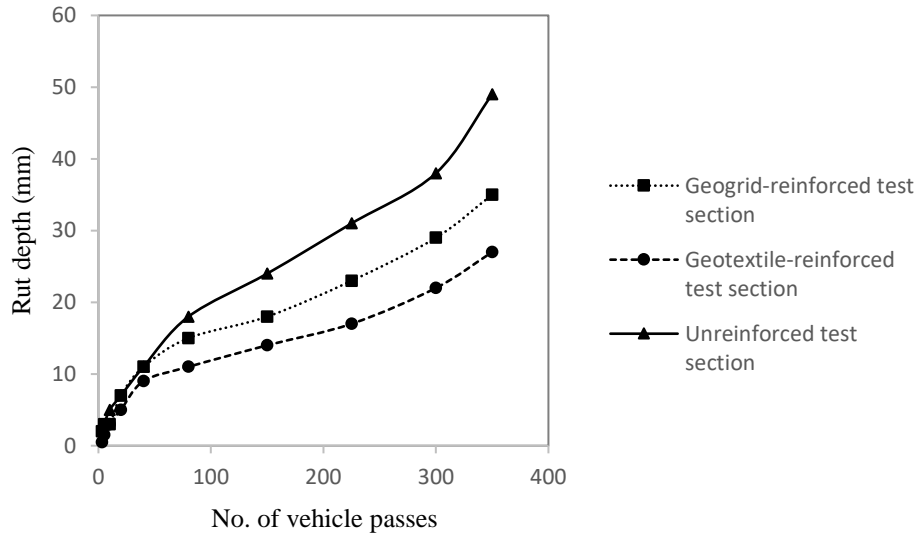
**Figure 7.8** Rut depth versus numbers of vehicle passes

7.4.3 DCP Tests

Dynamic Cone Penetrometer tests were carried out to estimate the strength of unreinforced and geosynthetic reinforced unpaved test sections. DCP test involves a 60˚ cone with 20mm base diameter driving into the test sections using an 8kg hammer dropped from a height of 575mm in accordance with ASTM 6951-03. Figure 7.9 presents the variation in the DCP blow counts with penetration depths. DCPI value was determined from the DCP test results and converted to CBR strength using correlations developed by webster et al., (1992) as shown in Eq. 1.

$$CBR = \frac{292}{DCPI^{1.12}} \tag{4}$$

DCP measurements were taken on section 1, section 2, and section 3 after the completion of moving wheel load tests. DCP test results were expressed in terms of dynamic cone penetration index (DCPI), which is defined as the penetration depth per blow of the hammer (mm/blow). DCPI values were determined based on the thickness of granular layer and subgrade. DCPI values obtained for unreinforced, geotextile-reinforced, and geogrid-reinforced test sections are 6.99 mm/blow, 5.66 mm/blow, and 5.82 mm/blow, respectively. Table 7.2 provides a

summary of DCPI values and CBR values. Lowest DCPI was obtained for geotextile-reinforced test section and highest DCPI was obtained for unreinforced test section. DCPI value indicates the resistance against penetration and this penetration resistance is more in geosynthetic-reinforced test section as compared to the unreinforced test section. DCP tests were performed at the center of each unpaved test section and DCPI values were calculated at the same depth for both unreinforced and geosynthetic-reinforced test sections as shown in Fig. 7.10. The profile shows the change in the strength of unreinforced and geosynthetic-reinforced test sections. Geosynthetic reinforcement has more benefits in improving the performance of unpaved test sections in terms of DCPI value.
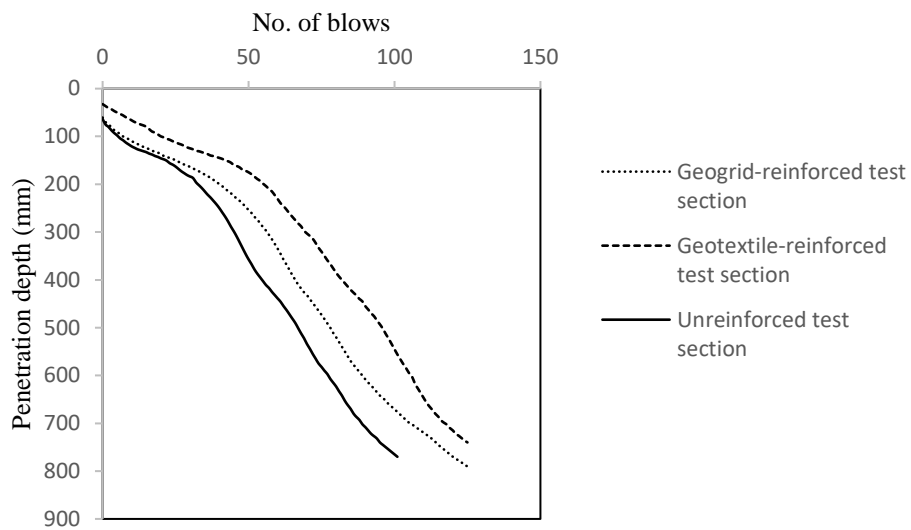
Figure 7.9 Variation in blow counts with penetration depth for unpaved test sections
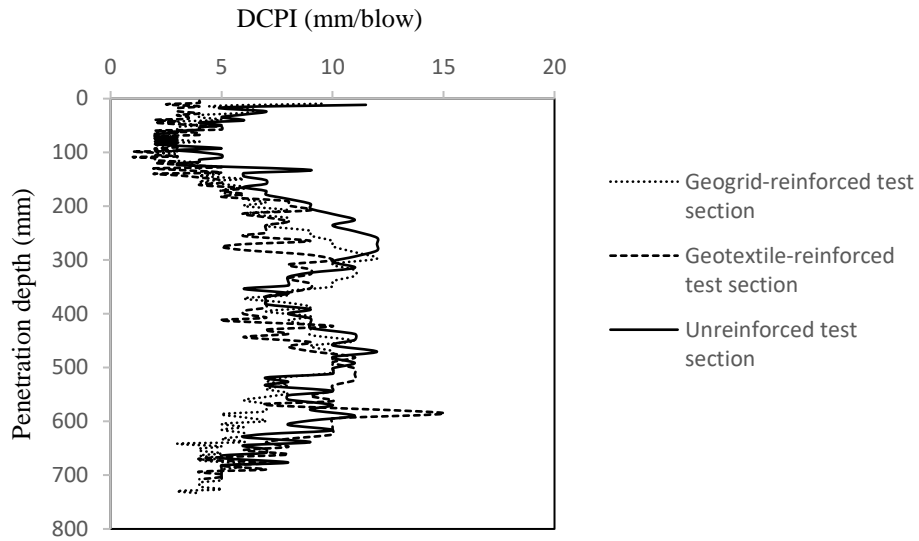
Figure 7.10 DCPI profile for unreinforced and geosynthetic-reinforced test section

Table 7.2 DCPI values and CBR values of unpaved test section

Unpaved test section	DCPI values (mm/blow)		CBR value (%)	
	Granular layer	Subgrade layer	Granular layer	Subgrade layer
Unreinforced test section	4.14	8.32	59.47	27.21
Geotextile-reinforced test section	3.03	6.91	84.68	29.55
Geogrid-reinforced test section	3.48	7.73	72.01	33.51

7.5 Conclusions

Moving wheel load tests were performed on unreinforced and geosynthetic-reinforced unpaved test sections. DCP tests were performed on the unpaved tests section after the completion of moving wheel load test. The main conclusions obtained are summarized below.

1. Unreinforced test section exhibited significantly greater surface deformation than the reinforced test section under the same numbers of vehicle passes.

2. Test results demonstrated that the use of both geotextile and geogrid reinforcement at base-subgrade interface significantly improve the stability of unpaved roads and reduce the surface deformation.

3. The analysis of transverse rut surface profiles indicated the benefits of geosynthetic reinforcement through the lateral restraint reinforcement mechanism at lower rut depth.

4. Traffic benefit ratio can be used to quantify the efficiency of geosynthetic reinforcement, which was calculated based on the rut depth measurements in the field. TBR value confirm that geotextile-reinforced test section exhibits the most effective geosynthetic reinforcement.

References

ASTM D6951-03. Standard Test Method for Use of the Dynamic Cone Penetrometer in Shallow Pavement Applications, *ASTM International* 2003; West Conshohocken, PA.

Abu-Farsakh MY, Chen Q. Evaluation of geogrid base reinforcement in flexible pavement using cyclic plate load testing. *International Journal of Pavement Engineering* 2011; 12(03):275-88. DOI: 10.1080/10298436.2010.549565.

Al-Qadi IL, Brandon TL, Valentine RJ, Lacina BA, Smith TE. Laboratory evaluation of geosynthetic-reinforced pavement sections. *Transp Res Rec* 1994; 25–31.

Al-Qadi IL, Dessouky SH, Kwon J, Tutumluer E. Geogrid in flexible pavements: validated mechanism. *Transportation Research Record* 2008; 2045(1):102-9.

Chen Q, Hanandeh S, Abu-Farsakh M, Mohammad L. Performance evaluation of full-scale geosynthetic reinforced flexible pavement. *Geosynthetics International* 2018; 25(1):26-36. https://doi.org/10.1680/jgein.17.00031.

Collin JG, Kinney TC, Fu X. Full scale highway load test of flexible pavement systems with geogrid reinforced base courses. *Geosynthetics International* 1996; 3(4):537-49.

Fannin RJ, Sigurdsson O. Field Observations on Stabilization of Unpaved Roads with Geosynthetics. *Journal of Geotechnical Engineering* 1996; 122:544–53. doi:10.1061/(ASCE)0733-9410(1996)122:7(544).

Giroud JP, Han J. Design Method for Geogrid-Reinforced Unpaved Roads. I. Development of Design Method. *Journal of Geotechnical and Geoenvironmental Engineering* 2004; 130 (8): 775–786. DOI: 10.1061/(ASCE)1090-0241(2004)130:8(775).

Giroud JP, Noiray L. Geotextile-reinforced unpaved road design. *Journal of Geotechnical Engineering* 1981;107(9):1233-54.

Haas R, Walls J, Carroll RG. Geogrid reinforcement of granular bases in flexible pavements. *Transportation Research Report* 1988; 19–27.

Holtz RD, Christopher BR, Berg RR. Geosynthetics Design and Construction Guidelines. U.S. Department of Transportation, Federal Highway Administration, Washington DC, Report No. FHWA-NHI-07-092, 592.

Hufenus R, Rueegger R, Banjac R, Mayor P, Springman SM, Brönnimann R. Full-scale field tests on geosynthetic reinforced unpaved roads on soft subgrade. *Geotext Geomembranes* 2006; 24:21–37. DOI: 10.1016/j.geotexmem.2005.06.002.

Imjai T, Pilakoutas K, Guadagnini M. Performance of geosynthetic-reinforced flexible pavements in full-scale field trials. *Geotextiles and Geomembranes* 2019; 47:217-229. https://doi.org/10.1016/j.geotexmem.2018.12.012.

Ingle GS, Bhosale SS. Full-Scale Laboratory Accelerated Test on Geotextile Reinforced Unpaved Road. *Int. J. of Geosynth. And Ground Eng*. 2017; 3:33. DOI: 10.1007/s40891-017-0110-x.

IRC: SP: 72. Guidelines for the design of flexible pavements for low volume rural roads. Indian Road Congress 2007; New Delhi.

Maxwell S, Kim W-H, Edil TB, Benson CH. Geosynthetics in stabilizing soft subgrades with breaker run. *Wisconsin Highway Research Program*. Final Report No. 0092-45-15; 2005. p. 88.

Mekkawy MM, White DJ, Suleiman MT, Jahren CT. Mechanically reinforced granular shoulders on soft subgrade: Laboratory and full-scale studies. *Geotextiles and Geomembranes* 2011 Apr 1;29(2):149-60.

Perkins SW, Ismeik M. A Synthesis and Evaluation of Geosynthetic-Reinforced Base Layers in Flexible Pavements: Part I. *Geosynth Int* 1997;4(6):549–604.

Tingle JS, Jersey SR. Cyclic Plate Load Testing of Geosynthetic-Reinforced Unbound Aggregate Roads. *Transportation Research Record* 2005; 1936:60–69.

Webster SL, Grau RH, Williams RP. Description and application of dual mass dynamic cone penetrometer. Vicksburg, MS, U.S. Army Engineer Waterways Experiment Station. Report Number GL-92-3.

Wu H, Huang B, Shu X, Zhao S. Evaluation of geogrid reinforcement effects on unbound granular pavement base courses using loaded wheel tester. *Geotextiles and Geomembranes* 2015; 43 (5): 462–469. doi.org/10.1016/j.geotexmem.2015.04.014.

Yang X, Han J, Pokharel SK, Manandhar C, Parsons RL, Leshchinsky D, Halahmi I. Accelerated pavement testing of unpaved roads with geocell-reinforced sand bases. *Geotextiles and Geomembranes* 2012; 32:95-103.

CHAPTER 8

CONCLUSIONS AND FUTURE RESEARCH

This chapter presents the conclusions of the research work focused on the performance evaluation of geosynthetic reinforced unpaved roads. Though conclusions have been given at the end of each chapter, the overall key findings have been presented in this chapter. Finally, it makes some recommendations for future research based on the experience from this research.

8.1 General

This thesis is the outcome of the laboratory experimental work, field experimental work and modelling to quantify the benefits of geosynthetic reinforcement in improving the performance of unpaved roads. Permanent deformation or rutting is the most common distress in unpaved roads. Extensive literature review on the studies of geosynthetic reinforcement in unpaved and paved roads reveals that it improves the service life of pavement, reduces the permanent deformation, reduces construction and operational cost, increases the bearing capacity of soft soil, reduces the required fill thickness and requires less periodical maintenance. This study focuses on the use of geotextile and geogrid reinforcement in unpaved roads through experimental and field studies.

In this research, an attempt has been made to conduct the California bearing ratio (*CBR*) tests on unreinforced and geosynthetic-reinforced subgrade soil, as well as on unreinforced and geosynthetic-reinforced subgrade-aggregate composite systems. Single and double layers of geosynthetic reinforcements were laid horizontally at varying depths within the subgrade soil. One of the major aspects of conducting *CBR* tests on subgrade soil is to determine the optimal location of geosynthetic reinforcement. Maximum benefits of geosynthetic reinforcement can be drawn only if it is placed at the optimal depth. This study investigated the effect of type of

geosynthetic reinforcement and the relative performance of various types of geosynthetics used. In addition, this research also presents the results of dynamic cone penetrometer tests and digital static cone penetrometer tests on unreinforced and geosynthetic-reinforced test sections to assess the potential benefits of geotextile and geogrid reinforcement. The load–displacement behavior of geosynthetic-reinforced test section was measured and determine resistance against penetration for reinforced test section in terms of dynamic cone penetration index. Further, this study introduces a fuzzy logic–based modeling approach for predicting the strength of geogrid-reinforced subgrade soil of unpaved roads with optimal depth of geogrid reinforcement. Triangular and Gaussian membership functions were used for the development of model in the investigation for input and output variables. To achieve the objectives of this study, moving wheel load tests were conducted on unreinforced and geosynthetic-reinforced unpaved test sections constructed in the field at Delhi Technological University. Performance of the test sections were evaluated in terms of rutting under moving wheel load tests. A single-axle testing vehicle of weight 1530 kg was used to traffic each unpaved test section. Measurements of transverse rut surface profiles were taken during trafficking after certain numbers of vehicle passes. The performance parameter of unreinforced and geosynthetic-reinforced test sections includes rut depth on the wheel path after trafficking and traffic benefit ratio. This chapter provides general conclusions from this study and recommendations for future research.

8.2 Conclusions

Based on the current study, the following general conclusions are made from each of the individual research aspects and the analysis of the literature.

1. This study confirms that inclusion of a single layer and double layers of geosynthetic reinforcements at varying depths in subgrade soil enhances the strength of the subgrade soil in terms of California bearing ratio (*CBR)* value.

2. The *CBR* value of the subgrade soil increases by 5 to 60 % when a single layer of reinforcement is placed within the subgrade soil and the strength increases by 112 to 325 % when it is reinforced with double layers of reinforcement. The amount of improvement depends upon the position of reinforcement layer and type of reinforcement.

3. Placing the geosynthetic reinforcement in the double layers within the subgrade soil yields the largest improvement regardless of the type of geosynthetic.

4. The optimum benefit of reinforcement is evident if it is placed at middle height of the thickness of subgrade soil specimen and for better improvement in strength, reinforcement layer should be placed in between the upper one-third layer and middle layer within the subgrade soil.

5. Among the three geosynthetics used in the laboratory CBR tests, Tenax 3D grid performed better than other two geosynthetics for soil reinforced with a single layer of reinforcement at $\xi=H/3=H/4$ and Tenax multimat performed better than other two geosynthetics for soil reinforced with double layers of reinforcement and single layer of reinforcement at $\xi=H/2$.

6. Optimum location of reinforcement was found as $0.3H$ to $0.36H$ for Tenax 3D grid reinforcement layer and $0.41H$ to $0.62H$ for both Glasgrid reinforcement layer and Tenax multimat reinforcement layer in laboratory CBR tests.

7. The reinforced subgrade-aggregate composite system with reinforcement at the interface of subgrade and aggregate layer performs better than the reinforced subgrade-aggregate composite system with double layer of reinforcement.

8. Geotextile and geogrid reinforcement proved to be the most effective reinforcement and the contribution of geomat was least in improving the performance of subgrade-aggregate composite system.

9. The reinforced subgrade-aggregate composite system performs better than the unreinforced subgrade-aggregate composite system only in case of geotextile and geogrid reinforcement placed at the interface of subgrade and aggregate layer.

10. Contribution of geosynthetic reinforcement would be ineffective if it is not implemented at the suitable location.

11. The DCP test results were found to be influenced by the inclusion of geosynthetic reinforcement. The lowest *DCPI* value was obtained for the geotextile-reinforced test section. *DCPI* indicates the resistance to penetration; a greater penetration resistance is observed for reinforced test section as compared to the unreinforced test section.

12. Overall DCPI values obtained for geogrid-reinforced, geotextile-reinforced and unreinforced test sections are 4.38 mm/blow, 2.04 mm/blow and 6.33 mm/blow, respectively.

13. The behavior of the reinforced test section was significantly better than that of the unreinforced test section, with the best performance served by the geotextile-reinforced test section.

14. The results demonstrated that DCP was able to detect significant changes in the strength of base and subgrade layers through the profile of the test section along with the depth. It can also be used to delineate the transition zone of the base course and subgrade layer. However, the digital SCP results did not reflect changes in layer because the device was

not able to penetrate up to the depth of the reinforcement layer with the application of load.

15. The geogrid has higher strength and stiffness than the geotextile, but the better performance was observed when the geotextile reinforcement layer was placed at the base-subgrade interface than that of the geogrid reinforcement layer placed at the same location. Higher resistance to penetration offered by the geotextile had more contribution in improving the performance of the test section.

16. Fuzzy logic modeling is a convenient approach for predicting the strength of geogrid-reinforced subgrade soil, thus saving time and resources in real-life projects.

17. The correlation coefficient is found to be closer to unity for both the developed models having Triangular membership function and Gaussian membership function, thus validating the results.

18. Sensitivity analysis evaluated the contribution of individual input parameters on the *CBR* value of geogrid-reinforced subgrade soil and it reveals that, the strength of the relationship between the input parameters and *CBR* of geogrid-reinforced subgrade soil is more than 0.7 for all the input parameters except for 'soaked/unsoaked condition'. This demonstrates the good selection of input parameters for the development of models.

19. As the availability of data on geogrid-reinforced subgrade soil increases in the literature, more accurate prediction model can be proposed for a wider range.

20. The range of the optimal depth of geogrid reinforcement is found as 36% to 60% of the thickness of the subgrade soil layer from fuzzy logic prediction model.

21. Unreinforced test section exhibited significantly greater surface deformation than the reinforced test section under the same numbers of vehicle passes during the moving wheel load tests in the field.

22. Field test results demonstrated that the use of both geotextile and geogrid reinforcement at base-subgrade interface significantly improve the stability of unpaved roads, reduce the surface deformation and extends the service life of pavement.

23. The analysis of transverse rut surface profiles indicated the benefits of geosynthetic reinforcement through the lateral restraint reinforcement mechanism at lower rut depth.

24. After maximum numbers of vehicle passes for this study, geotextile-reinforced and geogrid-reinforced test section reduced rut depth by 44.89% and 28.57%, respectively.

25. Traffic benefit ratio can be used to quantify the efficiency of geosynthetic reinforcement, which was calculated based on the rut depth measurements in the field. TBR value confirm that geotextile-reinforced test section exhibits the most effective geosynthetic reinforcement.

8.3 Future Research

The possible research ideas for future work are summarized below.

- The present study investigates the effect of geosynthetic reinforcement on the strength of subgrade-aggregate composite system in terms of *CBR* value. Further studies are to be carried out for better understanding of the strength behavior of subgrade-aggregate composite system with multiple layers of reinforcement and by varying the type of geosynthetic reinforcement.

- In future studies, more input variables can be included, such as specific property of geosynthetics, for developing the fuzzy logic model for predicting strength of geogrid-reinforced subgrade soil. The predictive capabilities of the proposed models with Triangular and Gaussian membership functions are limited to the range of the data used

for their calibration. As more data become available, by including them for other types of soils and test conditions, the proposed models can be improved to make more accurate predictions for a wider range.

- Full-scale field tests can be carried out by varying the thickness of granular layer, type of geosynthetic with different stiffness or aperture size, strength of subgrade, and location of geosynthetic reinforcement to evaluate the performance of geosynthetic-reinforced pavements. Field tests are necessary to validate the results of laboratory work.

- In the present study, only 350 passes of wheel load were applied to the unpaved test section for evaluating rutting in the field. Further study with higher numbers of vehicle passes may be carried out to give valuable results.